The Dissertation Committee for Heirberto Rivera Jr. Certifies that this is the approved version of the following dissertation:

A Direct, Concise and Stereoselective Formal Synthesis of Platensimycin

Committee:

Philip D. Magnus, Supervisor

Michael J. Krische

Dionicio R. Siegel

Richard A. Jones

Sean M. Kerwin

A Direct, Concise and Stereoselective Formal Synthesis of Platensimycin

by

Heriberto Rivera Jr., B.Sc.

Dissertation

Presented to the Faculty of the Graduate School of

The University of Texas at Austin

in Partial Fulfillment

of the Requirements

for the Degree of

Doctor of Philosophy

The University of Texas at Austin

December 2011

Dedication

To my mother, whose love, hard work, sacrifice and dedication has made everything possible.

Acknowledgements

Mrs. Maria Rivera: There are not enough words to describe what you have done for me.

Mr. Roberto Rivera, Mr. Francisco Rivera and Ms. Brenda Rivera: Your love and sacrifice will never be forgotten.

Ms. Lily Abbott: Thank you for helping me close a chapter in my life and helping me start a new one. I love you very much.

Dr. Ryan Littich: I am happy to consider you part of my family, brother.

Mr. Justin Dragna: Hermano, thank you for keeping me sane.

Mr. Dan Propheter: Shee-koo-koo-keek.

Mr. Chris Grant: Thank you for being a good friend and helping me become a better chemist.

Mr. Fernando Pedraza: Your advice hasn't failed me yet. Thanks for everything.

Mr. Alec Brozell: You rank as funniest man in my book.

Mrs. Negar Garizi: Your guidance was invaluable and your friendship irreplaceable.

Mr. David Hardin: You are truly an amazing teacher. Thank you for pushing me to my limits.

Mrs. Jackie Hester: Thank you for being a great teacher and wonderful friend.

Dr. Elizabeth Komives: Thank you for helping me find my path. I will always remember your generosity and kind heart.

Dr. Philip Magnus: Thank you for helping me grow as a scientist and as a person. I doubt I could have asked for a better mentor.

A Direct, Concise and Stereoselective Formal Synthesis of Platensimycin

Publication No._____

Heriberto Rivera Jr., Ph.D.

The University of Texas at Austin, 2011

Supervisor: Philip D. Magnus

Herein we describe the synthesis of (±) platensimycin, a potent antibiotic against gram-positive bacteria. The first chapter reviews (±) platensimycin's isolation, biological profile and previously reported studies relevant to the area. The second chapter describes our initial efforts to synthesize (±) platensimycin. The third chapter accounts our second generation synthesis and its completion. The fourth chapter entails the experimental details of the important compounds in our synthesis.

Table of Contents

List of Abbreviations

Å	angstrom
Ac	acetyl
Atm	atmosphere
bs	broad singlet
BINAP	2,2'-bis(diphenylphosphino)-1,1'-binaphthyl
Brsm	by recovered starting material
Bu	butyl
cat.	Catalytic
m-CPBA	*m*-chloroperoxybenzoic acid
d	doublet
DCE	dichloroethane
DCM	dichloromethane
dd	doublet of doublets
DEAD	diethyl azodicarboxylate
DIBAL-H	diisobutylaluminum hydride
Dioxane	1,4-dioxane
DMAP	4-Dimethylaminopyridine
DME	dimethoxyethane
DMF	dimethylformamide
DMM	dimethoxy methane
DMSO	dimethyl sulfoxide

h	hour
HATU	2-(1H-7-Azabenzotriazol-1-yl)--1,1,3,3-tetramethyl uronium hexafluorophosphate methanaminium
HFIP	hexafluoroisopropanol
HMPA	hexamethylphosphoramide
IC_{50}	half maximal inhibitory concentration
IR	infrared
LAH	lithium aluminum hydride
M	Molar
m	multiplet
MeA	methyl acrylate
min	minutes
MOM	methoxymethyl ether
MsCl	methanesulfonyl chloride
mw	microwave
NBS	*N*-bromosuccinimide
NMR	nuclear magnetic resonance
^{i}Pr	isopropyl
psi	Pounds per square inch
PTC	phase transfer catalyst
TBDMS	tert-butyl dimethylsilyl
TFA	Trifluoroacetic acid

TfOH	Trifluoromethanesulfonic acid
THF	Tetrahydrofuran
Triton B	Benzyltrimethylammonium hydroxide
TMSCl	trimethylsilyl chloride
TLC	thin layer chromatography
Tol	Toluene

Chapter 1: Platensimycin: The New Antibiotic

1.1 Introduction

The increasing number of antibiotic resistant bacteria and lack of new antibiotics, has greatly increased the need for researchers to make new discoveries. In 2006, Merck Laboratories discovered two new natural products with antibacterial properties, platensimycin **1** and platencin **2** (**Figure 1.1.1**).[1] They are produced by *Streptomyoces platensis,* a bacterium discovered in soil samples from South Africa and Spain. It was determined that both platensimycin and platencin function as potent inhibitors in cellular lipid biosynthesis, in a novel mode of action. Furthermore, they displayed great selectivity and low cytotoxic properties.

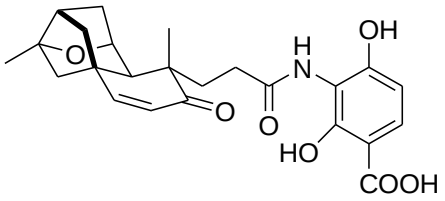

Platensimycin (**1**)

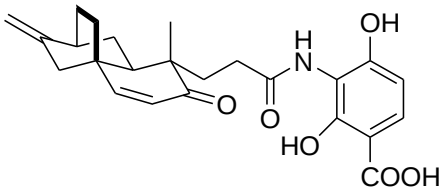

Platencin (**2**)

Figure 1.1.1: Structures of Platensimycin and Platencin

To complement its appealing antibacterial properties and novel mode of action, platensimycin also has a very unusual molecular architecture. It consists of two major fragments, a tetracyclic acid enone core and a 3-amino-2,4 hydroxy benzoic side chain (**Figure 1.1.2**) Although the disconnection at the amide bond is obvious, developing a

strategy for the synthesis of the individual components constitutes a synthetic challenge. Thus, it has been the focus of many synthetic groups over the last 5 years.

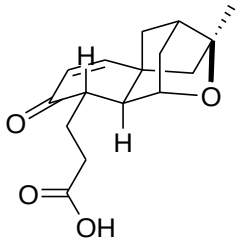

(**A**)

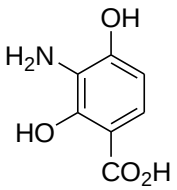

(**B**)

Figure 1.1.2: (A) tetracyclic acid enone core (B) amino benzoic acid side chain

1.2 Isolation and Structural Determination

Platensimycin was discovered by the use of new high throughput screening method developed at Merck.[2] This method employs an antisense differential sensitivity technique. Once it was determined that platensimycin was produced by *Streptomyces platensis*, fermentation was implemented to gain access to greater amounts of the natural product. The resulting broth was purified using a two-step process using Amberchrome and reverse phase HPLC chromatography.

The molecular formula was determined using HRESIFTMS and corroborated using ^{13}CNMR. Various ^{1}HNMR techniques (NOSEY, NOED, HMBS) were used to help determine the molecular structure and relative stereochemistry. Finally, crystallographic analysis of a 6'-bromo platensimycin (**Figure 1.2.1**) allowed for the unambiguous assignment of structure and absolute stereochemistry.[3]

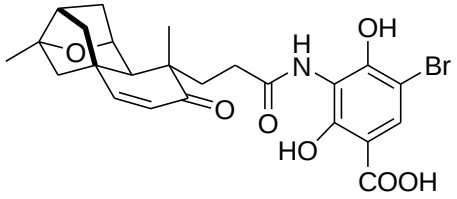

Figure 1.2.1: 6'-bromo platensimycin

1.3 Biological Profile

Discoveries in the realm of antibiotics in the last 50 years have been few and with limited success. Two of these in particular are cerulenin and thiolactomycin which target the FabF enzyme, a target for antibacterial agents for the past 30 years.[4] Fab F is an elongation condensing enzyme, a key component in fatty acid biosynthesis that is highly conserved among many important bacteria. As such, a successful drug designed to specifically bind FabF will make a potent antibiotic and allow it to be used for a wide range of pathogens.

Through high throughput screening techniques and *in vitro* experiments it was determined that platensimycin inhibited *S. aureus* FabF and *Escherichia coli* FabF/B enzymes with IC_{50} values of 48 and 160 nM, respectively. These inhibition concentrations were very promising when compared to IC_{50} values for cerulenin and thiolactomycin which range from 1.5-13 μg/mL. Astonishing results were also obtained for MRSA (Methicillin-resistant *Staphylococcus aureus*) and VRE (Vancomycin-Resistant *Enterococci*) with MIC values of .1-1 μg/mL. Furthermore, whole-cell labeling experiments show that platensimycin specifically bounds to *S. aureus* (without interfering with DNA, RNA, protein, or cell wall biosynthesis) with concentrations up to 500 μg/mL.[1]

Promising results were also obtained in *in vivo* experiments using mice. Mice infected with *S. aureus*, showed in a decrease of 4-5 log reduction of infection after 24 hours with treatment of platensimycin (100 μg ¯h). It is also important to note that no toxicity was observed in this particular case nor was it observed in examples where the mice were treated for elongated periods of time, up to 8 days.[1]

The major drawback of platensimycin is the need for continuous administration in order to be effective. This has spurred a significant interest in the synthesis of platensimycin analogs. To date, none of the analogs have shown improved efficacy upon administration.[5,6]

Platensimycin's potency and selectivity have made it an ideal candidate for more extensive research. Although it suffers from a poor pharmacokinetic profile, it still has the potential to have a major impact in the antibiotic arena. With many promising attributes, platensimycin has become a prime target for scientists.

1.4 Previous Syntheses

With an impressive pharmacological profile and complex molecular structure it is no surprise that platensimycin has been the focus of many synthetic groups, including our own. Since 2006 there have been two total syntheses[7,8], numerous formal syntheses[9,10,11,12,13,14] and formation of platensimycin analogues.[15,16] The proceeding sections will focus on key syntheses. The first will be the initial synthesis by Nicolaou, which has been the foundation for nearly all of the formal syntheses published. This will be succeeded by the work from the Mulzer group, which employs a similar strategy to our own. Lastly, I will briefly address the key reactions in the asymmetric syntheses of platensimycin.

1.4.1 The Nicolaou Synthesis

In 2006 the Nicolaou group published the first total synthesis of platensimycin.[7] They started with commercially available ethoxy enone **3** and performed a sequential alkylation to give compound **4** (**Scheme 1.4.1**). Compound **4** was reduced, hydrolyzed under acidic conditions and the allylic alcohol was re-protected to produce enone **5**. Cylcoisomerization of compound **5** using a ruthenium catalyst gave spirocycle **6**, in a 1:1 distereomeric ratio. They overcame this obstacle in subsequent work. Saegusa oxidation produced dienone **7**, which upon exposure to acid gave aldehyde **8**. Radical cyclization with SmI_2 afforded compound **9** in a 2:1 ratio favoring the desired diastereomer. Even though they were able to obtain the desired isomer as the major product they did so in poor yield (42% total yield). Next, compound **9** underwent an intramolecular cyclization to give compound **10**, the tetracyclic core of platensimycin. It is important to note that this compound is the target for all formal syntheses. Another set of sequential alkylations led to disubstituded enone **12**. Finally, olefin metathesis with Grubbs second generation catalyst and two subsequent oxidations gave carboxylic acid **15.** It was noted by the authors that more direct route could have been achieved using methyl acrylate instead of allyl bromide, but they were unable to obtain any conclusive results. With the first half of the platensimycin synthesized they directed their efforts toward the amino benzoic acid moiety.

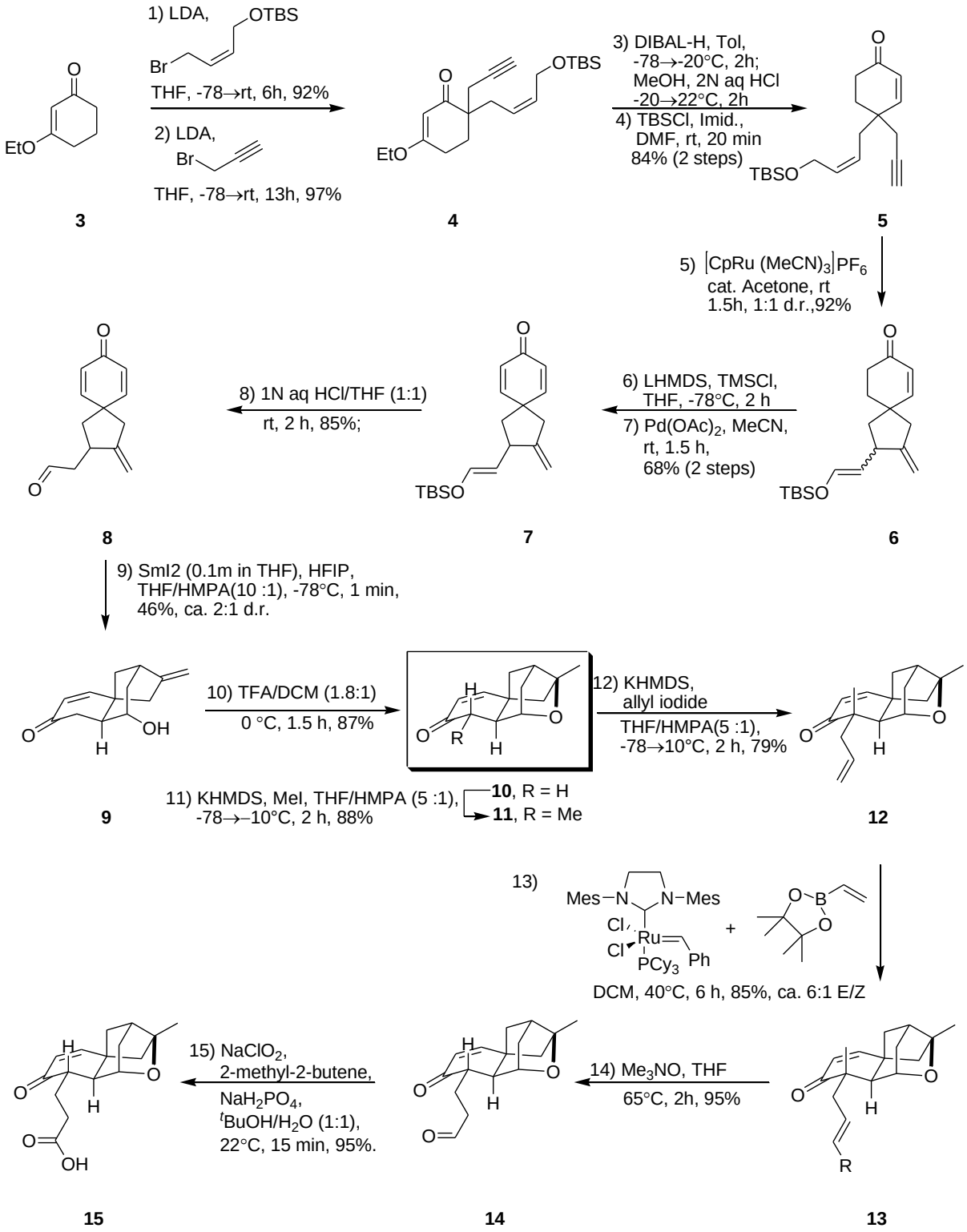

Scheme 1.4.1: Synthesis of the tetracylic acid enone core

The second half of the molecule started with commercially available 2-nitro resorcinol, **16** ($8/g) (**Scheme 1.4.2**). Protection of the hydroxyl groups and subsequent reduction of the nitro group gave aniline **18**. The aniline was protected under standard BOC conditions to afford compound **19**. The protected aniline was then silylated and carbonylated with methyl cyanoformate. Finally, the amine was deprotected by

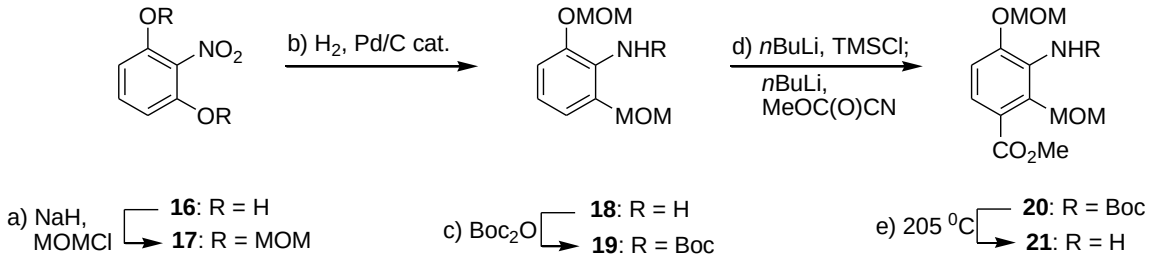

Scheme 1.4.2: Synthesis of the benzoic acid side chain

thermolysis to produce benzoic acid moiety **21**. An improved method for the synthesis of the trisubstituted benzoic acid chain was later developed by the Nicolaou group.

The last sequence of reactions starts with the coupling of the tetracylic acid enone core **15** and compound **21** under standard peptide coupling conditions using HATU (**Scheme 1.4.3**). Hydrolysis of the methyl ester and removal of the MOM groups completed the synthesis of platensimcyin.

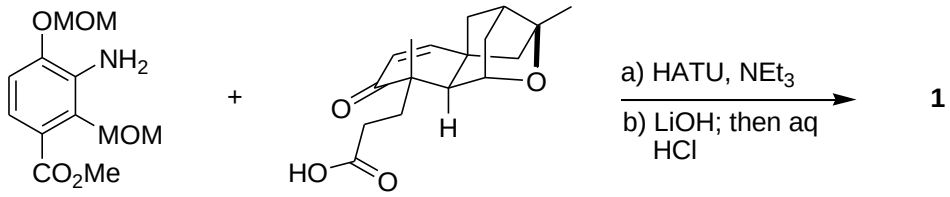

21 **15**

Scheme 1.4.3 Peptide coupling.

The Nicolaou group was able to achieve the synthesis of the tetracylic core in 15 linear steps and the total synthesis of platensimycin in 22 overall steps. Although their strategy suffered from stereochemical issues and low yields in key transformations, they produced the inaugural synthesis of platensimycin which provided the foundation for all succeeding formal syntheses. Furthermore, they were able to complete the synthesis in a short number of steps which still rivals the latest syntheses.

1.4.2 The Mulzer Synthesis

In 2007 the Mulzer group published the formal synthesis of platensimcyin.[17] This was of special importance to us because it directly involved the strategy we had devised, specifically using dienone **25** as a key intermediate. Their synthesis began with tetralone **22**, which is commercially available and relatively inexpensive (**Scheme 1.4.4**). They took tetralone **22** and converted it to carboxylic acid **23** in three steps using previously published procedures. The resulting unsaturated carboxylic acid **23** was reduced using standard hydrogenative conditions to give carboxylic acid **24**. Carboxylic acid **24** was

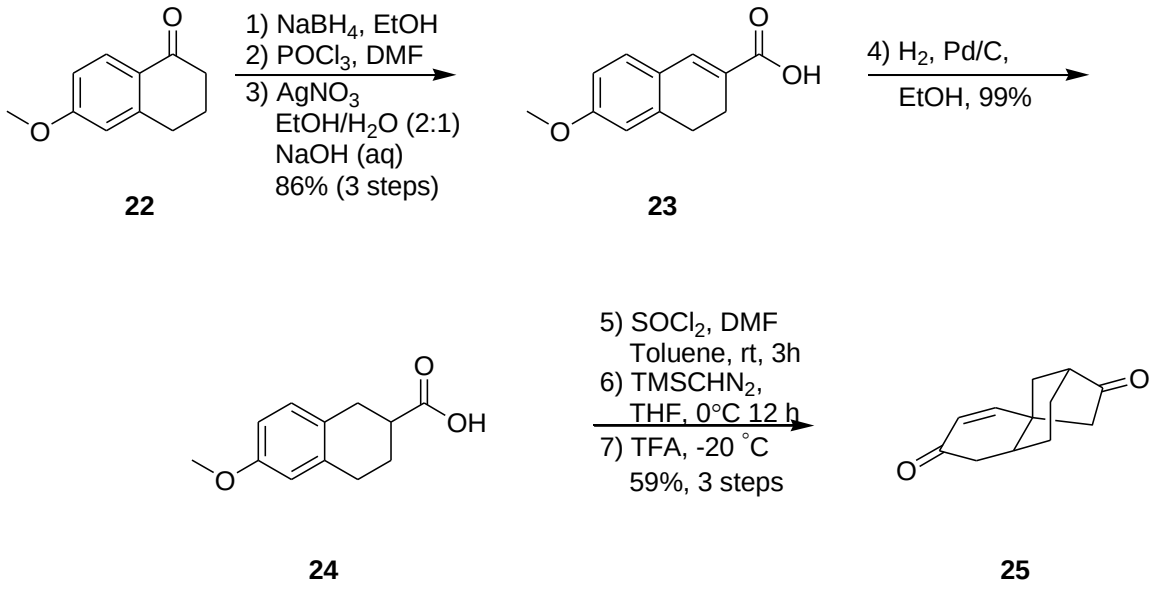

Scheme 1.4.4: Formation of key intermediate **25**

converted to the acyl chloride and treated to TMS-diazomethane to give the beta-hydrazido ketone. Finally, the resulting diazoketone was treated with TFA to give dienone **25** in 59% yield over 3 steps.

Their end game started with a Grignard addition into the saturated ketone **25** to give tertiary alcohol **26** with both regio- and stereoselectivity albeit in low yield. (**Scheme 1.4.5**). Compound **26** was then brominated at the γ-position using NBS. The resulting brominated compound **27** possessed the appropriate stereochemistry for an intramolecular SN_2 displacement.

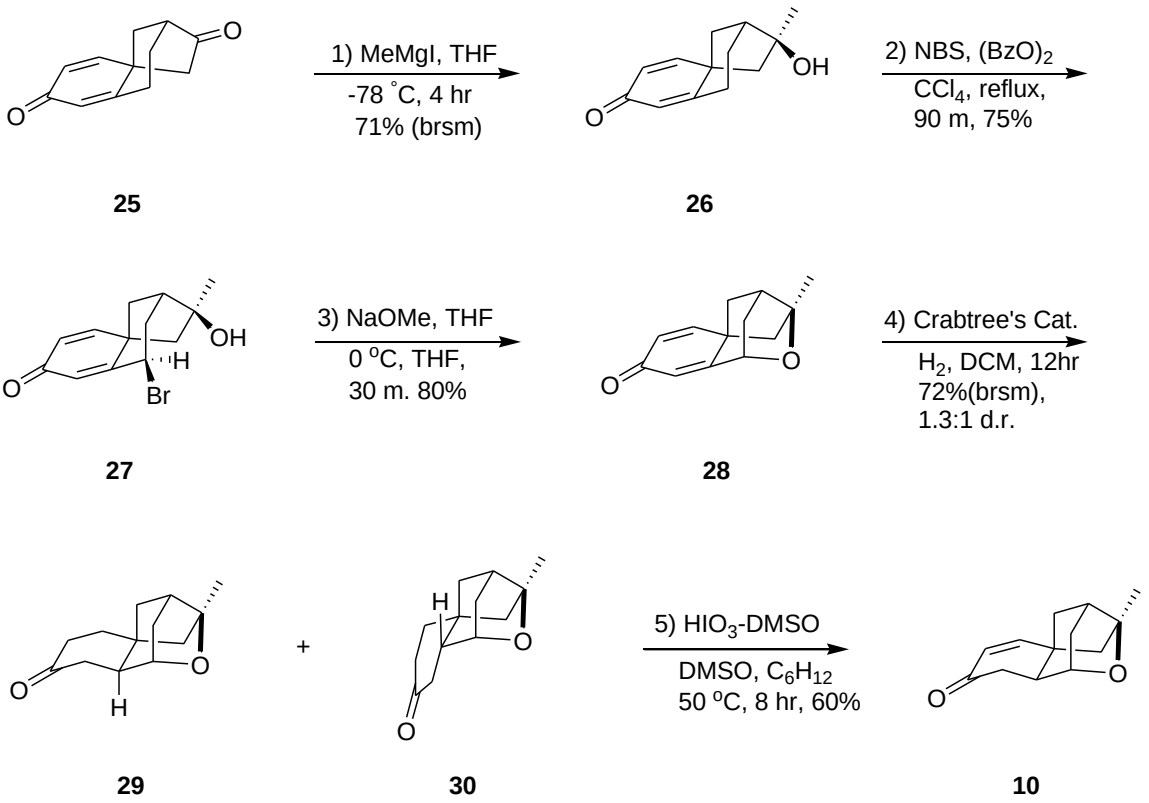

Figure 1.4.5 Completion of the Mulzer Synthesis

Upon treating bromide **27** with NaOMe in THF, the desired ether was formed to give tetracycle **28**. Compound **28** underwent global reduction upon exposure to Crabtree's Catalyst to produce saturated ketones **29** and **30**, giving a 1.3:1 distereomeric ratio. This step suffers from poor stereoseletivity and from a low yield. Furthermore it seems counterproductive to perform a global reduction only to have to reoxidize to the appropriate oxidation level. Finally, taking reduced product **29** and treating it to oxidative conditions gave mono-oxidized product **10** in 60% yield.

The Mulzer group was able complete the formal synthesis of platensimycin in 12 linear steps starting with commercially available materials. They devised a short and direct route to the tetracyclic core of platensimycin and did so in a protecting group free

fashion. Though the synthesis was efficient, it suffered from a few major drawbacks. First, the Grignard addition was low yielding, with an actual yield closer to 25%. The reduction itself also suffered from poor selectivity and low yield. Finally, as previously pointed out, it seems impractical to toggle between oxidation states (conversion of **28** to **10** in **Figure 1.4.5)**.

1.3.3 Asymmetric Syntheses

In this section we will highlight the key steps, in chronological order, of the asymmetric syntheses of (-)-platensimycin. Before we go into detail on work not yet addressed, I will briefly state that both the Mulzer (2010)[18] and Nicolaou (2009)[19,20] groups were able produce enantioselective syntheses. They performed key stereocontrolled reactions in the reduction of the unsaturated acid **23** and the cycloisomerization of compound **5**, respectively.

In 2007 the Yamamoto group published the second asymmetric synthesis of (-)-Platensimycin.[21] Their strategy involved two key transformations in which they were able to enforce the desired stereochemistry (**Scheme 1.4.6**). The first reaction involved an Diels-Alder reaction with methyl acrylate and cylcopentadiene using a Brønsted acid assisted chiral Lewis acid (**34+35**). They obtained cycloadduct **33** in high yield and high enantioselectivity. The second step, coincidently the final step of their synthesis, was a stereoselective intramolecular Michael addition of bicyclic compound **36**. They obtained the desired diastereomer **10** as the major product in good yield (80%).

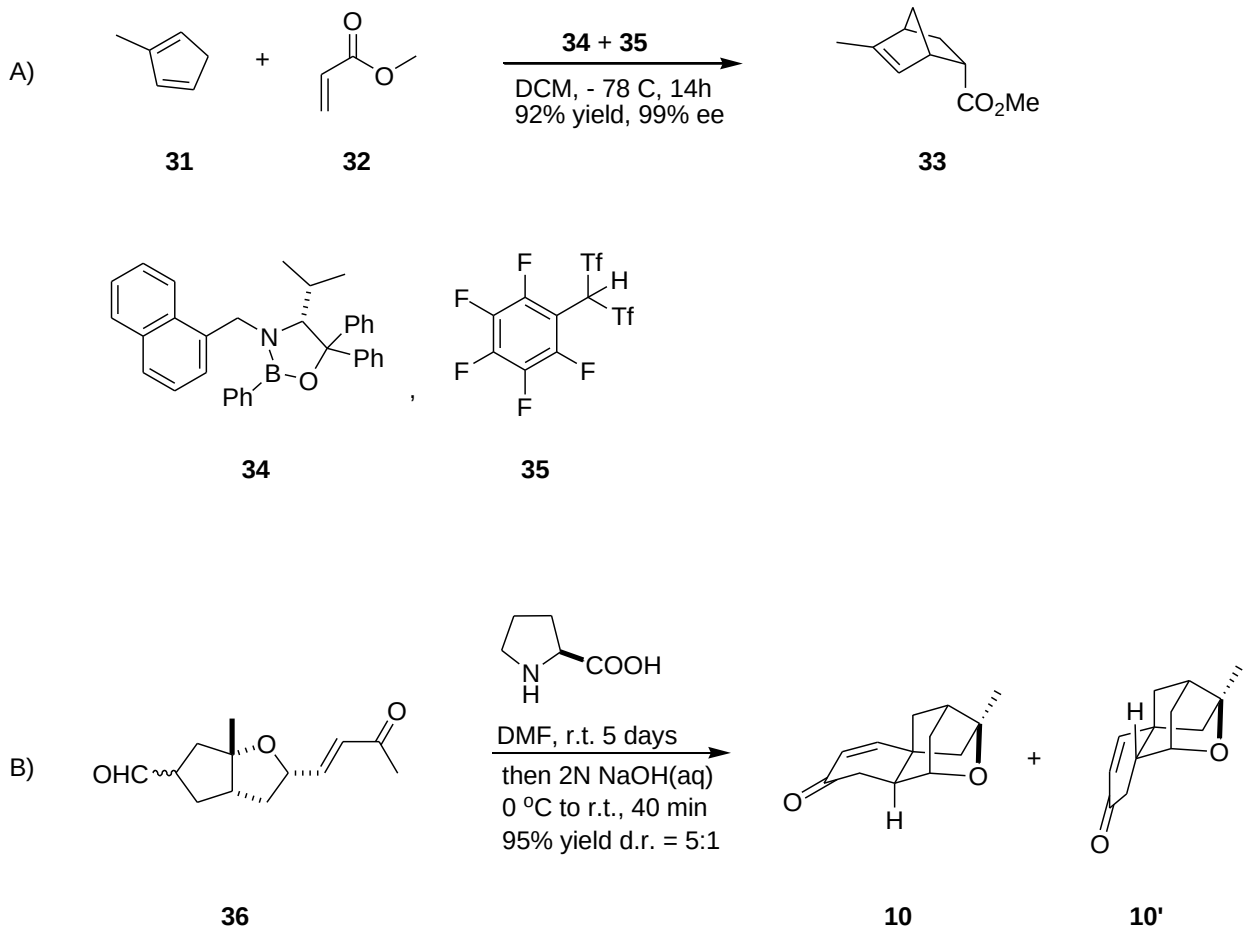

Scheme 1.4.6: (a) Stereoselective Diels-Alder (b) Stereoselective Michael addition

The next body of work was published by the Corey group.[22] The first reaction consists of an enantioselective conjugate addition of a 2-propenyl group into enone **37** using a rhodium catalyst (**Scheme 1.4.7**). The addition product was obtained in high yield and high enantioselectivity. The other step was a high pressure, rhodium catalyzed diastereoselective reduction of dienone **28**, which gave saturated ketone **29** in good yield.

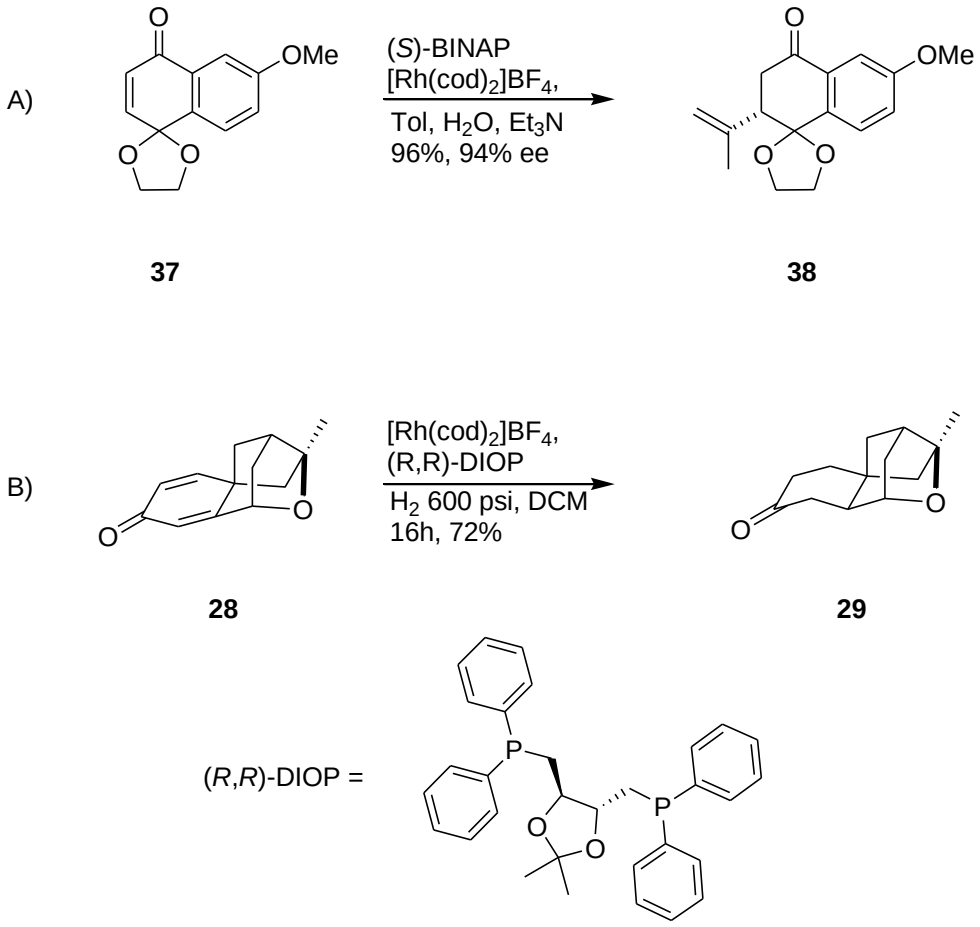

Figure 1.4.7: (A) Enantioselective conjugate addition (B) Diastereoseletive reduction

Matsuo and coworkers also took advantage of a stereoselective Diels-Alder reaction (**Scheme 1.4.8**).[23] They treated diene **40** with enone **39** to give bicyclic compounds **41** and **42** in 83% yield with 11:1 ratio in favor of the desired product.

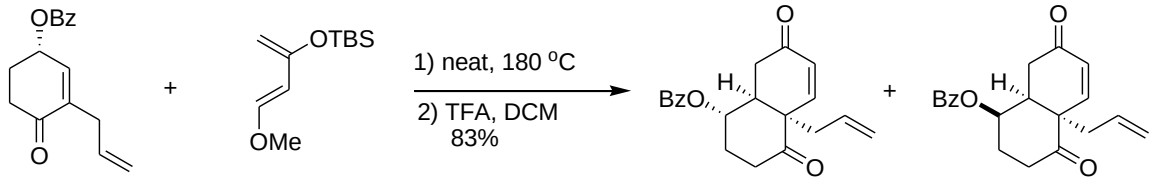

39 **40** **41** **42**

(11:1)

Scheme 1.4.8: Matsuo's diastereoselective Diels-Alder reaction

Two years later the Lear[24] group and Canesi[25] groups published asymmetric syntheses. The Lear group utilized an organocatalyst in a diastereoselective reduction. They took dienone **43** and treated it to *tert*-butyl D-phenylalanine then exposed it to sequential Hantzsch and Pd/C based reductions to produce ketones **29** and **30** (**Scheme 1.4.9**). Although they were able to isolate compounds **10** and **44**, they observed large of amounts of degradation upon purification, so the crude was directly submitted to the second reduction.

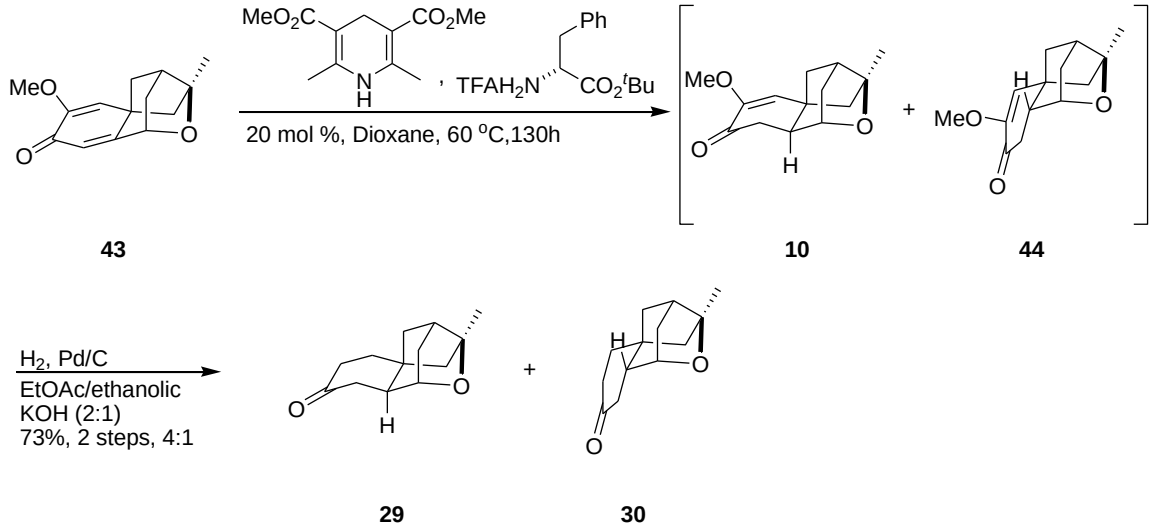

43 **10** **44**

29 **30**

Scheme 1.4.9: Sequential reductions to afford compound 30 enantioselectively

The Canesi group utilized a stereoselective oxidative Prins-Pinacol tandem process to transform compound **45** to spirocycle **46** in 64% yield over 2 steps (**Scheme 1.4.10**). This spirocycle is similar to intermediate **6** in the Nicolaou synthesis and the succeeding transformations mirror closely what was done in the Nicolaou synthesis to obtain enone **10**.

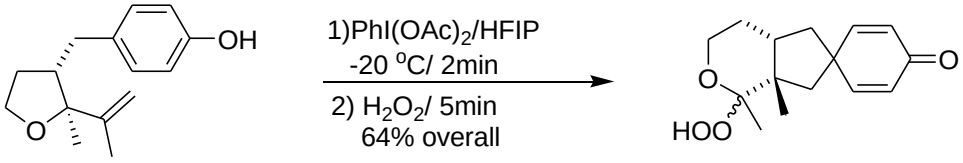

45 **46**

Scheme 1.4.10: Formation of spirocycle **46**

The latest asymmetric synthesis was published by the Nakada group which centered on an enantioselective catalytic asymmetric intramolecular cyclopropanation.[26] They synthesized α-diazosulfone **47** and subjected it to a chiral copper catalyst to produce cyclopropyl compound **48** in 72% yield (**Scheme 1.4.11**). This compound was elaborated to an intermediate in the Snider synthesis and eventually transformed to enone **10**.

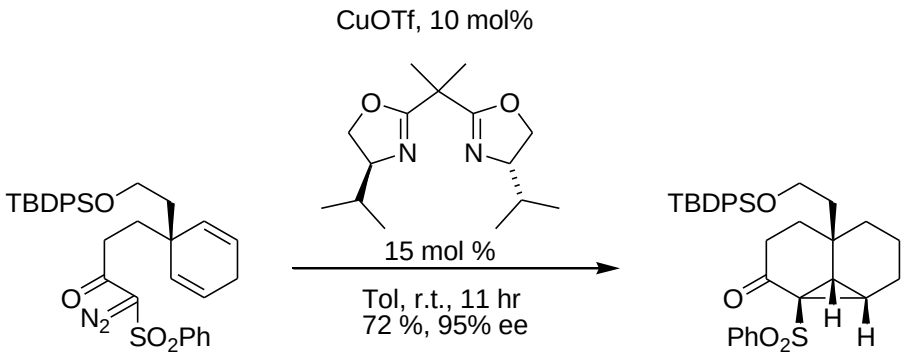

47 **48**

Scheme 1.4.11 Enantioselective formation of cyclopropane **48**

Although these formal syntheses allowed for the asymmetric synthesis of (-)-platensimycin, they had many shortcomings. Devising an asymmetric strategy required many of these groups to add several steps, accept low yields and in some cases report comparable stereoselectivities. To date the Nicolaou asymmetric synthesis offers the best example of an asymmetric synthesis.

1.5 Conclusions

Platensimycin's potency, selectivity and molecular complexity have made it an appealing target for synthetic chemists. Though a multitude of syntheses had been published, we believed a more concise and direct route could be developed. In the following chapters we will describe our synthetic strategy of the platensimycin core.

1.5 References

(1) Wang, J. Soisson, S. M. Young, K. Shoop, W. Kodali, S. Galgoci, A. Painter, R. Parthasarathy, G. Tang, Y. S. Cummings, R. Ha, S. Dorso, K. Motyl, M. Jayasuriya, H. Ondeyka, J. Herath, K. Zhang, C. Hernandez, L. Allocco, J. Basilio, Á. Tormo, J. R. Genilloud, O. Vicente, F. Pelaez, F. Colwell, L. Lee, S. H. Michael, B. Felcetto, T. Gill, C. Silver, L. L. Hermes, J. D. Bartizal, K. Barrett, J. Schmatz, D. Becker, J. W. Cully, D.; Singh, S. B. Platensimycin is a selective FabF inhibitor with potent antibiotic properties. *Nature* **2006**, *441*, 358-361.

(2) Young, K. Jayasuriya, H. Ondeyka, J. G. Herath, K. Zhang, C. Kodali, S. Galgoci, A. Painter, R. Brown-Driver, V. Yamamoto, R. Silver, L. L. Zheng, Y. Ventura, J. I. Sigmund, J. Ha, S. Basilio, A. Vicente, F. Tormo, J. R. Pelaez, F. Youngman, P. Cully, D. Barrett, J. F. Schmatz, D. Singh, S. B.; Wang, J. Discovery of FabH/FabF Inhibitors from Natural Products. *Antimicrob. Agents Chemother.* **2006**, *50*, 519-526.

(3) Singh, S. B. Jayasuriya, H. Ondeyka, J. G. Herath, K. B. Zhang, C. Zink, D. L. Tsou, N. N. Ball, R. G. Basilio, A. Genilloud, O. Diez, M. T. Vicente, F. Pelaez, F. Young, K.; Wang, J. Isolation, Structure, and Absolute Stereochemistry of Platensimycin, A Broad Spectrum Antibiotic Discovered Using an Antisense Differential Sensitivity Strategy. *Journal of the American Chemical Society* **2006**, *128*, 11916-11920.

(4) Wright, H. T.; Reynolds, K. A. Antibacterial targets in fatty acid biosynthesis. *Current Opinion in Microbiology* **2007**, *10*, 447-453.

(5) Shen, H. C. Ding, F.-X. Singh, S. B. Parthasarathy, G. Soisson, S. M. Ha, S. N. Chen, X. Kodali, S. Wang, J. Dorso, K. Tata, J. R. Hammond, M. L. MacCoss, M.; Colletti, S. L. Synthesis and biological evaluation of platensimycin analogs. *Bioorganic & Medicinal Chemistry Letters* **2009**, *19*, 1623-1627.

(6) Singh, S. B. Herath, K. B. Wang, J. Tsou, N.; Ball, R. G. Chemistry of platensimycin. *Tetrahedron Letters* **2007**, *48*, 5429-5433.

(7) Nicolaou, K. C. Li, A.; Edmonds, D. J. Total Synthesis of Platensimycin. *Angewandte Chemie International Edition* **2006**, *45*, 7086-7090.

(8) Ghosh, A. K.; Xi, K. Total Synthesis of (−)-Platensimycin, a Novel Antibacterial Agent. *The Journal of Organic Chemistry* **2009**, *74*, 1163-1170.

(9) Xing, S. Pan, W. Liu, C. Ren, J.; Wang, Z. Efficient Construction of Oxa- and Aza-[n.2.1] Skeletons: Lewis Acid Catalyzed Intramolecular [3+2] Cycloaddition of Cyclopropane 1,1-Diesters with Carbonyls and Imines. *Angewandte Chemie International Edition* **2010**, *49*, 3215-3218.

(10) Zou, Y. Chen, C.-H. Taylor, C. D. Foxman, B. M.; Snider, B. B. Formal Synthesis of (±)-Platensimycin. *Organic Letters* **2007**, *9*, 1825-1828.

(11) Oblak, E. Z.; Wright, D. L. Highly Substituted Oxabicyclic Derivatives from Furan: Synthesis of (±)-Platensimycin. *Organic Letters* **2011**, *13*, 2263-2265.

(12) McGrath, N. A. Bartlett, E. S. Sittihan, S.; Njardarson, J. T. A Concise Ring-Expansion Route to the Compact Core of Platensimycin. *Angewandte Chemie International Edition* **2009**, *48*, 8543-8546.

(13) Kaliappan, K. P.; Ravikumar, V. An Expedient Enantioselective Strategy for the Oxatetracyclic Core of Platensimycin. *Organic Letters* **2007**, *9*, 2417-2419.

(14) Nicolaou, K. C. Tang, Y.; Wang, J. Formal synthesis of (+/-)-platensimycin. *Chem. Commun.* **2007**, 1922-1923.

(15) Yeung, Y.-Y.; Corey, E. J. A Simple, Efficient, and Enantiocontrolled Synthesis of a Near-Structural Mimic of Platensimycin. *Organic Letters* **2008**, *10*, 3877-3878.

(16) Nicolaou, K. C. Stepan, A. F. Lister, T. Li, A. Montero, A. Tria, G. S. Turner, C. I. Tang, Y. Wang, J. Denton, R. M.; Edmonds, D. J. Design, Synthesis, and Biological Evaluation of Platensimycin Analogues with Varying Degrees of Molecular Complexity. *Journal of the American Chemical Society* **2008**, *130*, 13110-13119.

(17) Tiefenbacher, K.; Mulzer, J. Protecting-Group-Free Formal Synthesis of Platensimycin. *Angewandte Chemie International Edition* **2007**, *46*, 8074-8075.

(18) Tiefenbacher, K. Trendlin, L. Mulzer, J.; Pfaltz, A. An expeditious asymmetric formal synthesis of the antibiotic platensimycin. *Tetrahedron* **2010**, *66*, 6508-6513.

(19) Nicolaou, K. C. Li, A. Ellery, S. P.; Edmonds, D. J. Rhodium-Catalyzed Asymmetric Enyne Cycloisomerization of Terminal Alkynes and Formal Total Synthesis of (−)-Platensimycin. *Angewandte Chemie International Edition* **2009**, *48*, 6293-6295.

(20) Nicolaou, K. C. Pappo, D. Tsang, K. Y. Gibe, R.; Chen, D. Y.-K. A Chiral Pool Based Synthesis of Platensimycin. *Angewandte Chemie International Edition* **2008**, *47*, 944-946.

(21) Li, P. Payette, J. N.; Yamamoto, H. Enantioselective Route to Platensimycin: An Intramolecular Robinson Annulation Approach. *Journal of the American Chemical Society* **2007**, *129*, 9534-9535.

(22) Lalic, G.; Corey, E. J. An Effective Enantioselective Route to the Platensimycin Core. *Organic Letters* **2007**, *9*, 4921-4923.

(23) Matsuo, J.-ichi; Takeuchi, K.; Ishibashi, H. Stereocontrolled Formal Synthesis of (±)-Platensimycin. *Organic Letters* **2008**, *10*, 4049-4052.

(24) Eey, S. T.-C.; Lear, M. J. A Bismuth(III)-Catalyzed Friedel−Crafts Cyclization and Stereocontrolled Organocatalytic Approach to (−)-Platensimycin. *Organic Letters* **2010**, *12*, 5510-5513.

(25) Beaulieu, M.-A. Sabot, C. Achache, N. Guérard, K. C.; Canesi, S. An Oxidative Prins–Pinacol Tandem Process and its Application to the synthesis of (−)-Platensimycin. *Chem. Eur. J.* **2010**, *16*, 11224-11228.

(26) Hirai, S.; Nakada, M. Enantioselective divergent approaches to both (-)-platensimycin and (-)-platencin. *Tetrahedron* **2011**, *67*, 518-530.

Chapter 2: First Generation Synthesis

2.1 Introduction

Platensimycin is a potent antibiotic against gram-positive bacteria that was discovered in 2006 by Merck. Complementing its impressive biological profile is its molecular complexity. The unusual structural motif of platensimycin has aroused significant attention from the synthetic community. Although many syntheses have been published we felt that we could produce a more precise and stereospecific synthesis.

2.2 Synthetic Approach

We devised a strategy beginning with 6-methoxy-1-tetralone **22.** Tetralone **22** was chosen because it is both commercially available and inexpensive. Tetralone **22** is elaborated to carboxylic acid **24**. Carboxylic acid **24** is converted to dienone **25**, a compound that has been previously produced in gram scale.

The next phase of the synthesis begins with a Grignard addition into dienone **25** to give tertiary alcohol **26**. Dienone **26** is converted to dialkylated compound **49**, providing the appropriate oxidation level at the enone. Hydroboration and cyclization of compound **49** gives cyclic ether **50**. Hydrolysis of compound **50** would afford carboxylic acid **15**, thereby completing the formal synthesis. Successful execution of this route would provide the shortest route to the platensimycin core.

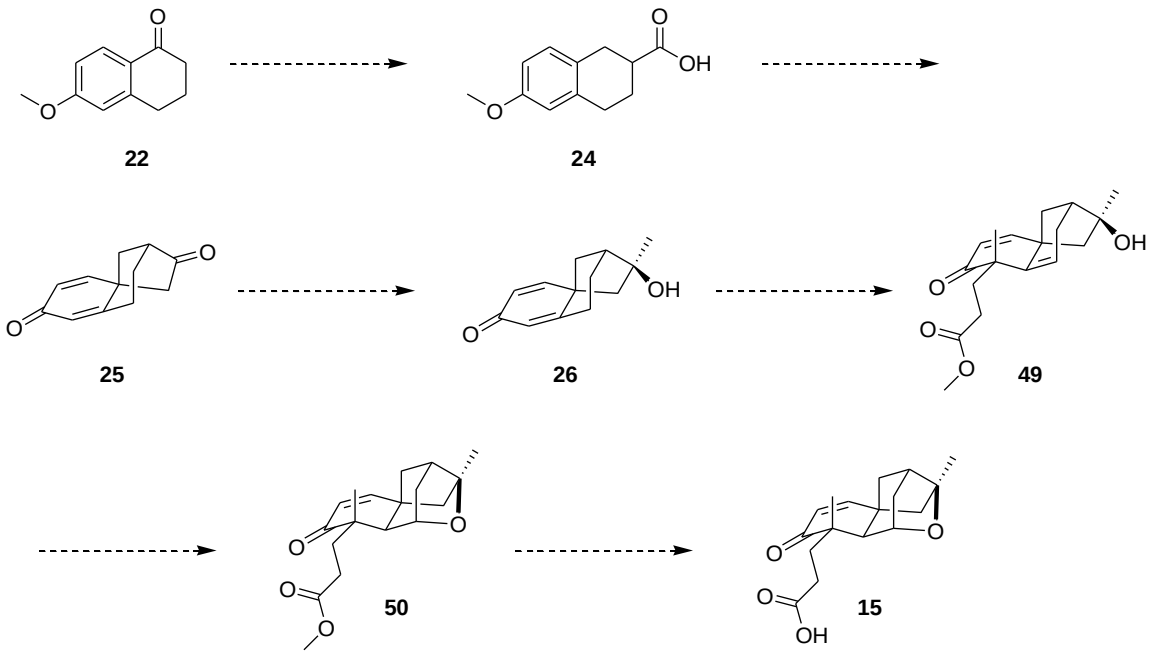

Scheme 2.2.1: Synthetic Approach

2.3 Background for the Dienone 25

In the early 1970's Mander published a series of papers displaying the synthesis of various intermediates directed toward the formation of tetracylic diterpenes.[1,2,3,4] The structure that caught our attention was dienone **25** (**Figure 2.3.1**). It piqued our interest for various reasons. First, it contained all but one carbon in the carbocyclic framework of

25 **10**

Figure 2.3.1: Mander's Dienone **25** and Nicolaou's Enone **10**

enone **10**. Mander went on to show that compound **25** reacts stereoselectively upon treatment with sodium borohydride (**Figure 2.3.2**). These results lead us to believe that compound **25** treated with methyl Grignard could produce compound **10** on gram scale.

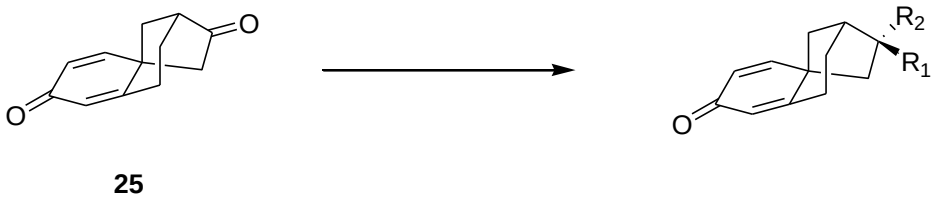

25

	R_1	R_2
51	OH	H
52	H	OH
53	$-OCH_2CH_2O-$	

Figure 2.3.2: Examples of regioselectivity

2.4 Synthesis of Dienone 25

The synthesis of enone **25** began with the acylation of 6-methoxy-1-tetralone **22**.[5] Tetralone **22** was added to a mixture of dimethyl carbonate and NaH and heated to provide α,β-ketoester **54** (**Scheme 2.2**). α,β-ketoester **54** was directly reduced to methyl ester **55**.[6] The methyl ester was hydrolyzed to provide carboxylic acid **24** as an off white solid. Carboxylic acid **24** was produced in 84% yield over 3 steps and with a single purification. It is worthwhile noting that both the R- and S-enantiomers of acid **24** are available from the microbial reduction of 1-tetralone-2-carboxy ethyl esters.[7] Hence, it is possible to execute this route asymmetrically.

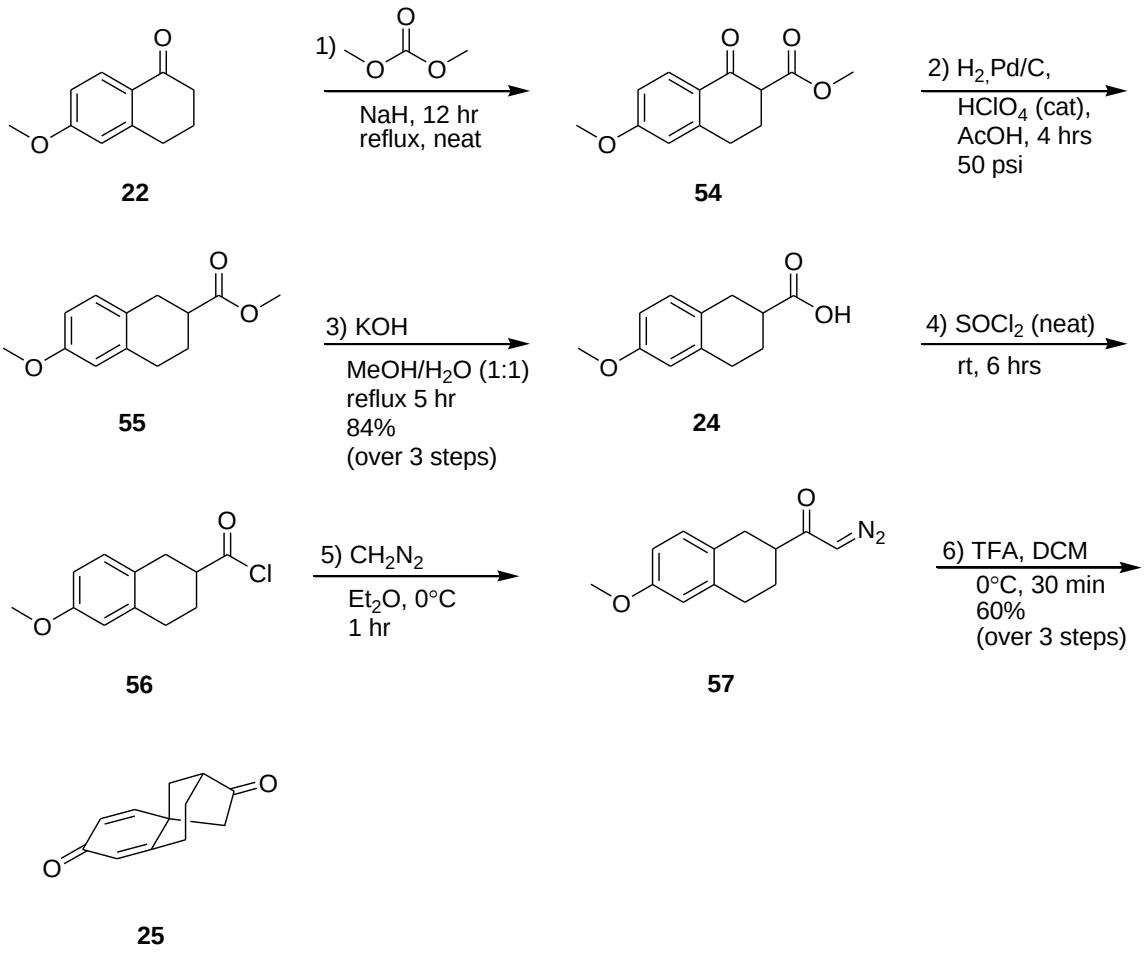

Scheme 2.4.1: Synthesis of dienone **25**

Carboxylic acid **24** was converted to acyl chloride **56** upon treatment with thionyl chloride. Acyl chloride **56** was treated with freshly prepared diazomethane to give α-diazoketone **57**. The resulting mixture was exposed to TFA to give key intermediate **25**. Dienone **25** was obtained in 61% yield over three steps and with a single purification.

We were able to obtain dienone **25** in 6 steps, 1 less step than the Mulzer group, and in gram quantities. We were now situated to perform the Grignard addition.

2.5 Grignard Addition

As we were approaching this step in our synthesis, the Muzler work was published. Although they were fruitful in producing the tertiary alcohol **26**, it was reported as an ambiguous 71% yield (brsm = by recovered starting material, **Scheme 2.5.1**). It was no surprise that when Mulzer's conditions were used a paltry yield of 26% was obtained (**Scheme 2.5.1**). Thus, we set our efforts to improve this transformation.

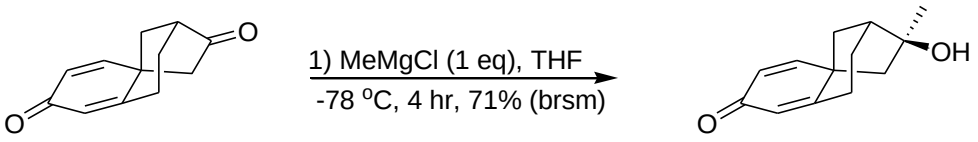

25 **26**

Scheme 2.5.1: Mulzer's conversion of dienone **25** to tertiary alcohol **26**

We began exploring this transformation by choosing Grignard reagents with different halogen counteranions (**Table 2.5.1**). The differences between MeMgI, MeMgBr, and MeMgCl were minimal (Entry A-C). For quality purposes fresh solutions of MeMgBr and MeMgI were prepared but offered no advantage over the commercially available reagents (Entry D-E). The reactions performed with different solvents yielded unreacted starting material (Entry F-K). This was possibly due solubility issues. The reactions were normally run at 0.3 M because it was determined this was the optimal reaction concentration (Entry A-C). However, using dimethyl ether or dimethoxy methane (DMM) required the reaction to be diluted to .03 M. We believe this huge decrease in reaction concentration was responsible for our results. Finally, varying the reaction temperature had little impact on the yield (Entry L). Having exhausted the

possible avenues utilizing different Grignard reagents we decided to test other methyl nucleophilic sources.

Entry	Grignard (1eq)	Temp (°C)	Solvent	Time (h)	Yield (%)
A	MeMgI	-78	THF	4	25
B	MeMgBr	-78	THF	4	24
C	MeMgCl	-78	THF	4	28
D	MeMgI	-78	THF	4	23
E	MeMgBr	-78	THF	4	22
F	MeMgI	-78	Et_2O	4	sm
G	MeMgBr	-78	Et_2O	4	sm
H	MeMgCl	-78	Et_2O	4	sm
I	MeMgI	-78	DMM	4	sm
J	MeMgBr	-78	DMM	4	sm
K	MeMgCl	-78	DMM	4	sm
L	MeMgI	-78 to rt	THF	4	25

Table 2.5.1: Grignard Addition

The reaction conditions from the Grignard addition were maintained with the exception of the nucleophile source (**Table 2.5.2**). Using MeLi gave a 13% yield (Entry A). All other reagents failed to produce any positive results (Entry B-E).[8,9] When the reactions were run at 0 ºC and allowed to warm to ambient temperature, only $TiCl_3Me$ managed to give any of the desired product albeit in low yield (Entry F-H).[10,11] Although this was a low yield, further reactions were performed using $TiCl_3Me$. When the reaction was run at higher temperatures or with an excess of the reagent, a multitude of unidentifiable compounds were obtained (Entry I,K). Changing the solvent resulted in recovered starting material (Entry J).

Entry	Reagent (1 eq)	Temp (°C)	Solvent	Time (h)	Yield (%)
A	MeLi	-78	THF	4	13
B	$(CH_3)_2CuLi$	-78	THF	4	sm
C	$TiCl_3Me$	-78	THF	4	sm
D	$Al(CH_3)_3$	-78	DCM	4	0
E	$CH_2(MgBr)_2$	-78	THF	4	0
F	MeLi	0-rt	THF	4	sm
G	$TiCl_3Me$	0-rt	THF	4	5
H	$(CH_3)_2CuLi$	0-rt	THF	4	sm
I	$TiCl_3Me$	rt-50C	THF	4	0
J	$TiCl_3Me$	0-rt	DCM	4	sm
K	$TiCl_3Me$ (3 eq)	0-rt	THF	4	0

Table 2.5.2: Use of different methylating sources

One thing that had caught our attention was that the experiments run with MeLi (**Table 2.5.2** Entry A,E). We were partially surprised to have not obtained the desired product at 0 °C. This led us to believe that a competition was occurring between the reagent acting as base instead of nucleophile. We devised a quick and easy experiment where dienone **25** was treated to previous conditions except that the reaction was quenched with D_2O instead of H_2O (**Scheme 2.5.2**). Deuterated compound **57** was isolated and the ^1H NMR indicated the incorporation of deuterium by the disappearance of the indicated proton. These results strongly suggested it was an issue of enolization versus addition.

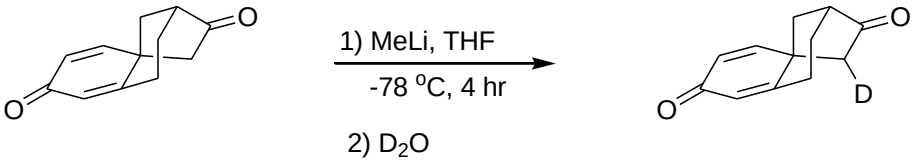

25 **57**

Scheme 2.5.2: Deuterium exchange experiment

The issue of enolization versus addition is not without precedent. It has been shown that using $CeCl_3$ helps to deter the path of enolization and favor Grignard addition.[12] Although, how it actually impedes enolization is not completely understood. Reaching this conclusion, the experiments using Grignard reagents were re-run in the presence of $CeCl_3$ (**Table 2.5.3**). These reactions were run with 1 equivalent of $CeCl_3$ and at a 0.08 mM concentration. Running the reaction under previous conditions produced poor results. Increasing the reaction temperature had little to no effect with about 50% decrease in yield (Entry A-C). Preparing our own Grignard reagent gave similar results (Entry D). Increasing the reaction temperature had little to no effect (Entry F-H). In the instances where MeLi was used, only starting material was recovered

Entry	Grignard (1eq)	Temp (^{O}C)	Solvent	Time (h)	Yield (%)
A	MeMgI	-78	THF	4	15
B	MeMgBr	-78	THF	4	12
C	MeMgCl	-78	THF	4	15
D	MeMgI	-78	THF	4	14
E	MeLi	-78	THF	4	sm
F	MeMgI	-78-rt	THF	4	13
G	MeMgBr	-78-rt	THF	4	11
H	MeMgCl	-78-rt	THF	4	14
I	MeLi	-78-rt	THF	4	sm

Table 2.5.3: Grignard addition in the presence of $CeCl_3$

(E, I). We had reached major roadblock and had to seriously consider continuing this feat or accept the yields obtained from Mulzer's work.

We came up with one final idea before retreating; we would simply increase the equivalents of the Grignard reagent (**Table 2.5.4**). As the equivalents of MeMgCl were increased, the yield increased as well (Entry A-C). Eventually it was determined that best yield was obtained using 3 eq of MeMgCl (Entry C). A 61 % isolated yield of tertiary alcohol **26** represents almost a 250% increase in yield from the Muzler procedure (**Table 2.5.4**).

Entry	Grignard	Eq	Temp (°C)	solvent	Time (h)	Yield (%)
A	MeMgCl	1	-78	THF	4	28
B	MeMgCl	2	-78	THF	4	46
C	MeMgCl	3	-78	THF	4	61
D	MeMgCl	4	-78	THF	4	57
E	MeMgCl	5	-78	THF	4	55

Table 2.5.4: Increasing the amount of MeMgCl

These experiments were repeated with other Grignard reagents and MeLi but gave inferior results. Varying temperature and reaction times also failed to provide further improvement.

Ultimately, dienone **25** dissolved it in THF and MeMgCl (3 eq.) was added to give tertiary alcohol **26** in 60% yield (**Scheme 2.5.3**).

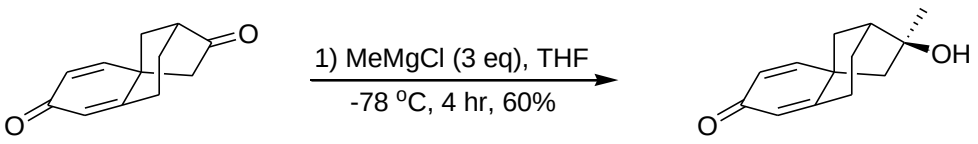

25 **26**

Scheme 2.5.3: New found conditions for the formation of tertiary alcohol **26**

2.6 Alkylation

Now that the Grignard addition had been adequately solved, we continued with the subsequent sequence of alkylations. Dienone **26** was submitted to standard alkylating conditions to give α-methyl dienone **58** in good yield and without any trace of the germinal dimethylation product (**Scheme 2.6.1**).[13]

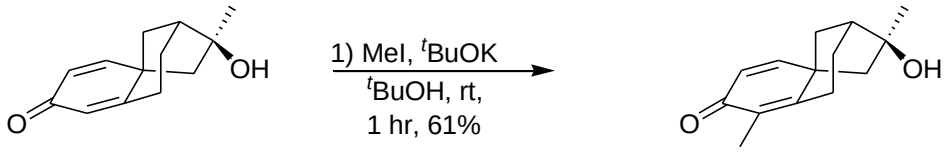

26 **58**

Scheme 2.6.1: Methylation of dienone **26**

The succeeding alkylation with methyl acrylate (MeA) was performed under similar conditions as the methyl addition but was unfruitful (**Table 2.6.**1, Entry A).[14] Varying the conditions provided similar results. Increasing the equivalents of methyl acrylate or ^{t}BuOK resulted in recovered starting material (Entry B-D). Increasing the temperature from ambient temperature to 60 ºC resulted in a mixture of unidentifiable compounds (Entry E). Utilizing triton-B, previously shown to affect the desired transformation, resulted in recovered starting material (Entry F).[15] Similar experiments

were implemented using ethyl bromoacetate in lieu of methyl acrylate, but these conditions also failed to provide any positive results.

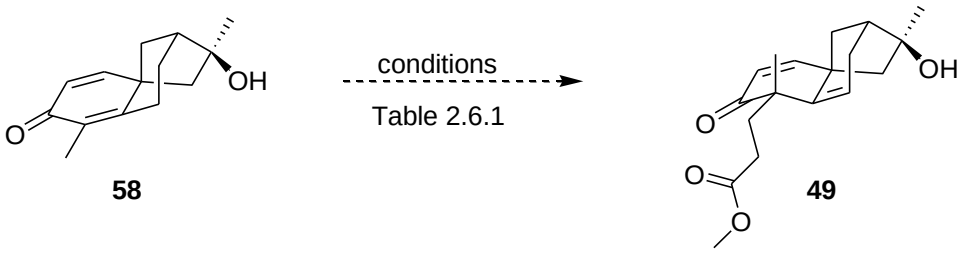

58 **49**

Scheme 2.6.2: Attempted alkylation of dienone **58**

Entry	Base	Base eq	Methyl Acrylate (eq)	Solvent	Temp (°C)	Time (h)	Yield (%)
A	^{t}BuOK	2.2	1	^{t}BuOH	rt	6	sm
B	^{t}BuOK	2.2	2	^{t}BuOH	rt	6	sm
C	^{t}BuOK	2.2	5	^{t}BuOH	rt	6	sm
D	^{t}BuOK	4	1	^{t}BuOH	rt	6	sm
E	^{t}BuOK	2.2	1	^{t}BuOH	rt-60	3	0
F	K_2CO_3/ Triton B (cat)	2.2	1	DCE	rt-reflux	12	sm

Table 2.6.1: Conditions for methyl acrylate alkylation of **58**

It was evident that the formation of the quaternary center was not going to be as straight forward as imagined. We believed that we might affect this transformation by simply reversing the order of alkylation. Dieneone **26** was treated to alkylating conditions but this proved to be an unfruitful endeavor (**Table 2.6.2**). Varying the amount of methyl acrylate had no effect (Entry A-C). When the reaction was heated, an inextricable mixture was obtained (Entry D). Lack of success led us to abandon the use methyl acrylate and seek a suitable alternative.

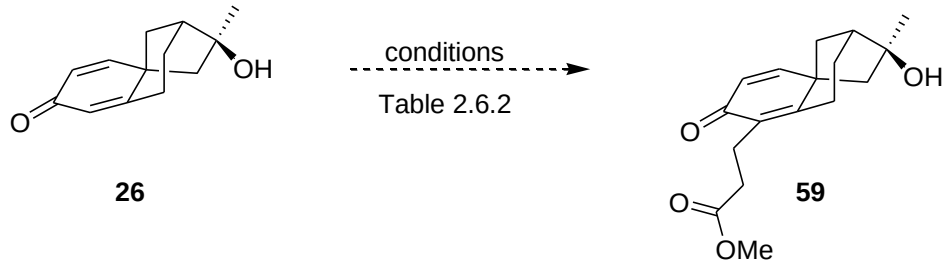

26 **59**

Scheme 2.6.3: Attempted alkylation with methyl acrylate

Entry	Base	MeA (eq)	Solvent	Temp (°C)	Time (h)	Yield (%)
A	^{t}BuOK	1	^{t}BuOH	rt	6	sm
B	^{t}BuOK	2	^{t}BuOH	rt	6	sm
C	^{t}BuOK	5	^{t}BuOH	rt	6	sm
D	^{t}BuOK	1	^{t}BuOH	60	6	0

Table 2.6.2: Conditions for alkylation of dienone **26** with methyl acrylate

We decided to pursue an alkylation with allyl bromide. Since the Nicolaou group already had success with allyl bromide as an alkylating agent, we saw this as a viable option. Although this would provide an earlier intermediate in the Nicolaou synthesis than originally planned, successful execution would still provide a short and concise formal synthesis.

Following the previous rationale, dienone **26** was alkylated with allyl bromide to give α-allyl dienone **60** in 67% yield (**Scheme 2.6.4**). The second alkylation with MeI was attempted but without success. The reaction was monitored *via* TLC and quenched upon consumption of the starting material. Following purification only dienone **26** was recovered. Initially this was a bit confusing. The reaction was repeated additional times, taking greater care in the way the product was isolated but continued to give similar

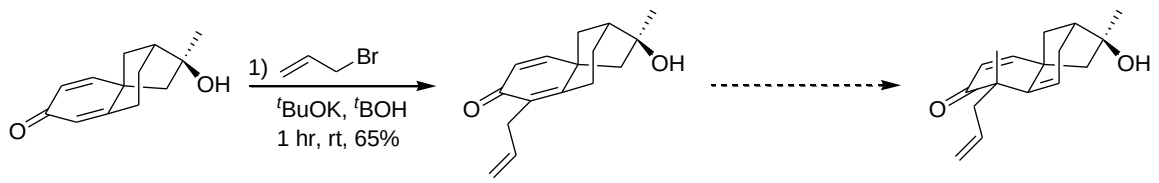

26 **60** **61**

Scheme 2.6.4: Allylation and subsequent alkylation of dienone **26**

results. We postulated that a competition between *O* and *C*-alkylation was occurring, with *O*-alkylation dominating the reaction. We proceeded to reverse the sequence of alkylation believing that if *O*-alkylation was indeed impeding the formation of the quaternary center we could force a Claisen rearrangement to give us the desired product (**Scheme 2.6.5**).

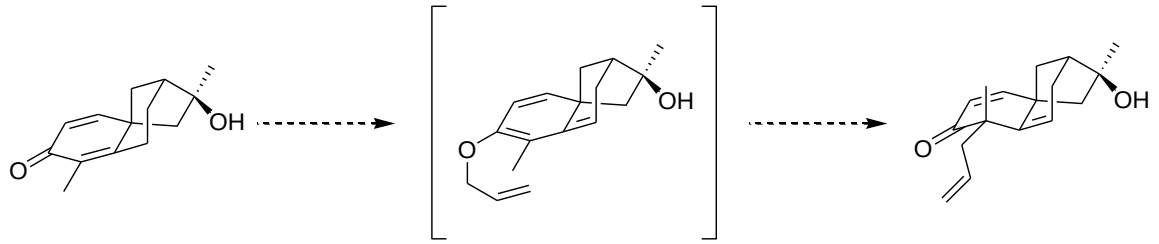

58 **62** **61**

Scheme 2.6.5: Proposed Claisen rearrangement

On a side note, the alkylation of dienone **26** with methyl acrylate was revisited. This was in response to work published by the Corey group of a platensimycin analog.[16] They reported the alkylation of enone **63** with methyl acrylate in good yield (**Scheme 2.6.6**). However, when this alkylation was attempted using their method none of the

desired product was obtained. Minor modifications were made to the procedure but all attempts failed to show any promise. This idea was quickly abandoned.

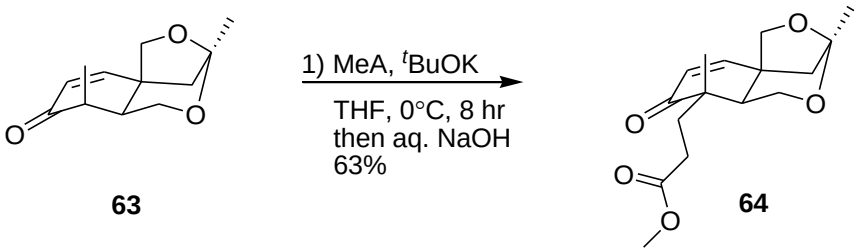

Scheme 2.6.6: Corey's alkylation with Methyl Acrylate

Subjecting α-methyl dienone **58** to deconjugative alkylating conditions gave epimers **61** and **65** in a 1:3 ratio (**Scheme 2.6.7**). Structures of enones **61** and **65** were assigned by IR and NMR. Their relative stereochemistries were later assigned through crystallographic data. It was determined that the minor product, enone **61**, was that of the desired stereochemistry (**Figure 2.6.1**). We were surprised to obtain two different compounds, since we expected to have a bias toward the desired stereochemistry. This notion stems from the Nicolaou synthesis, where they observed complete stereoselectivity in their sequence of alkylations (**Scheme 1.3.1.**). We had assumed that the structure of dienone **26** was comparable to the structure of enone **10** that we would observe the same selectivity, unfortunately this was not the case.

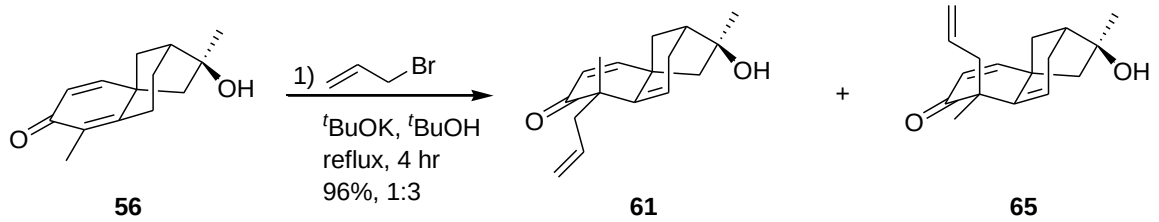

Scheme 2.6.7: Enones **61** and **65**

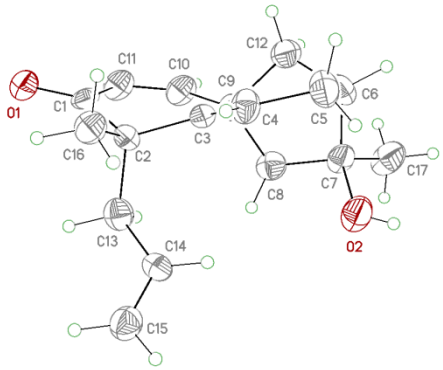

Figure 2.6.1: Crystal Structure of enone **61**

Upon closer examination of the structure, published literature and molecular models we realized that the critical difference between our intermediate and those published was the hybridization of the β-carbon (**Figure 2.6.2**). In the structure of enone **61** and **65** the β-carbon is sp^2 hybridized and in the Nicolaou synthesis it is sp^3 hybridized. This change of hybridization has a major influence on the stereochemistry at the α-carbon due to the differences in conformation because of the γ-carbon (**Figure 2.6.2**).

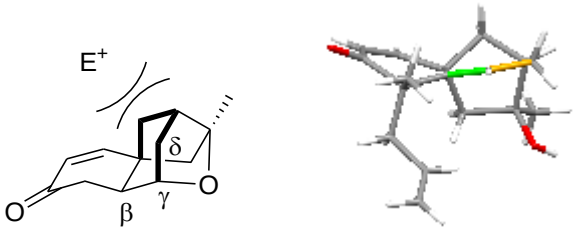

Figures 2.6.2: Steric effects caused by difference in hybridization

The top face of Nicolaou's intermediate **10** is unavailable to electrophiles do to the steric congestion from the axial methylene groups (bold bonds) (**Figure 2.6.2**). This conformation gives complete stereoselectivity in forming the α-quaternary center. As can be seen from the crystal structure, the β-carbon of enone **61** is trigonal planar, forcing the bond between the β- and γ-gamma carbons (highlighted green) to be skewed down. This geometric restriction forces the δ-methylene (highlighted orange) to be moved away from the top face, exposing the top of the molecule to electrophiles. It is this difference in hybridization that has reversed the stereoselectivity of this alkylation.

2.7 Conclusion

We were successful in obtaining dienone **25** in gram quantities and in one step less than the Mulzer synthesis. Furthermore, were able to improve the Grignard addition giving us an actual yield as opposed to a "brsm" yield. When we were unsuccessful in using methyl acrylate to install the α-quaternary center, we opted to use allyl bromide. Although success was met in forming the α-quaternary center using allyl bromide, the resulting mixture of enones favored undesired epimer **65** in a 3:1 ratio. We were able to surmise that the hybridization at the β-carbon had enough influence to affect the stereochemical outcome of this alkylation. These results compelled us to conceive a different strategy.

2.8 References

(1) DJ Beames and LN Mander Studies on intramolecular alkylation. l. the preparation of tricyclic intermediates for the synthesis of diterpene alkaloids. *Aust. J. Chem.* **1971**, *24*, 343-351.

(2) Beames, D. J. Klose, T. R.; Mander, L. N. Intramolecular C-alkylation in diazo-ketones. *J. Chem. Soc. D* **1971**, 773-774.

(3) Beams, DJ. Mander, LN Studies on intramolecular alkylation. IV. The preparation of spirodienones from phenolic diazoketones. *Aust. J. Chem.* **1974**, *27*, 1257-1268.

(4) Beames, D.J.; Klose, T.R.; Mander, L.N., D. J. Studies on intramolecular alkylatoin. V. Intramolecular alkylation of the aromatic ring in tetrahydronaphthyl diazomethyl ketones. *Aust. J. Chem.* **1974**, *27*, 1269-1275.

(5) Brown, D. S. Marples, B. A. Smith, P.; Walton, L. Epoxidation with dioxiranes derived from 2-fluoro-2-substituted-1-tetralones and -1-indanones. *Tetrahedron* **1995**, *51*, 3587-3606.

(6) Weinstock, J. Gaitanopoulos, D. Oh, H. J. Pfeiffer, F. R. Karash, C. B. Venslavsky, J. W. Sarau, H. M. Flaim, K. E. Hieble, J. P.; Kaiser, C. Synthesis and dopaminergic activity of some halogenated mono- and dihydroxylated 2-aminotetralins. *Journal of Medicinal Chemistry* **1986**, *29*, 1615-1627.

(7) Buisson, D.; Cecchi, R.; Laffitte, J.; Guzzi, U.; Azerad, R. Microbial Reduction of 1-Tetralone 2-Carboxyesters as a Source of New Asymmetric Synthons. *Tet. Lett.* **1994**, *35*, 3091-3094.

(8) Mole, T. and Surtrees, J.R. Organoaluminium compounds. V. Reactions of oragnoaluminium compounds with benzophenone. *Aust. J. Chem.* **1964**, *17*, 961-966.

(9) Bruin, J. W. Schat, G. Akkerman, O. S., Bickelhaupt, F. Some applications of the methylene di-Grignard reagent for the synthesis of main group IV organometallic compounds. *Journal of Organometallic Chemistry* **1985**, *288*, 13-25.

(10) Reetz, M. T. Kyung, S. H., llmann, M. $CH_3Li/TiCl_4$: A non-basic and highly selective Grignard analogue. *Tetrahedron* **1986**, *42*, 2931-2935.

(11) Reetz, M. T. Hugel, H.; Dresely, K. The relative reactivity of cyclic ketones towards methyltitanium reagents. *Tetrahedron* **1987**, *43*, 109-114.

(12) Imamoto, T. Takiyama, N. Nakamura, K. Hatajima, T.; Kamiya, Y. Reactions of carbonyl compounds with Grignard reagents in the presence of cerium chloride. *Journal of the American Chemical Society* **1989**, *111*, 4392-4398.

(13) Jansen, B. J. M. Kreuger, J. A.; De Groot, A. The conversion of (-)- and (+)-dihydrocarvone into chiral intermediates for the synthesis of (-)-polygodial, (-)-warburganal and (-)-muzigadial. *Tetrahedron* **1989**, *45*, 1447-1452.

(14) House, H. O. Roelofs, W. L.; Trost, B. M. The Chemistry of Carbanions. XI. Michael Reactions with 2-Methylcyclopentanone and 2-Methylcyclohexanone1a. *The Journal of Organic Chemistry* **1966**, *31*, 646-655.

(15) Cartlier, D.; Levy, J. Synthese d'acetoacetaldehydes mono- et di-substitues par des chaines fonctionnalisees. *Tetrahedron* **1990**, *46*, 5295-5304.

(16) Yeung, Y.-Y.; Corey, E. J. A Simple, Efficient, and Enantiocontrolled Synthesis of a Near-Structural Mimic of Platensimycin. *Organic Letters* **2008**, *10*, 3877-3878.

Chapter 3: Second Generation Synthesis

3.1 Introduction

As we have not yet achieved the desired stereoselectivity, we went on to devise a new strategy that would enforce the desired selectivity. From the Nicolaou synthesis and close examination of our work we knew it was crucial to form the ether linkage prior to alkylation. Consequently, our second generation strategy would revolve around this idea.

3.2 Synthetic Approach

Our new strategy started with dienone **26.** Dienone **26** would be converted to extended enol ether **66**. Epoxidation of enol ether **66** would give epoxide **67.** Hydrolysis of enol ether **67** would afford γ-hydroxy dienone **68**.[1,2,3] A hydroxyl-directed reduction of dienone **68** to enone **69** followed by cyclization would give final product **10**. Enone **10** was chosen as our new goal because the succeeding alkylation had already been successfully accomplished by the Nicolaou group.

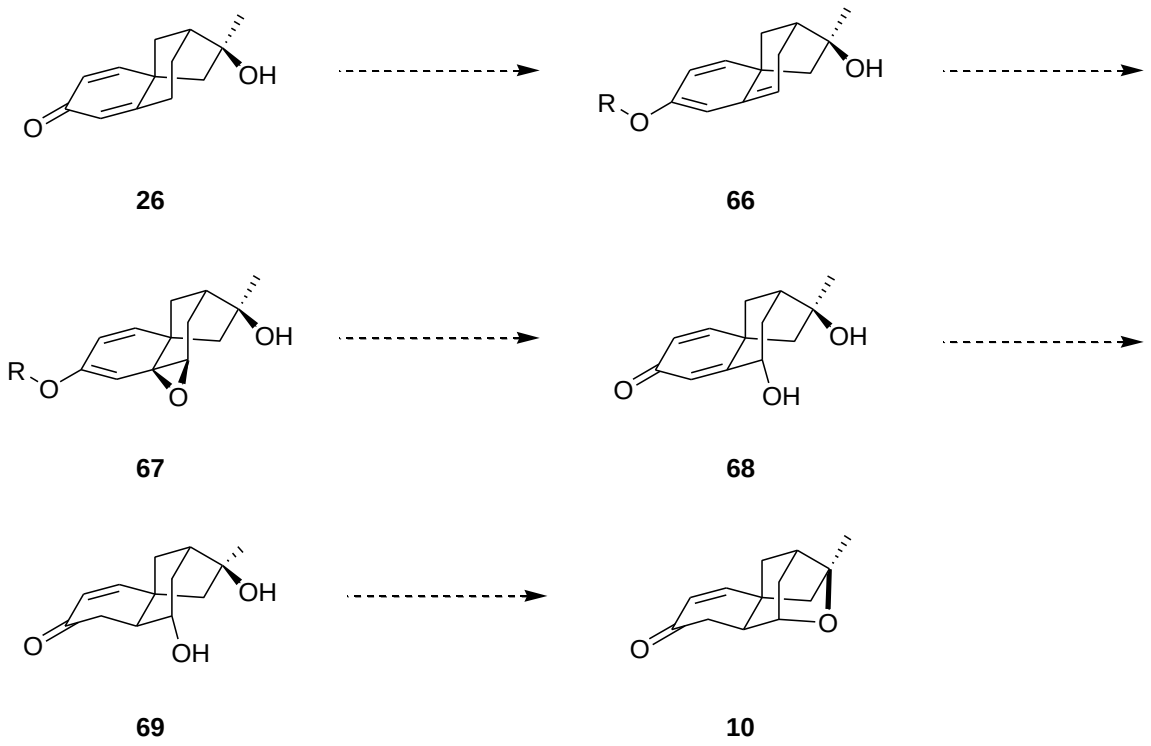

Scheme 3.2.1: Route to cyclic either **10**.

3.3 Formation of he Extended Enol Ether

Initial attempts to make extended enol ether **66** using acetic anhydride failed to give any of the desired products (**Scheme 3.3.1)**. This transformation was then attempted using TBDMS to form silyl enol ether **71**. TBDMS was used because we assumed that a TMS group would be too labile, as can be evidenced by how readily the methyl enol ether postulated to form in the alkylation of compound **59,** hydrolyzed. Dienone **26** was treated under standard silyl enol ether forming conditions but gave mostly recovered starting material and a minor product (~5%). After purification it was determined that the minor product was γ-hydroxy dienone **68**.

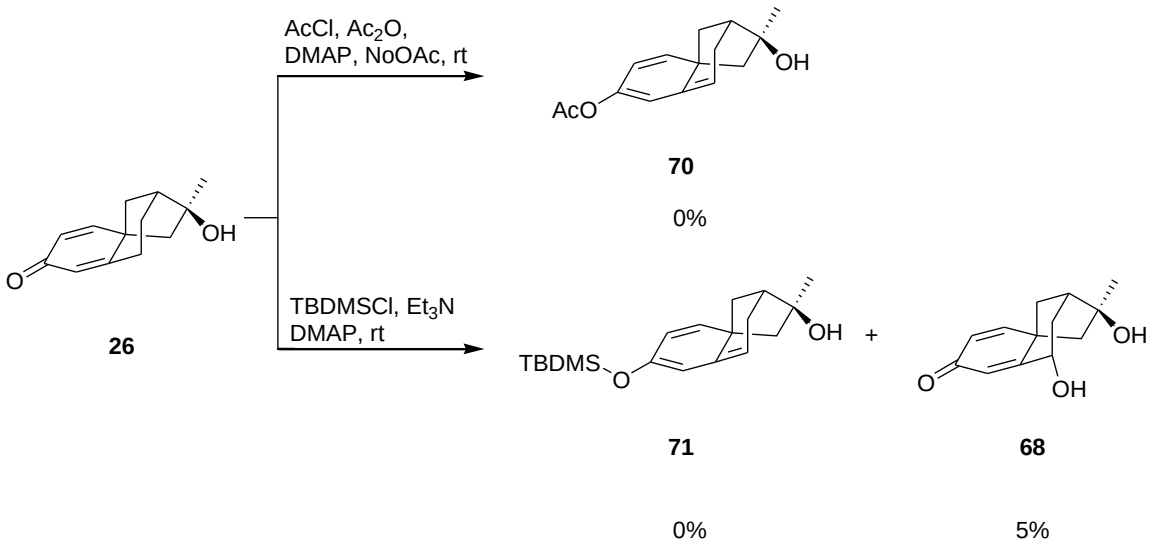

Scheme 3.3.1: Formation of the extended enol ether **66**.

The direct formation of γ-hydroxy dienone **68** from dienone **26** was a fortuitous result because it shortened our intended route by two steps (**Scheme 3.3.2**). Our efforts were now directed toward understanding and improving this transformation.

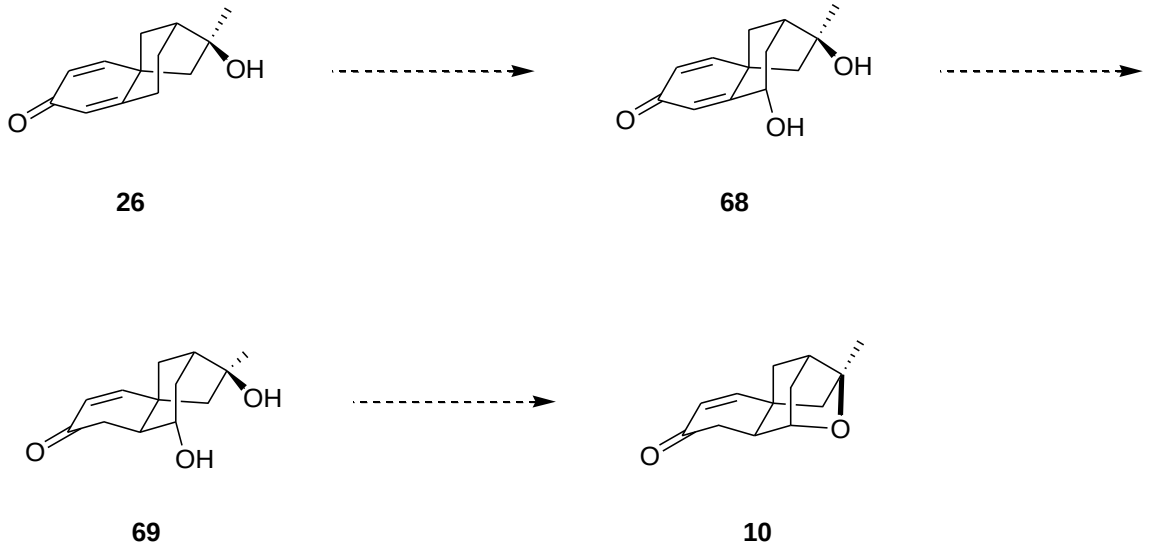

Scheme 3.3.2: Modified Synthetic Scheme.

3.4 Autoxidation

The origin of γ-hydroxy dienone **68** was uncertain so we explored this transformation by repeating the previous experiments. The results were poor with yields of **68** ranging from 4-7 %, with no signs of the desired enol ether. During these trials it was concluded that the process responsible for the oxidation at the γ-position was autoxidation ($^3O_2$). Furthermore, a result from a concurrent literature search gave further support to the notion that this reaction was occurring *via* an autoxidation process. Aladro and coworkers treated bicyclic enone **72** under autoxidation conditions to obtain γ-hydroxy enone **73** in 100% yield (**Scheme 3.4.1**).[4]

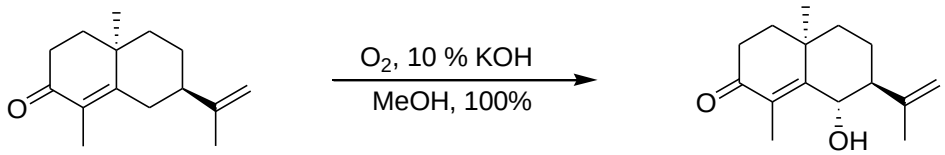

72 **73**

Scheme 3.4.1: Aldaro autoxidation.

The investigation proceeded with taking enone **26** and treating under the same conditions used by Aladro (**Table 3.4.1**). The reactions were left open to atmosphere unless otherwise noted. Under these conditions only a 10% yield was obtained (Entry A). No improvement was observed when the temperature or reaction

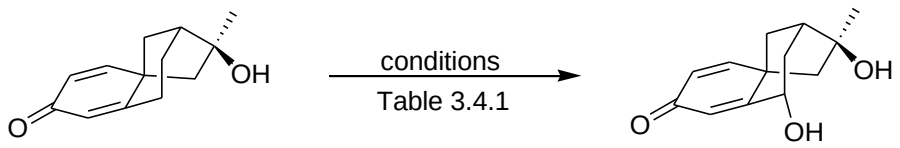

26 **68**

Scheme 3.4.2: Autoxidation of dienone **26**.

Entry	Base	Solvent	Temp (°C)	Time (h)	Yield (%)
A	KOH	MeOH	rt	48	10
B	KOH	MeOH	60	48	0
C	KOH	MeOH	rt	96	8
D	^{t}BuOK	MeOH	rt	48	6
E	KOH	THF	rt	48	3
F	^{t}BuOK	THF	rt	48	3
G*	KOH	MeOH	rt	48	10

*The reaction was run under an atmosphere of oxygen

Table 3.4.1: Autoxidation conditions for dienone **26**

time were increased. (Entry B,C). Changing to a stronger base or changing the solvent also failed to produce any positive results (Entry D-F). The use of an oxygen balloon had no impact on the yield (Entry G).

Having little success using dienone **26,** α-methyl dienone **58** was used instead. This was done in order to mirror more closely what the Diaz group published (**Scheme 3.4.2**). By simply substituting dienone **26** with α-methyl dienone **58**, γ-hydroxy compound **74** was obtained in 27% yield, almost a 3-fold increase in yield (**Table 3.4.2**, Entry A). Further changes to the procedure were fruitless. Prolonging the reaction from 48 h to 96 h had little effect (Entry B,C). Changing the base or the solvent caused a slight drop in yield (Entry D-F).[5,6] The use of an oxygen balloon had little impact on the yield (Entry G).

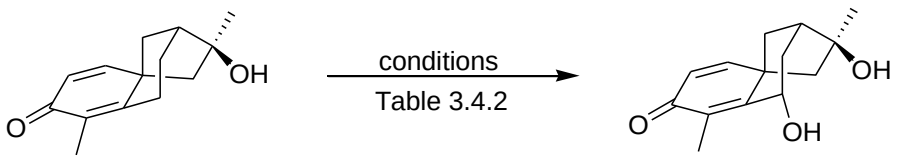

58 **74**

Scheme 3.4.2: Autoxidation of α-methyl dienone **58**.

Entry	Base	Solvent	Temp (°C)	Time (h)	Yield (%)
A	KOH	MeOH	rt	48 h	27
B	KOH	MeOH	rt	72 h	21
C	KOH	MeOH	rt	96 h	19
D	^{t}BuOK	MeOH	rt	48 h	20
E	KOH	THF	rt	48h	20
F	^{t}BuOK	THF	rt	48h	21
G*	KOH	MeOH	rt	48 h	24

*the reaction was run under an atmosphere of oxygen

Table 3.4.2: Autoxidation conditions for α-methyl dienone **58**

Three new pieces of information were obtained from this reaction. First, due to the increase in yield, enough of the product was collected to obtain an x-ray structure of γ-hydroxy dienone **74** and the relative stereochemistry was assigned (**Figure 3.4.1**). The image displayed is a view from the bottom of the molecule to help show the *syn*-relationship of the hydroxyl groups. The γ-hydroxyl group was of the desired stereochemistry, perfectly situated for the envisioned hydroxyl-directed reduction. Furthermore, the γ-hydroxyl group was in proximity for the final transformation which was imagined to proceed under an acid catalyzed etherification *via* the tertiary carbocation.

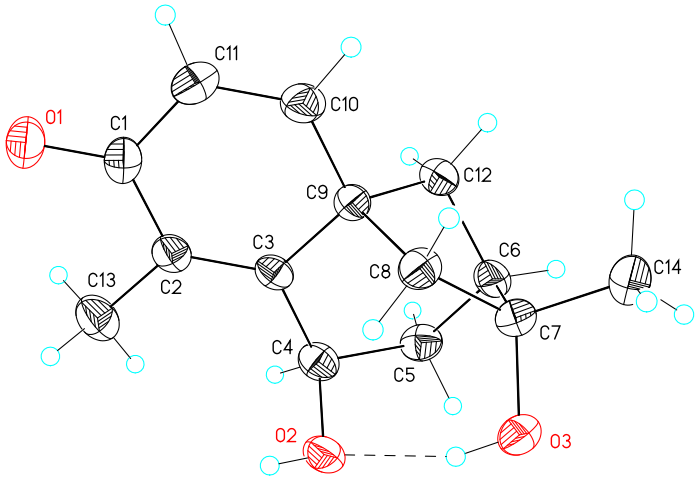

Figure 3.4.1: Crystal structure γ-hydroxy dienone **74**

It was discovered that a major reason for the low yield of dienone **74** was the formation of ketone **76** which was isolated in 16-19% yield (**Figure 3.4.2**). Ketone **76** was thought to arise from the over oxidation of dienone **74.** It was postulated that when the peroxide formed at the γ-position, excess base deprotonated the remaining γ-proton to give ketone **76.** Since it accounted for such a significant percentage of the products isolated, it was imperative that we find a solution. Our initial thought was that using reducing agent might help deter this pathway by cleaving the oxygen-oxygen bond of the

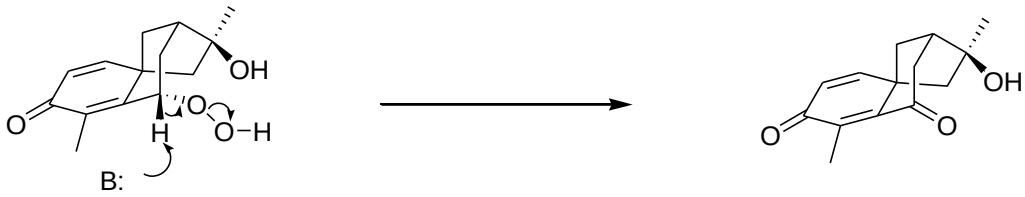

75 **76**

Figure 3.4.2: Formation of ketone **73**

the peroxide before deprotonation occurred.

A commonly utilized reducing agent in autoxidation is $P(OEt)_3$.[7] The previous set of trials were repeated in the presence $P(OEt)_3$ (**Scheme 3.4.3**). Overall the addition of $P(OEt)_3$ caused a drop in the yield of ketone **76**. Additionally, the reaction time was significantly reduced. However, there was little improvement in the yield of the desired compound. The one reaction that caught our attention was the use of ^{t}BuOK in THF (Entry E). This set of conditions produced the lowest yield of ketone **76**, while still providing a comparable yield of the desired product. The reason for this was not well understood but we shifted our attention to using ^{t}BuOK instead of KOH.

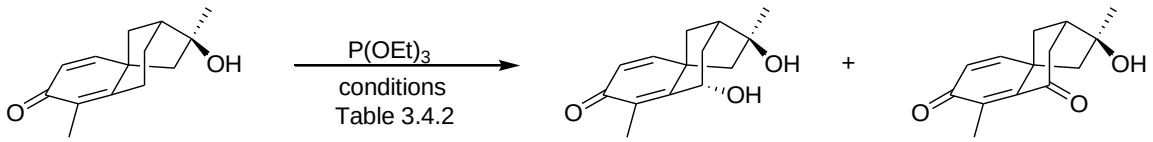

Scheme 3.4.3: Auto-oxidation in the presence of $P(OEt)_3$.

Entry	Base	Solvent	Temp (°C)	Time (h)	Yield (%) **74**	Yield **(%) 76**
A	KOH	MeOH	rt	2.5	26	8
B	KOH	MeOH	60	2.5	0	0
C	^{t}BuOK	MeOH	rt	2.5	20	7
D	KOH	THF	rt	2.5	21	8
E	^{t}BuOK	THF	rt	2.5	23	4

Figure 3.4.3: Conditions for the autoxidation with $P(OEt)_3$.

Increasing the amount of $P(OEt)_3$ which had little impact on the yield (**Table 3.4.4**, Entry A-C). Raising or lowering the reaction temperature didn't provide any significant improvement (Entry D,E). Changing the solvent to ^{t}BuOH had paralleled the

Entry	Base (2.5 eq)	$P(OEt)_3$ (eq)	Solvent	Temp (°C)	Time (h)	Yield(%) **74**	Yield(%) **76**	Yield(%) **77**
A	^{t}BuOK	1	THF	rt	2.5	25	4	0
B	^{t}BuOK	2	THF	rt	2.5	25	5	0
C	^{t}BuOK	5	THF	rt	2.5	26	4	0
D	^{t}BuOK	1	THF	60	2.5	0	0	0
E	^{t}BuOK	1	THF	0	2.5	19	6	0
F	^{t}BuOK	1	^{t}BuOH	rt	2.5	22	5	0
G	^{t}BuOK	1	^{t}BuOH/ THF(1:1)	0	2.5	21	8	0
H	^{t}BuOK	1	^{t}BuOH/ THF(1:1)	-40	2.5	20	7	5
I	^{t}BuOK	1	^{t}BuOH/ THF(1:1)	-78	2.5	0	0	8
J	^{t}BuOk	1	^{t}BuOH/ THF(1:1)	rt	2.5	27	5	0
K	^{t}BuOK	5	^{t}BuOH/ THF(1:1)	rt	2.5	30	5	0

Table 3.4.4: Autoxidation of **58** using ^{t}BuOK.

results when THF was used (Entry F). This new development sparked interest into using ^{t}BuOH as a solvent. Realizing that when the temperature was increased loss of starting material was observed we decided to experiment with lower temperatures. THF had to be used as a co-solvent to prevent solidification of ^{t}BuOH at lower temperatures. Decreasing the temperature lowered the yield slightly but gave rise to a new side product (Entry G-I). It was determined that this side product was α-hydroxy enone **77** (Scheme **3.4.4**). It was not too surprising since similar conditions have been employed to produce α-hydroxy ketones.[8] Enone **77** helped us to conceive a possible mechanism for the autoxidation of α-methyl dienone **58** which will be later examined in detail. When the reaction was performed at room temperature with in THF/^{t}BuOH (1:1) mixture a slight increase in yield was observed (Entry J). Finally, when the amount of $P(OEt)_3$ was

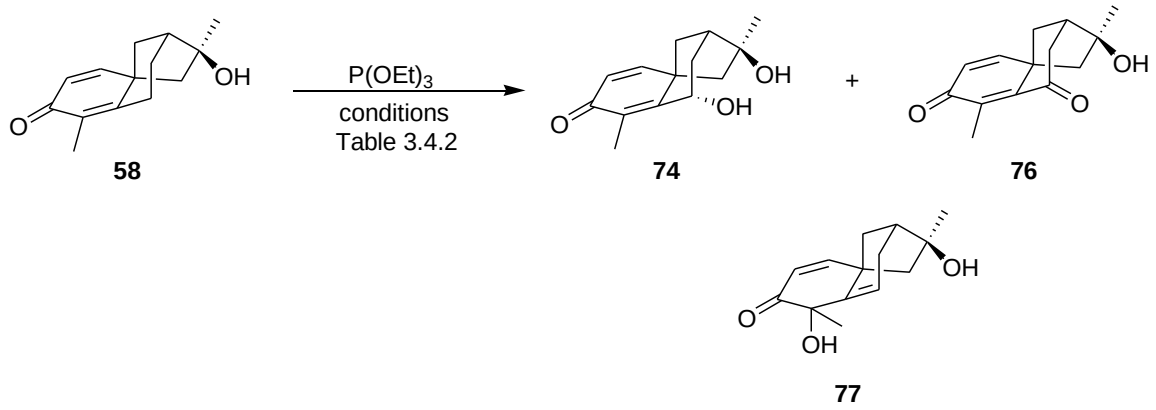

58 **74** **76** **77**

Scheme 3.4.4: Products formed from the autoxidation of **58**.

increased a 30% yield was obtained with a minimal amount of ketone. These were the optimal conditions obtained thus far. Changing the amount of base, reductant, ratio of solvents or reaction time failed to improve these results. It is also important to mention that other reductants were used (PBu_3, PPh_3) but provided inferior results.

Obtaining α-hydroxy enone **77** and studying molecular models allowed us to suggest a mechanism for the autoxidation and help understand its stereoselectivity (**Figure 3.4.3**). The reaction begins with deprotonation at the γ-position forming the extended enolate. Single electron transfer then occurs from the negatively charged oxygen to triplet oxygen. Homolytic cleavage of the alpha double bond leads to the formation of the carbonyl and alpha-peroxy bonds. It is at this step that the peroxide can either do an 2,3 sigmatropic rearrangement or be reduced to give α-hydroxy ketone **77**.[9] Molecular models helped us understand that proper orbital overlap for the 2,3-sigmatropic rearrangement can only be achieved when the peroxide is on the bottom face of the molecule. After the 2,3 sigmatropic shift the peroxide can either be cleaved by $P(OEt)_3$ to give γ-hydroxy dienone **74** (red arrows) or the reminaing γ-proton can be abstracted by ^{t}BuOK leading to ketone **76** (blue arrows).

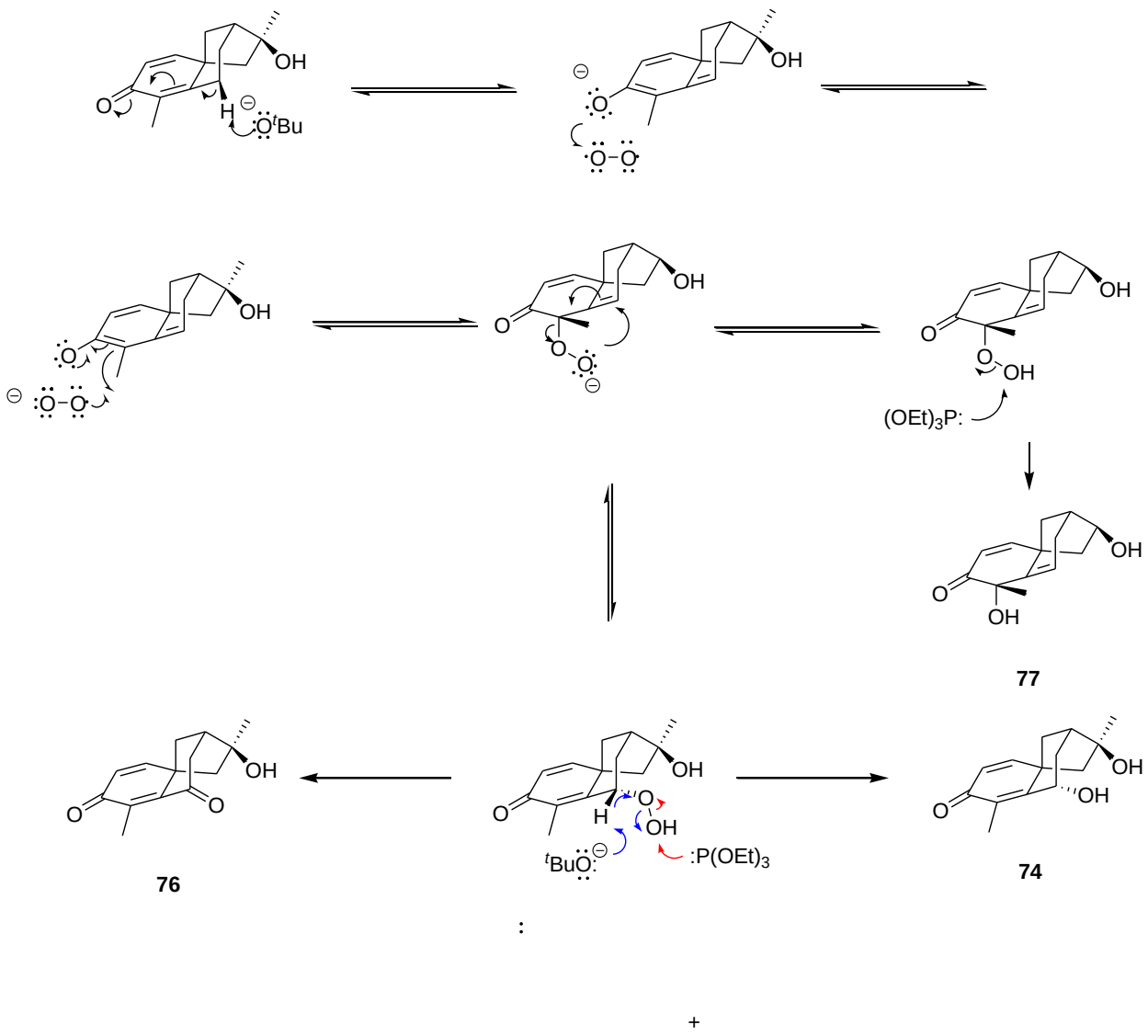

Figure 3.4.3: Autoxidation mechanism.

Although we had improved our yield to a consistent 30% and greatly reduced the amount of ketone **76**, it was still at best a modest yield. Furthermore the best results were obtained when the reaction was run on a small scale (30 mg). Running the reaction on

larger scales dropped the yield significantly. For these reasons we sought out alternatives in forming the γ-hydroxy dienone **74**.

We started by attempting an allylic oxidation with SeO_2 (**Table 3.4.5**, Entry A). At lower temperatures there was no visible change but when the temperature was raised only degradation of the starting material was observed. Similar results were obtained for all the other trials as well. When a source of electrophilic oxygen was used degradation of the starting material occurred (Entry B).[10] Allylic acetate formation resulted in complex mixtures (Entry C-E).[11] It was thought that successful formation of the allylic acetate could yield γ-hydroxy dienone **74** *via* hydrolysis.

Entry	Conditions	Yield (%)
A	SeO_2, Dioxane, rt to reflux	0
B	^tBuOK, ^tBuOOH, Et_3N, ^tBuOH	0
C	$Pd(OAc)_2$, Benzoquinone, AcOH, rt, 6 h	0
D	$Pb(OAc)_4$, AcOH, 60 °C, 4 h	0
E	Hippuric Acid, NaOAc, AcOH, rt to reflux	0

Table 3.4.5: Alternative allylic oxidation methods.

During this time we made another discovery in the literature. The Yoshioka group had published a paper on the functionalization of the Wieland-Miescher ketone at the γ-position.[12] By using water as a co-solvent they completely eliminated the presence of ketone **80** (**Scheme 3.4.5**). Running the reaction under different conditions had

produced a substantial amount of ketone **80**. These conditions were applied to the autoxidation of dienone **58**.

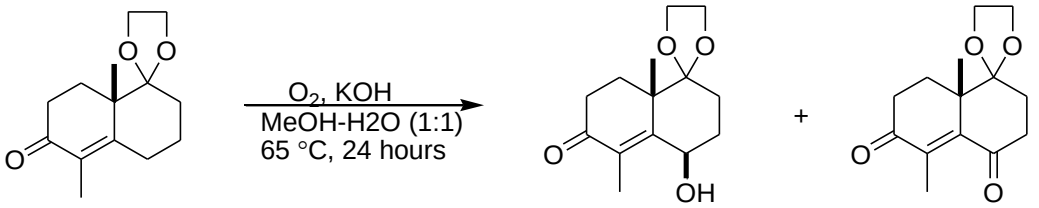

Scheme 3.4.5: Yoshioka's Autoxidation.

Running the reaction under the same conditions yielded a small amount of product but without yielding any of the undesired ketone **76** (**Table 3.4.6**, Entry A). When the temperature was increased or the base changed from KOH to ^{t}BuOK no significant improvement was made (Entry B,E,F). However, when ^{t}BuOH was used as a co-solvent a significant improvement in yield was observed (Entry C). Increasing the reaction temperature lead to a reduction in yield by about 50% (Entry D). Unexpectedly, the mixture of base with a ^{t}BuOH/H_2O formed a biphasic system. This observation lead us to explore the use of phase transfer catalysts (PTCs).

Entry	Base (10%)	Solvent	Time (days)	Temp (°C)	Yield(%) **74**	Yield(%) **76**
A	KOH	MeOH/ H_2O(1:1)	5	rt	7	0
B	KOH	MeOH/ H_2O(1:1)	5	65	4	0
C	KOH	^{t}BuOH/ H_2O (1:1)	5	rt	53	0
D	KOH	^{t}BuOH/ H_2O (1:1)	5	65	23	0
E	tBuOK	^{t}BuOH/ H_2O(1:1)	5	rt	10	0
F	tBuOK	^{t}BuOH/ H_2O (1:1)	5	65	4	0

Table 3.4.6: Autoxidation using Yoshioka conditions.

By screening various PTCs at 10 mol % it was determined that Bu_4NBr showed the most promise in improving the yield so further experiments were performed using only Bu_4NBr (**Table 3.4.7**). The first trial showed improvement in yield and a reduction in reaction time by 2 days (Entry A). Increasing the amount of PTC had a slight increase in yield but more importantly decreased the reaction time to 2 days (Entry B-F). Changing the solvent, base, or temperature provided inferior results. Furthermore, this reaction was performed on a 100 mg scale, 3 times greater than previous scale.

Entry	Base (10%)	Solvent	PTC %	Time (days)	Temp	Yield (%)
A	KOH	^{t}BuOH/ H_2O(1:1)	10	3	rt	60
B	KOH	^{t}BuOH/ H_2O(1:1)	20	3	rt	60
C	KOH	^{t}BuOH/ H_2O(1:1)	30	2.5	rt	62
D	KOH	*t*BuOH/ H_2O(1:1)	40	2.5	rt	62
E	KOH	^{t}BuOH/ H_2O(1:1)	50	2.5	rt	63
F	KOH	^{t}BuOH/ H_2O(1:1)	100	2	rt	65

Table 3.4.7: Autoxidation using aBu_4NBr.

Through these experiments the optimal conditions for producing γ-hydroxy dienone **74** in 65% yield were obtained (**Scheme 3.4.6**). Moreover, it was discovered that the use of water as a co-solvent helped to deter over oxidation to unwanted ketone **76.** We were able to gain a working hypothesis as to the mechanism that was operating in the autoxidation. Finally, the crystal structure was solved and showed that we had obtained the desired relative stereochemistry (**Figure 3.4.1**)

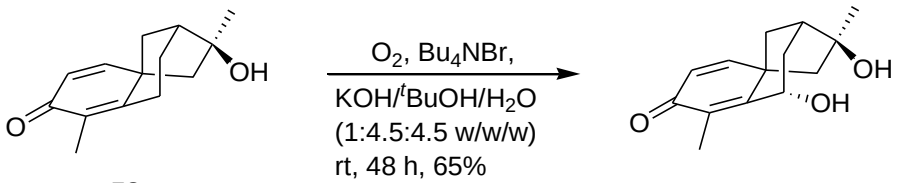

58 **74**

Scheme 3.4.6: Optimal autoxodation conditions.

3.5 Hydroxyl-Directed Conjugate Reduction

Having been able to unambiguously assign the stereochemistry of the γ-hydroxyl group put us in good position to attempt the desired hydroxyl directed conjugate reduction. At the onset we had two ideas on how to achieve this objective. The first was a reduction based on an intramolecular hydrosilylation and the second a reduction based on LAH.

We started by silylating γ-hydroxy dienone **74** to give compound **81** (**Scheme 3.5.1).** This compound was then treated to a variety of conditions to affect the conjugate reduction (**Tabel 3.5.1**). Treating compound **81** to Wilkinson's catalyst resulted in degradation of the reactant (Entray A).[13] The use of Lewis acids resulted in desilylation (entry B,C).[1415] Using I_2O_5 resulted in the degradation of the starting material.[16] Having shown little promise we shifted our attention to an LAH reduction.

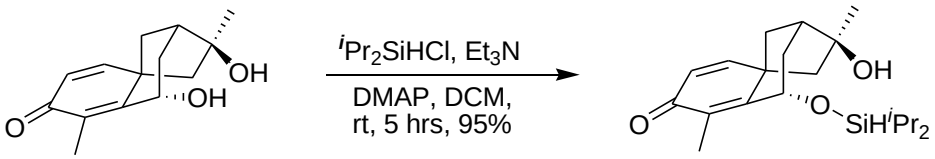

74 **81**

Scheme 3.5.1: Formation of silyloxy compound **81**.

Entry	Conditions	Yield (%)
A	$(Ph_3P)_3RhCl$, THF, 6 h, rt - reflux	0
B	$SnCl_4$, DCM, -78° C, 3 h	0
C	$TiCl_4$, DCM, - 78 °C 3 h	0
D	I_2O_5, rt, DCM, 5 h	0

Table 3.5.1: Conditions for the intramolecular hydrosylation.

The idea for the LAH reduction stemmed from work published by the Liotta group (**Scheme 3.5.2**).[17] They treated dieone **82** with LAH and obtained diastereomer **83** in 90% yield. These conditions were taken and applied to γ-hydroxy dienone **74** (**Table 3.5.2**). All the reactions were done in THF with LAH (1eq). When the reaction was done at ambient temperature a distribution of three compounds were isolated, enone **84**, **85**, and dieneone **74** (Entry A). As the temperature was decreased a greater amount of enones **84** and **85** were isolated (Entery A,C,E). When the reaction continued until complete consumption of dienone **74**, low yields and poor mass balance were observed (Entry B,D,F). The best results were obtained when there reaction was performed at –78 °C for one minute (Entry E). The same experiments were performed with the addition CuI/HMPA, which have been shown to aid LAH in conjugate reductions, but offered no advantage over the previous examples.[18,19,20]

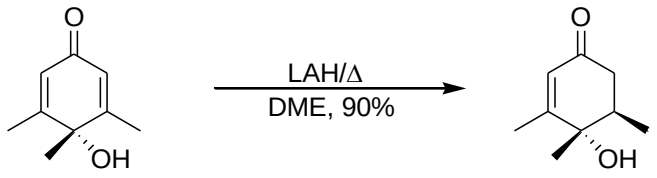

82 **83**

Scheme 3.5.2: Liotta's conjugate reduction of dienone **82**.

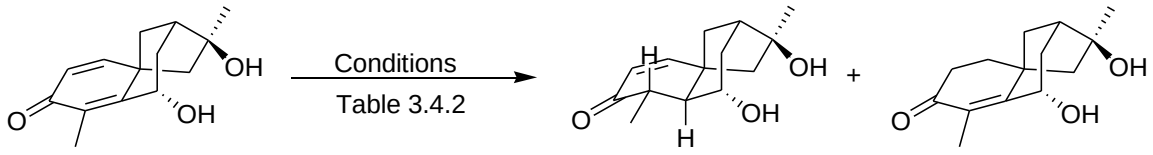

74 **84** **85**

Scheme 3.5.3: Conjugate reduction using LAH.

Entry	Temp (°C)	Time (min)	Yield (%) **84**	Yield (%) **85**	Yield (%) **74**
A	rt	1	7	16	55
B	t	5	4	19	0
C	0	1	15	24	30
D	0	12	11	23	0
E	-78	1	32	32	34
F	-78	45	14	26	0

Table 3.5.2: Conditions for LAH reduction.

The next improvement came upon an observation using a new bottle of LAH. When the reduction was performed under the current conditions only a small amount of the products were obtained (~10% combined) with a poor mass balance. It had then occurred to us that the bottle that we had been using was a bit older and postulated that

moisture may have entered the original bottle thereby forming $LAH_x(OH)_y$ adducts. These adducts would stand to be less reactive that pure LAH.

Previous studies had been done on the reactivity of LAH reagents modified with alkoxy groups by the Brown and Ashby Groups.[21,22] The general trend they observed for reactivity of these adducts was OH ≥MeOH >EtOH > iPrO >>tBuOH. The number of alkoxy groups on the LAH moiety also affected its reactivity, with the greater number of displaced hydrides the more reactivity decreased. Based on previous results we decided to start the next set of experiments with a $LAH_x(EtO)_y$ adducts (**Table 3.5.3**). When only one hydride was displaced and the reaction run at -78 °C a bias toward the desired product was observed (Entry A). When the reactivity was decreased by adding a second ethoxy group complete selectivity was obtained (Entry B). Adding an additional ethoxy

Entry	Adduct	Temp (°C)	Time (min)	Yield(%) **84**	Yield(%) **85**	Yield(%) **74**
A	$LiAlH_3OEt$	-78	15	40`	19	35
B	$LiAlH_2(OEt)_2$	-78	20	64	0	30
C	$LiAlH(OEt)_3$	-78	60	0	0	99
D	$LiAlH_3OEt$	0	5	20	35	35
E	$LiAlH_2(OEt)_2$	0	15	45	15	35
F	$LiAlH_2(OEt)_2$	rt	5	5	30	10

Table 3.5.3: Conjugate reduction with LAH-ethoxy adducts.

failed to provide any new results as was expected with only one available hydride. As the temperature was raised yields decreased and the desired selectivity was lost (Entry C-F). The use of isopropoxy or tertbutoxy groups failed to provide any of the reduced products at low temperatures. When the reactions were run at high temperatures using

these reagents (+60 °C) the starting material was consumed and inextricable mixtures were obtained.

The end result was a 65% yield of enone **84** when γ-hydroxy dienone **74** was treated to $LAH_2.OEt_2$ at – 78 °C (**Scheme 3.5.4**). The crystal structure was obtained and the relative stereochemistry assigned (**Figure 3.5.1**). It is clear that the hydrogen on the β-carbon was delivered from the bottom face, signaling that this was indeed a hydroxyl directed reduction. The major drawback of this reaction is the purification. It was very difficult to separate the starting material from the products. As such, the subsequent transformation was undertaken with a mixture of dienone **74** and **84**. It is worthy of note that other reducing reagents/methods failed to give any positive results (Alane, Borane, DIBAL-H, and Birch).

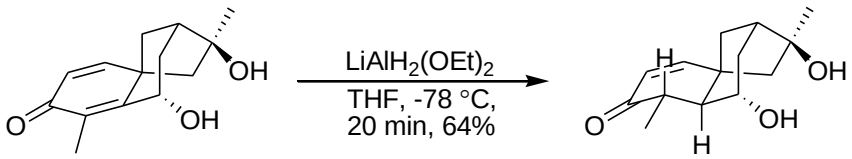

74 **84**

Scheme 3.5.4: Hydroxy directed conjugate reduction.

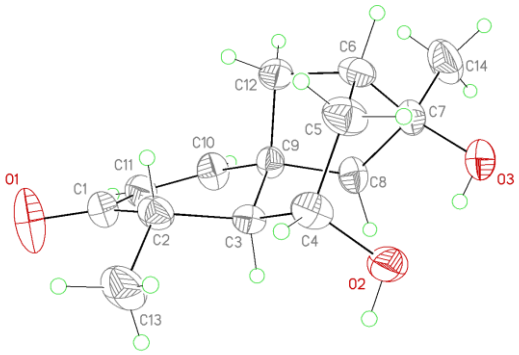

Figure 3.5.1: Crystal structure of enone **84**.

3.6 Cyclization

The final step of our synthesis was the cyclization of enone **84**. It was initially envisioned that this transformation could be achieved *via* acid catalysis. This method was employed by Nicolaou in the etherification of compound **9** (**Scheme 3.6.1**). These

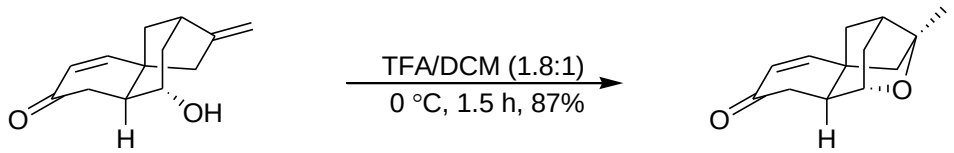

9 **10**

Scheme 3.6.1: Nicolaou's acid induced cyclization

conditions were taken and applied to substrate **74** (**Scheme 3.6.2**). The results were discouraging and surprising (**Table 3.6.1**). At best only 6% of the desired product was obtained, along with *epi*-compound **87** and cyclized dienone **88** (Entry A). Using stronger acids lead solely to the cyclized dienone (Entry B,C,E).[23] When weaker acids

were employed only the yield of cyclized dienone increased. (Entry D). The formation of *epi*-compound **87** was not surprising, since it is known that tetrahydrofurans are readily cleaved under acidic conditions. What was surprising was other sources reported this transformation in moderate to good yields (57-87%) without any epimerization.

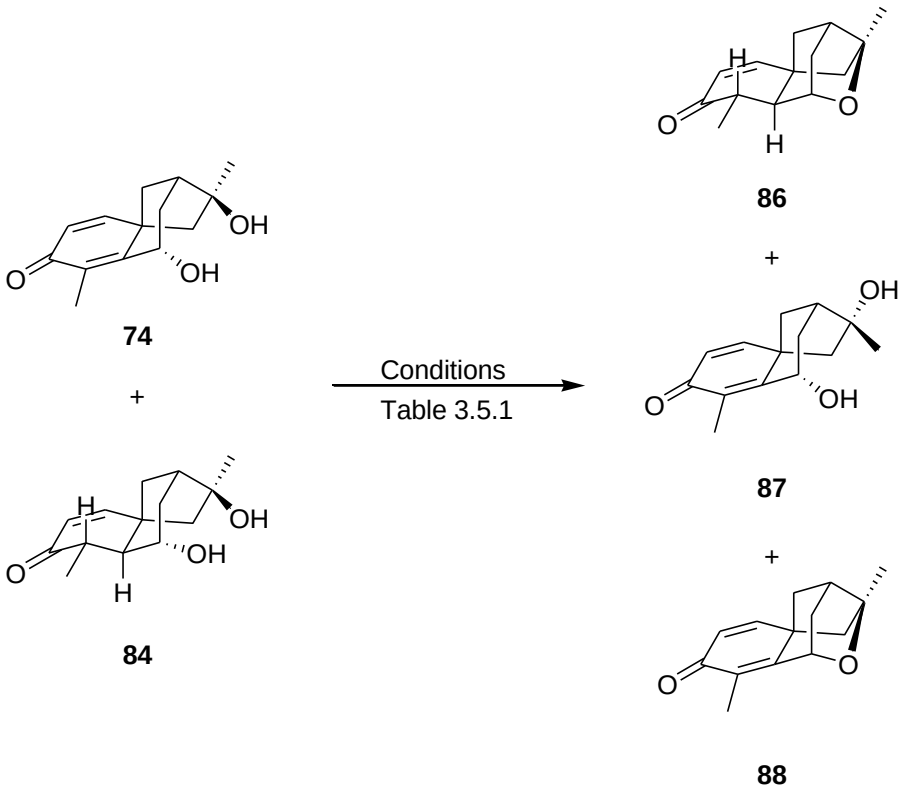

Scheme 3.6.2: Formation of cyclic ether **86.**

Entry	Acid	Solvent	Time (h)	Temp (°C)	Yield(%) **86**	Yield(%) **87**	Yield(%) **88**
A	TFA	DCM	2	0	6	3	56
B	TfOH	DCM	1.5	-78	0	0	23
C	HCl	Dioxane	2	0	0	0	28
D	AcOH	neat	24	40	0	0	67
E	Nafion	DCE	12	rt	0	0	60

Table 3.6.1: Acid catalyzed conditions for the ether formation.

Short of any promising results we looked to inverting the stereochemistry of the secondary alcohol and perform an intramolecular SN_2 displacement. This displacement would be done under basic conditions, thus avoiding the opening of the furan ring. We began by exploring Mitsunobu chemistry (**Table 3.6.2**). When standard or modified conditions were employed the starting material was destroyed (Entries A, B).[24] It has been shown that Cyanomethylene/triemthylphosporane (CMMP/ Tsunoda's Reagent), a modified Mitsunobu reagent, could enact an inversion and intramoleuclar cyclization in one pot.[25,26] When CMMP was used only degradation products were isolated (Entry C). Foregoing Mitsunobu chemistry, Appel chemistry was attempted but that failed to give the desired bromide (Entry D). The use of P_2I_4 resulted in degradation of starting material (Entry E).[27] Attempting to form the bromide by displacing the mesylate also failed to give any new results (Entry F).

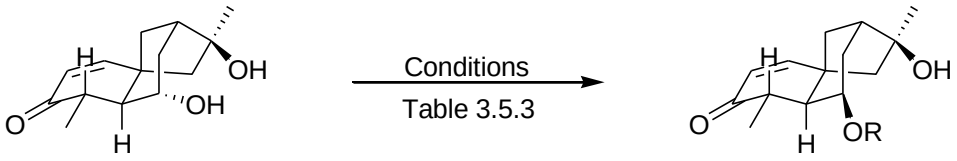

84 **89**

Scheme 3.6.3: Inversion of the secondary alcohol.

Entry	Conditions	Yield (%)
A	standard Mitsunobu	0
B	DEAD, Ph_3P, $Zn(OTs)_2$, THF, 3 hr	0
C	CMMP, THF, 65 °C, sealed tube	0
D	Ph_3P, CBr_4, DCM, rt	0
E	P_2I_4, THF, 0 °C, 5 h	0
F	MsCl, NEt_3, DCM, rt then LiBr	0

Table 3.6.2: Conditions for the inversion of the secondary alcohol.

Lacking any positive results from the previous experiments we looked at forming the cyclic ether by forming a carbonate moiety with the two hydroxyl groups. With this compound we envisioned enforcing an intramolecular cyclization to produce compound **11**. Initial attempts with thionyl chloride, phosgene and methyl carbonate all provided inextricable mixtures. However, when DMSO was utilized we were able to affect the desired transformation in 65% yield (**Scheme 3.5.5**).[28]

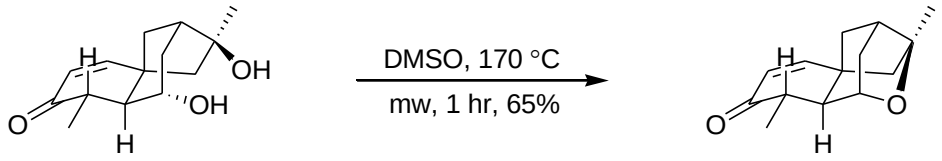

84 **11**

Scheme 3.6.5: Cyclization using DMSO.

We postulate that the ether formation is occurring *via* the tertiary carbocation. Ionization of the hydroxyl group followed by ring closure from the secondary alcohol gives compound **11** (Figure 3.6.1). We believe were able to achieve this etherification due to the relatively neutral reaction conditions, whereas when acidic conditions were employed only degradation and inversion products were isolated.

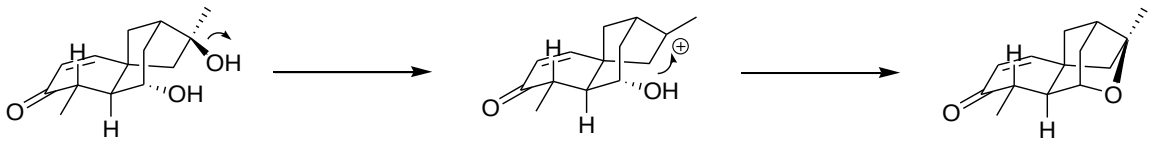

84 **11**

Figure 3.6.1 Mechanism for the ether formation.

3.7 Conclusion

We were able to achieve a concise, direct and stereoselective formal synthesis of platensimycin. This was accomplished in 11 linear steps starting from commercially available 6-methoxy-1-tetralone in a 5% overall yield. To date this is the shortest route to α-methyl enone **11**.

Our original plan did not materialize for two reasons. The first, a minor impediment, was the inability to successfully install the α-quaternary center using methyl acrylate. This was circumvented with the use of allyl bromide in a Claisen rearrangement. However, the issue of stereoselectivity was irreparable and forced us to re-work our strategy.

The second generation synthesis centered on forming the ether linkage prior to alkylation to affect the desired stereoselectivity. This route was almost immediately

improved due to serendipitous results. The autoxidation of α-methyl dienone **58** proved to be a useful intermediate, shortening the planned synthetic route by 2 steps. Furthermore, we achieved the desired stereochemistry at all the newly formed stereocenters. Finally, we were able to form the ether linkage in relatively neutral conditions to complete the formal synthesis of platensimycin.

3.7 References

(1) Holland, H. L.; Auret, B. J. The Mechanism of the Microbial Hydroxylation of Steroids. Part 2. Hydroxylation of a Δ4-3-Ketosteroid Analog by Rhizopus arrhizus ATCC 11145. *Canadian Journal of Chemistry* **1975**, *53*, 2041-2044.

(2) Mahajan, J. R. Dutt, P.; Dutta, P. C. 1012. Synthetic studies in the santonin series. *J. Chem. Soc.* **1957**, 5069-5073.

(3) Zheng, G. Chen, J. Fang, L. Tang, Z.; Li, Y. A novel approach for introduction of C-1 oxygenated group on decalin skeleton: first asymmetric total synthesis of 1[α],6[α]-dihydroxy-eudesm-3-ene. *Tetrahedron* **2004**, *60*, 6177-6182.

(4) Aladro, F. J. Guerra, F. M. Moreno-Dorado, F. J. Bustamante, J. M. Jorge, Z. D.; Massanet, G. M. Enantioselective synthesis of (+)-decipienin A. *Tetrahedron* **2001**, *57*, 2171-2178.

(5) Wender, P. A.; Mucciaro, T. P. A new and practical approach to the synthesis of taxol and taxol analogs: the pinene path. *Journal of the American Chemical Society* **1992**, *114*, 5878-5879.

(6) Bartok, W. Rosenfeld, D. D.; Schriesheim, A. Anionic Oxidation of Heterocyclic Nitrogen Bases and the Effect of Solvent on Such Reactions *The Journal of Organic Chemistry* **1963**, *28*, 410-412.

(7) Gardner, J. N. Carlon, F. E.; Gnoj, O. One-step procedure for the preparation of tertiary α-ketols from the corresponding ketones. *The Journal of Organic Chemistry* **1968**, *33*, 3294-3297.

(8) Magnus, P. Ujjainwalla, F. Westwood, N.; Lynch, V. Taxane diterpenes 4: Autoxidation, epimerization and isomerization for the introduction of functionality into the taxane ABC ring system. *Tetrahedron* **1998**, *54*, 3069-3092.

(9) Beckwith, A. L. J. Davies, A. G. Davison, I. G. E. Maccoll, A.; Mruzek, M. H. The mechanisms of the rearrangements of allylic hydroperoxides: 5[α]-hydroperoxy-3[β]-hydroxycholest-6-ene and 7[α]- hydroperoxy-3[β]-hydroxycholest-5-ene. *J. Chem. Soc., Perkin Trans. 2* **1989**, 815-824.

(10) Aav, Riina; Kanger, Tonis; Pehk, Tonis; Lopp, Margus Oxidation of Substitutes Cycyclo [4.4.0] decen-3-ones. *Proc. Estonian Acad. Sci. Chem.* **2001**, *3*, 138-146.

(11) Alam, Zafar; Ahman, Mohammad; Khan, Najm The Allylic Acetoxylation of Steroidal Enones. *Journal of Chemical Research* 288-289.

(12) Shimizu, Takeshi; Hrianuma, Sayoko; Yoshioka, Hirosuke Regio- and Steroselective Functionalizations of the Wieland-Miesher Ketone Derivatives at the C-8 Position. *Chemical and Pharmaceutical Bulletin* **1989**, *37*, 1963.

(13) Ojima, I.; Kogure, T. Selective reduction of α,β-unsaturated terpene carbonyl compounds using hydrosilane-rhodium(I) complex combinations. *Tet. Lett.* **1972**, *13*, 5035-5038.

(14) Anwar, S.; Davis, A. P. The application of difunctional organosilicon compounds to organic synthesis; 1,3-asymmetric induction in the reduction of [β]-hydroxy-ketones. *J. Chem. Soc., Chem. Commun.* **1986**, 831-832.

(15) Anwar, S. Bradley, G.; Davis, A. P. 1,3-versus 1,2-Asymmetric induction in the reduction of β-hydroxy ketones by intramolecular hydrosilylation. *J. Chem. Soc., Perkin Trans. 1* **1991**, 1383-1389.

(16) Mu, R. Liu, Z. Liu, Z. Yang, L. Wu, L.; Liu, Z.-L. A Metal-Free Catalytic Reduction of α,β-Unsaturated Carbonyl Compounds with Phenyldimethylsilane. *J. Chem. Res.* **2005**, *7*, 469-470.

(17) Solomon, M. Jamison, W. C. L. McCormick, M. Liotta, D. Cherry, D. A. Mills, J. E. Shah, R. D. Rodgers, J. D.; Maryanoff, C. A. Ligand-assisted nucleophilic additions. Control of site and face attack of nucleophiles on 4-oxido enones. *Journal of the American Chemical Society* **1988**, *110*, 3702-3704.

(18) Tsuda, T. Fujii, T. Kawasaki, K.; Saegusa, T. Copper(i)-catalysed conjugate reduction of [α][β]-unsaturated carbonyl compounds by lithium aluminium hydride. *J. Chem. Soc., Chem. Commun.* **1980**, 1013-1014.

(19) Overman, L. E. Ricca, D. J.; Tran, V. D. Total Synthesis of (±)-Scopadulcic Acid B. *Journal of the American Chemical Society* **1997**, *119*, 12031-12040.

(20) Paquette, L. A. Yang, J.; Long, Y. O. Concerning the Antileukemic Agent Jatrophatrione: The First Total Synthesis of a [5.9.5] Tricyclic Diterpene. *Journal of the American Chemical Society* **2002**, *124*, 6542-6543.

(21) Brown, H. C.; Shoaf, C. J. Selective Reductions. III. Further Studies of the Reaction of Alcohols with Lithium Aluminum Hydride as a Route to the Lithium Alkoxyaluminohydrides. *Journal of the American Chemical Society* **1964**, *86*, 1079-1085.

(22) Ashby, E. C. Dobbs, F. R.; Hopkins, H. P. Composition of lithium aluminum hydride, lithium borohydride, and their alkoxy derivatives in ether solvents as

determined by molecular association and conductance studies. *Journal of the American Chemical Society* **1975**, *97*, 3158-3162.

(23) Olah, G. A. Fung, A. P.; Malhotra, R. Synthetic Methods and Reactions; 991. Preparation of Cyclic Ethers over Superacidic Perfluorinated Resinsulfonic Acid (Nafion-H) Catalyst. *Synthesis* **1981**, *1981*, 474,476.

(24) Galynker, I.; Still, W. C. A simple method for tosylation with inversion. *Tetrahedron Letters* **1982**, *23*, 4461-4464.

(25) Sakamoto, I. Kaku, H.; Tsunoda, T. *Chemical & Pharmaceutical Bulletin* **2003**, *51*, 474-476.

(26) Hioki, H. Motosue, M. Mizutani, Y. Noda, A. Shimoda, T. Kubo, M. Harada, K. Fukuyama, Y.; Kodama, M. Total Synthesis of Pseudodehydrothyrsiferol. *Org. Lett.* **2009**, *11*, 579-582.

(27) Lauwers, M. Regnier, B. Van Eenoo, M. Denis, J. N.; Krief, A. Diphosphorus tetraiodine (P2I4) a valuable reagent for regioselective synthesis of iodoalkanes from alcohols. *Tet. Lett.* **1979**, *20*, 1801-1804.

(28) Gillis, B. T.; Beck, P. E. Formation of Tetrahydrofuran Derivatives from 1,4-Diols in Dimethyl Sulfoxide1. *The Journal of Organic Chemistry* **1963**, *28*, 1388-1390.

Chapter 4: Experimental Section

4.1 General Information

All moisture sensitive reactions were performed under an atmosphere of dry Ar, with glassware pre-dried at 125 °C. THF was dried via distillation over Na/benzophenone and ^{t}BuOH by distillation over Na(m). All other reagents or solvents were used as received, without further purification, unless otherwise stated. Infrared spectra were recorded on a Nicolet FT-IR spectrophotometer in methylene chloride. ^{1}H and ^{13}C NMR spectra were recorded on a QE 300, Varian Unity+ 300 spectrometer at 300 or 600 MHz and 75 or 150 MHz, respectively, and are reported in ppm relative to tetramethylsilane. All NMR spectra were taken with $CDCl_3$ as solvent unless otherwise noted. Mass spectra were obtained on a VG ZAB2E or a Finnigan TSQ70. Column chromatographic separations were carried out on silica gel (SilicaGel 60, 230-400 mesh) under pressure.

4.2 Experimental Conditions and Compound Data

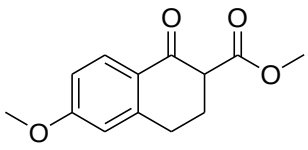

54

α-β Keto ester (54). Sodium hydride (60% suspension in mineral oil, 3.4g, 85 mmol) was added to methyl carbonate (71.0 mL, 740 mmol) under argon. After about 0.5 h tetralone **22** (10.0 g, 56.8 mmol) was added to this suspension. The reaction mixture was heated to about 80 °C for about 5 h. The reaction mixture was allowed to cool to ambient temperature and acidified with an aqueous solution of HCl (2M). The aqueous layer was then extracted with EtOAc (3 x 50 mL). The organic layers were combined, washed with a saturated aqueous solution of $NaHCO_3$ and brine, and dried over Na_2SO_4. The solvent was removed under reduced pressure to afford dark brown solid (13.3 g, 56.8 mmol). The crude mixture was carried on to the next step. IR (thin film) 2950, 1740, 1676, 1600 cm^{-1}; ^1H NMR (300 MHz, $CDCl_3$): δ 8.03 (1H, d, *J* = 6.9 Hz), 6.85 (1H, dd, *J* = 6.9, 1.8 Hz), 6.70 (1H, d, *J* = 1.8), 3.87 (3H, s), 3.79 (3H, s), 3.61-3.57 (1H, m), 3.04-2.96 (2H, m), 2.51-2.31 (2H, m); ^{13}C NMR (75 MHz, $CDCl_3$): δ 192.0, 171.1, 164.2, 146.4, 130.5, 125.5, 113.7, 112.8, 55.7, 54.4, 52.6, 28.2, 26.7; HRMS calcd. for $C_{13}H_{15}O_4$ [MH^+]: 235.097; found: 235.096

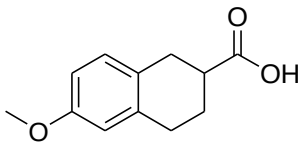

24

Carboxylic Acid 24. A crude mixture of **54** (56.8 mmol, crude), AcOH (140 mL), 10% Pd/C (3.00 g, 2.83 mmol) and 70% $HClO_4$ (5.0 mL, 83 mmol) was subjected to pressurized hydrogen gas (45 psi) for about 5 h. After about 5 h NaOAc (3.5 g, 43 mmol) was added and stirred for about 15 min. The resulting mixture was filtered over celite, and the filtrate was concentrated *in vacuo* to produce a light brown oil. The crude mixture was dissolved in MeOH (75 mL). To this was added a solution of KOH (7.0 g, 125 mmol), dissolved in H_2O (75 mL), and maintained at ambient temperature for about 7 h. The MeOH was removed under reduced pressure, and the resulting aqueous layer was washed with Et_2O (2 x 50 mL). The aqueous layer was then acidified with an aqueous solution of HCl (2M) and extracted with EtOAc (3 x 50 mL). The organic extracts were combined, washed with water and brine, and dried over Na_2SO_4. The solvent was then removed under reduced pressure to afford white solid **24** (9.8 g, 84% yield over two steps). IR (thin film) 2935, 2838, 1688, 1609 cm^{-1}; ^1H NMR (300 MHz, $CDCl_3$): δ 7.05 (1H, d, *J* = 8.4 Hz), 6.73 (1H, d, *J* = 8.4 Hz), 6.66 (1H, br s,), 3.80 (3H, s), 3.07-2.77 (5H, m), 2.28–2.24 (1H, m), 1.99–1.87 (1H, m); ^{13}C NMR (75 MHz, $CDCl_3$): δ 182.1, 158.0, 136.9, 130.2, 126.9, 113.6, 112.5, 55.5, 40.3, 30.9, 28.9, 25.8; 176.6, 156.7, 136.1, 129.0, 126.4, 112.5, 111.3, 54.3, 39.1, 30.0, 27.9, 24.9; HRMS calcd for $C_{12}H_{15}O_3$ [MH^+]: 207.1021; found: 207.1023.

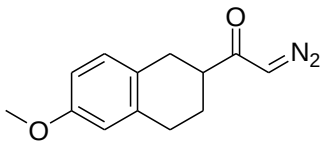

57

Diazoketone 57. Carboxylic acid **24** (4.00 g, 19.3 mmol) was dissolved in $SOCl_2$ (21 mL, 289 mmol) and stirred under argon for about 5 h at ambient temperature. The thionyl chloride was removed under reduced pressure, and the resulting mixture was concentrated under vacuum (5mm). The residue was dissolved in Et_2O (20 mL) and added to a freshly prepared solution of diazomethane (3.42 g, 81.5 mmol) in Et_2O (150 mL) at about 0°C. The reaction was maintained at about 0°C for about 30 min. The reaction mixture was allowed to warm to ambient temperature and then gently refluxed for about 1 h. The solvent was then removed under reduced pressure to produce diazoketone **57** as a yellow solid (4.73 g, 19.3 mmol). The diazoketone was immediately carried on to the next reaction. IR (thin film) 3092, 2932, 2837, 2103, 1636 cm^{-1}; ^1H NMR (300 MHz, $CDCl_3$): δ 7.02 (1H, d, *J* = 8.4 Hz), 6.72 (1H, dd, *J* = 8.3, 2.7 Hz), 6.65 (1H, d, *J* = 2.4 Hz), 5.38 (1H, bs), 3.80 (3H, s), 2.93-2.83 (4H, m), 2.65 (1H, bs), 2.09–2.07 (1H, m), 1.87–1.85 (1H, m); ^{13}C NMR (75 MHz, $CDCl_3$): δ 197.7, 158.0, 137.0, 130.2, 127.2, 113.7, 112.5, 55.5, 54.1, 46.2, 31.3, 29.2, 26.3; HRMS calcd for $C_{13}H_{15}N_2O_2[MH^+]$: 231.1134; found: 231.1135

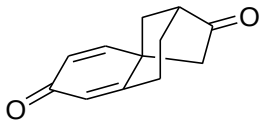

25

Dienone 25: Diazoketone **57** (4.73 g, 19.3 mmol, crude) was dissolved in DCM (20 mL) and cooled to about -10 °C. TFA (10 mL) was then added slowly and the reaction was maintained at about -10 °C for about 30 min. The reaction mixture was diluted with water (10 mL), removed from the cold bath, and neutralized with a saturated aqueous solution of $NaHCO_3$. The aqueous layer was extracted with DCM (3 x 30 mL). The organic extracts were then combined, washed with water and brine, and dried over Na_2SO_4. The mixture was filtered and the solvent was removed *in vacuo*. The crude product was purified by silica column chromatography (solvent gradient from 5/95 EtOAc/Hex to 60/40 EtOAc/Hex) to produce dienone **25** as a yellow solid (2.19 g, 60% yield over three steps). IR (thin film) 2953, 1745, 1661, 1624 cm^{-1}; ^1H NMR (300 MHz, $CDCl_3$): δ 6.75 (1H, d, *J* = 9.6 Hz), 6.19 (1H, dd, *J* = 9.6, 1.8 Hz), 5.98 (1H, d, *J* = 1.8 Hz), 2.61-2.11 (6H, m), 1.98-1.90 (1H, m), 1.66-1.60 (2H, m); ^{13}C NMR (75 MHz, $CDCl_3$): δ 216.3, 186.5, 163.0, 152.1, 129.0, 124.2, 48.8, 46.6, 46.3, 42.1, 29.3, 28.7; HRMS calcd. for $C_{12}H_{13}O_2$ [MH^+]: 189.0915; found: 189.0913.

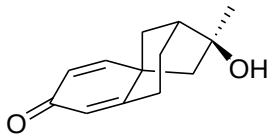

26

Tertiary alcohol 26. Dienone **25** (5.0 g, 27 mmol) was dissolved in anhydrous THF (78 mL) under argon and cooled to about -78 °C. To the solution was added 3.0 M MeMgCl in THF (27 mL, 80 mmol), and the reaction was maintained at about -78 °C for about 4 h. The reaction was removed from the cold bath, quenched with water (20 mL), and neutralized with a saturated aqueous solution of NH_4Cl. The aqueous layer was then extracted with EtOAc (3 x 50 mL). The organic layers were combined, washed with brine and dried over Na_2SO_4. The organic layer was then filtered and removed under reduced pressure. The crude mixture was purified through silica column chromatography (solvent gradient from 5/95 EtOAc/DCM to 50/50 EtOAc/DCM). Tertiary alcohol **26** was obtained as a pale yellow solid (3.42 g, 63% yield). IR (thin film) 3403, 2955, 2936, 2860, 1654, 1615, 1599 cm^{-1}; ^1H NMR (300 MHz, $CDCl_3$): δ 6.68 (1H, d, J = 9.6 Hz), 6.22 (1H, d, J = 9.9 Hz), 6.03 (1H, s), 2.98-2.86 (1H, m), 2.43 (1H, dd, J = 15.9, 6.3 Hz), 2.28-2.17 (2H, m), 2.00 (1H, d, J = 14.4 Hz), 1.89 (1H, dd, J = 14.3, 2.4 Hz), 1.61-1.56 (1H, m), 1.55 (3H, s), 1.50 (1H, dd, J = 11.1, 2.1 Hz); ^{13}C NMR (75 MHz, $CDCl_3$) δ 187.4, 169.3, 154.6, 129.0, 122.1, 80.0, 51.2, 49.3, 46.8, 44.7, 33.1, 30.3, 28.1; HRMS calcd. for $C_{13}H_{17}O_2$ [MH^+]: 205.1229 found 205.1231.

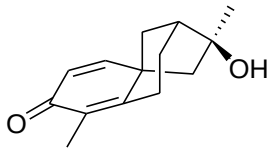

58

α-Methyl dienone 58. Dienone **26** (3.00 g, 14.7 mmol) was dissolved in anhydrous ^{t}BuOH (48 mL) under argon. To the reaction mixture ^{t}BuOK (3.62 g, 32.3 mmol) was added and the resulting solution was stirred at ambient temperature for about 1 h. Freshly distilled MeI (0.91 mL, 14.7 mmol) was added and the reaction mixture was maintained at ambient temperature for about 1 h. The resulting mixture was quenched with water (15 mL) and then neutralized with an aqueous solution of HCl (1M). The aqueous layer was extracted with EtOAc (3 x 35 mL). The organic extracts were combined, washed with brine, and dried over Na_2SO_4. The organic layer was then filtered and the solvent removed in *vacuo*. The crude mixture was purified by silica column chromatography (solvent gradient from 5/95 EtOAc/Hex to 40/60 EtOAc/Hex). Methyl dienone **58** was obtained as pale yellow solid (1.96 g, 61%). IR (thin film) 2953, 2924, 2852, 1653, 1616, 1599 cm^{-1}; ^{1}H NMR (300 MHz, $CDCl_3$): δ 6.61 (1H, d, *J* = 10.2 Hz), 6.23 (1H, d, *J* = 9.6 Hz), 2.81 (1H, dd, *J* = 16.2, 9 Hz), 2.74-2.67 (1H, m), 2.27-2.06 (3H, m), 1.97 (1H, d, *J* = 14.7 Hz), 1.88 (3H, s), 1.84 (1H, dd, *J* = 14.7, 3.0 Hz), 1.67-1.54 (1H, m), 1.53 (3H, s), 1.48 (1H, dd, *J* = 11.1, 2.4 Hz); ^{13}C NMR (75 MHz, $CDCl_3$): δ 165.6, 160.6, 153.9, 127.8, 79.7, 51.4, 48.7, 46.3, 43.9, 32.7, 29.6, 27.3, 25.8, 10.4; HRMS calcd. for $C_{14}H_{19}O_2$ [MH^+]: 219.3148 found 219.3149.

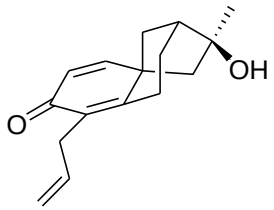

60

α-Allyl dienone 60. Dienone **26** (200 mg, 0.98 mmol) was dissolved in anhydrous ^{t}BuOH (5 mL) under argon. To the reaction mixture ^{t}BuOK (242 mg, 2.16 mmol) was added, and the resulting solution was stirred at ambient temperature for about 1 h. Allyl bromide (0.09 mL, 0.98 mmol) was added, and the reaction mixture was maintained at ambient temperature for about 4 h. The reaction was quenched with water (5 mL) and neutralized with an aqueous solution of HCl (1M). The aqueous layer was extracted with EtOAc (3 x 15 mL). The organic extracts were combined, washed with brine, and dried over Na_2SO_4. The organic layer was then filtered, and the solvent removed in *vacuo*. The crude mixture was purified by silica column chromatography (solvent gradient from 5/95 EtOAc/Hex to 60/40 EtOAc/Hex). Allyl dienone **60** was obtained as pale yellow solid (160.4 mg, 67%). IR (thin film) 3421, 2961, 2864, 1654, 1616, 1597 cm^{-1}; ^{1}H NMR (300 MHz, $CDCl_3$): δ 6.63 (1H, d, *J* = 9.6 Hz), 6.23 (1H, d, *J* = 9.3 Hz), 5.84-5.75 (1H, m), 4.95 (1H, s), 4.95 - 4.89 (1H, m), 3.18-3.16 (2H, m), 2.75-2.68 (2H, m), 2.35 - 2.09 (3H, m), 1.97 (1H, d, *J* = 14.4), 1.90 (1H, dd, *J* = 14.4, 2.1 Hz), 1.53 (3H, s), 1.49 – 1.45 (2H, m); ^{13}C NMR (75 MHz, $CDCl_3$): δ 185.9, 163.0, 154.4, 135.0, 128.9, 128.2, 114.5, 80.1, 51.7, 49.2, 46.6, 44.6, 32.9, 28.7, 27.9, 26.1; HRMS calcd. for $C_{16}H_{21}O_2$ [MH^+]: 245.1545 found 245.1542.

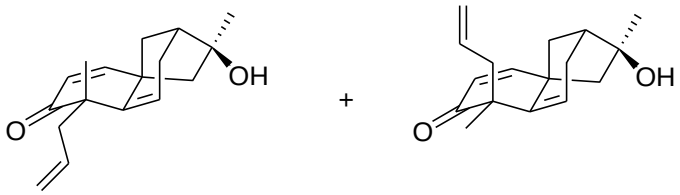

61 **65**

Enones 61 and 65. Dienone **26** (459 mg, 2.11 mmol) was dissolved in anhydrous ^{t}BuOH (24 mL). To the reaction mixture ^{t}BuOK (1.71g, 6.31 mmol) was added, and the resulting solution was maintained at ambient temperature under argon for 1 h. The solution was treated with allyl bromide (0.36 mL, 4.21 mmol) and the resulting solution was refluxed in a sealed tube for about 1 h. The reaction was then quenched with water (15 mL) and neutralized with a saturated aqueous solution of NH_4Cl. The aqueous layer was then extracted with EtOAc (3 x 30 mL). The organic layers were combined, washed with brine, and dried over Na_2SO_4. The organic layer was filtered, and the solvent was removed under reduced pressure. The crude mixture was purified by silica column chromatography (1:3 EtOAc/Hex). Products **61** and **65** were obtained as white crystals in a 1:3 diastereomeric ratio (521 mg, 95% yield).

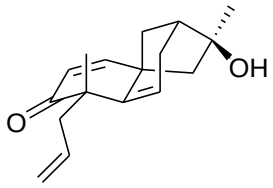

61

61: IR (thin film) 3452, 2966, 2928, 2865, 1671, 1652 cm^{-1}; ^{1}H NMR (300 MHz, $CDCl_3$): δ 6.43 (1H, d, *J* = 9.0 Hz), 5.86 (1H, d, *J* = 10.2 Hz), 5.54-5.49 (2H, m), 4.92 (2H, m), 2.72 (1H, dd, *J*= 14.7, 6.0 Hz), 2.51 (1H, dd, *J*= 17.7, 3.6 Hz), 2.41 (1H, dd, *J* = 15.3, 7.2 Hz), 2.28-2.10 (5H, m), 1.86 (1H, d, *J* = 14.1 Hz), 1.8 (1H, d, *J* = 5.1 Hz), 1.74 (1H, dd, *J* = 11.1, 3.0 Hz), 1.37 (3H, s), 1.25 (3H, s); ^{13}C NMR (75 MHz, $CDCl_3$): δ

201.9, 153.3, 144.3, 135.2, 126.1, 121.2, 116.7, 79.8, 57.1, 50.1, 45.5, 44.2, 42.9, 40.0, 31.4, 31.3, 29.0; HRMS calcd. for $C_{17}H_{22}O_2$ [MH^+]: 259.1698 found 259.1701.

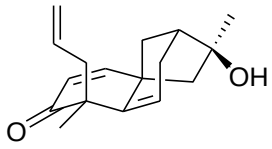

65

65: IR (thin film) 3471, 2962, 2926, 2870, 1672, 1653 cm^{-1}; ^1H NMR (300 MHz, $CDCl_3$): δ 6.49 (1H, d, *J* = 9.6 Hz), 5.92 (1H, d, *J* = 10.2 Hz), 5.68-5.62 (1H, m), 5.49 (1H, t,), 5.12-4.99 (2H, m), 2.60-2.53 (1H, m), 2.36- 2.19 (5H, m), 1.92-1.86 (2H, m), 1.74 (1H,dd, *J* = 11.1, 3.6 Hz), 1.45 (3H, s), 1.21 (3H, s); ^{13}C NMR (75 MHz, $CDCl_3$): δ 202.1, 153.2, 143.2, 133.2, 125.4, 121.3, 118.5, 79.9, 55.4, 51.4, 45.2, 45.2 44.7, 43.5, 31.3, 29.2, 17.7; HRMS calcd. for $C_{17}H_{22}O_2$ [MH^+]: 259.1698. Found 259.1699.1756

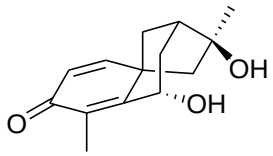

74

γ-Hydroxy dienone 74. A biphasic system was prepared by dissolving KOH (1 g, 17.8 mmol) in ^{t}BuOH (4.5 g) and water (4.5 mL). A portion of the aqueous layer (2 mL) and a portion of the organic layer (2 mL) were combined and treated with compound **58** (100 mg, 0.46 mmol) at ambient temperature. Following dissolution of **58**, the mixture was treated with $N(n\text{-}Bu)_4Br$ (147.7 mg, 0.46 mmol) and maintained at ambient temperature, open to atmosphere, for about 2 days. The reaction mixture was then diluted with water (5 mL) and neutralized with an aqueous solution of HCl (1 M). The aqueous layer was extracted with EtOAc (3x10 mL). The organic layers were combined, washed with brine, and dried over Na_2SO_4. The crude mixture was filtered and the solvent removed under reduced pressure. After column chromatography (solvent gradient from 5/95 EtOAc/DCM to 40/60 EtOAc/DCM), hydroxyl dienone **74** was obtained as a white solid (69.8 mg, 65%). IR (thin film) 3293, 2965, 2928, 2868, 1656, 1618 cm^{-1}; ^{1}H NMR (300 MHz, $CDCl_3$): δ 6.65 (1H, d, *J* = 9.6 Hz), 6.24 (1H, d, *J* = 9.6 Hz), 5.17 (1H, br), 4.97 (1H, d, *J* = 6.0 Hz), 4.85 (1H, br), 2.42 (1H, d, *J* = 15.3 Hz), 2.22-2.17 (2H, m), 2.12-2.02 (2H, m), 1.96 (3H, s), 1.93-1.84 (3H, m), 1.49 (3H, s); ^{13}C NMR (75 MHz, $CDCl_3$): δ 187.6, 157.4, 155.7, 131.5, 127.7, 79.2, 65.0, 50.9, 48.1, 46.6, 43.7, 35.1, 31.2, 10.7; HRMS calcd. for $C_{14}H_{19}O_3$ [MH^+] 235.1334. Found 235.1334.

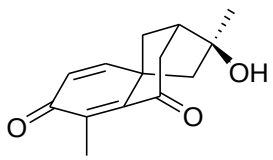

76

Ketone 76. IR (thin film) 3447, 2959, 2925, 2853, 1696, 1653, 1623 cm^{-1}; ^{1}H NMR (300 MHz, $CDCl_3$): δ 6.76 (1H, d, *J* = 10.2 Hz), 6.35 (1H, d, *J* = 9.9 Hz), 3.13 (1H, d, *J* = 16.2 Hz), 2.51-2.35 (3H, m), 2.31 (1H, s) 2.09 (3H, s), 1.99 (1H, dd, *J* = 12.3, 2.6 Hz). 1.87 (1H, dd, *J* = 15.0, 2.6 Hz), 1.55 (3H, s); ^{13}C NMR (75MHz, $CDCl_3$): δ 202.2, 186.9, 153.5, 152.2, 134.8, 128.4, 79.8, 51.5, 49.7, 46.9, 46.2, 43.5, 32.1, 10.7; HRMS calcd. for $C_{14}H_{17}O_3$ [MH^+] 233.1178. Found 233.1181.

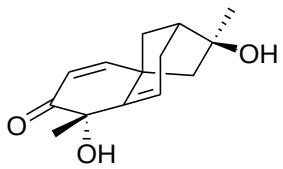

77

α-Hydroxy enone 77. IR (thin film) 3376, 2925, 2856, 1683, 1652 cm^{-1}; ^{1}H NMR (600 MHz, $CDCl_3$): δ 6.57 (1H, d, *J* =4.8 Hz), 6.03 (1H, d, *J* = 4.8 Hz), 5.95 (1H, t, *J* = 0.9 Hz), 2.97 (1H, bs), 2.61-2.56 (1H, m), 2.44-2.55 (1H, bs), 2.27-2.23 (2H, m), 2.16 (1H, dd, *J* = 7.5, 1.5 Hz), 1.91 (1H, d, *J* = 6.9 Hz), 1.88-1.85 (1H, m), 1.74 (1H, dd, *J* = 5.7, 1.8 Hz), 1.47 (3H, s), 1.38 (3H, s); ^{13}C NMR (150 MHz, $CDCl_3$): δ 198.1, 154.1, 143.3, 125.2, 124.8, 79.6, 74.0, 57.8, 45.8, 45.0, 42.3, 31.5, 29.3, 23.8; HRMS calcd. for $C_{14}H_{19}O_3$ [MH^+] 235.1334. Found 235.1338.

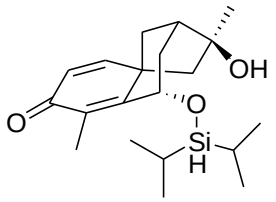

81

Silyloxy dienone 81. A solution of $^{i}Pr_2SiHCl$ (0.09mL, 0.52mmol), DMAP (20mg, 17 mmol), Et_3N (0.072 mL, 17 mmol) dissolved in DCM (8 mL) was added a solution of γ-hydroxy dienone **74** (100 mg, 0.13 mmol) in DCM (6 mL) *via* syringe. The reaction was maintained at ambient temperature for about 12 h. The reaction was then diluted with water (15 mL) and extracted with DCM (3 x 15 mL). The organic layers were combined, washed with brine, and dried over Na_2SO_4. The solvent was removed under reduced pressure and purified by column chromatography (5:95 EtOAc/Hex). The silyloxy dienone was obtained as a yellow solid (119 mg, 99%). IR (thin film) 3290, 2940, 2865, 2100, 1653, 1617 cm^{-1}; ^{1}H NMR (300 MHz, $CDCl_3$): δ 6.62 (1H, d, *J* =9.9 Hz), 6.27 (1H, d, *J* = 9.9 Hz), 4.99 (1H, d, *J* = 6.0 Hz), 4.23 (1H, s), 2.44 (1H, d, 15.3), 2.23-2.18 (2H, m), 2.14-2.03 (3H, m), 1.99 (3H, s), 1.95-1.87 (1H, m) 1.51 (3H, s) 1.11-0.98 (14H, m); ^{13}C NMR (75 MHz, $CDCl_3$): δ 187.5, 157.2, 155.4, 131.6, 127.8, 79.2, 65.2, 51.9, 48.0, 46.6, 43.6, 35.0, 31.3, 17.4, 12.9, 10.7; HRMS calcd. for $C_{20}H_{33}O_3Si$ [MH^+] 349.2199. Found 349.2198.

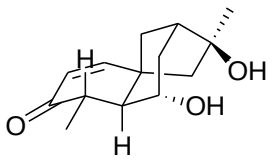

84

Enone 84. Dienone **74** (50 mg, 0.21 mmol) was dissolved in THF (2.13 mL) and cooled to about -78^{o}C under an atmosphere of argon. To the resulting solution was added $LiAH_2$•$(OEt)_2$ (0.12 mL, 1.8 M, 0.21 mmol). After about 0.5 h the reaction was quenched with MeOH (5mL) and diluted with water (10 mL). The solution was neutralized with an aqueous solution of HCl (1M). The resulting solution was extracted with EtOAc (3x10 mL). The organic layers were combined, washed with brine, and dried over Na_2SO_4. The solvent was removed *in vacuo* and to give pale yellow oil. The crude mixture was purified by column chromatography (5-50% EtOAc/DCM) to provide a mixture (2:1) of enone **84** and dienone **74** (48 mg, 64%) as a white solid. IR (thin film) 3280, 2964, 2927, 2874, 2855, 1670 cm^{-1}; ^{1}H NMR (300 MHz, $CDCl_3$): δ 6.63 (1H, d, *J* = 9.9 Hz), 5.93 (1H, d, *J* = 9.9 Hz), 4.15 (1H, d, *J* = 5.4 Hz), 2.44 (1H, d, *J* = 2.1 Hz), 2.39-2.2.29 (3H, m), 2.11-2.03 (2H, m), 1.91-1.83 (2H, m), 1.73-1.63 (2H, m), 1.46 (3H, s), 1.31-1.18 (3H, m); ^{13}C (75 MHz, $CDCl_3$): δ 20.2, 158.8, 127.8, 78.9, 67.2, 55.9, 53.5, 45.9, 44.6, 41.4, 37.4, 32.7, 31.4, 13.5; HRMS calcd. for $C_{14}H_{21}O_3$ [MH^+] 237.1491. Found 237.1491.

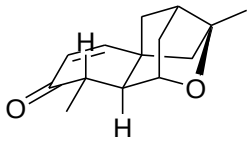

11

Cyclized enone 11. A mixture (2:1) of compounds **74** and **84** (50 mg, 0.13 mmol) was dissolved in DMSO (1 mL) and delivered to a microwave reaction vessel. The reaction was heated for about 1 h at 170 ^{o}C. The reaction was allowed to cool to ambient temperature, and water was added (3 mL). The resulting solution was extracted with Et_2O (3x10 mL). The organic layers were combined, washed with brine, and dried over Na_2SO_4. The solvent was removed under reduced pressure resulting in dark brown oil. The crude mixture was purified by column chromatography (solvent gradient from 0/100 EtOAc/hexanes to 30/70 EtOAc/hexanes) to give **11** (21 mg, 65%). IR (thin film) 2962, 2927, 2871, 1683 cm^{-1}; ^{1}H NMR (600 MHz, $CDCl_3$): δ 6.51(1H, d, *J*= 9.6 Hz), 5.90 (1H, d, *J* = 9.6 Hz), 4.33 (1H, t, *J* = 4.2 Hz), 2.37-2.30 (2H, m), 2.05 (1H, d, *J* = 13.8 Hz), 1.96-1.91 (1H, m), 1.92-1.88 (1H, m), 1.85 (1h, d, *J* = 11.4 Hz), 1.77 (1H, dd, *J*= 12, 3.6 Hz), 1.73-1.70 (1H, m), 1.6 (1H, d, *J* = 10.8), 1.42 (3H, s), 1.11 (3H, d, *J* = 6.6 Hz); ^{13}C NMR (75 MHz, $CDCl_3$): δ 201.6, 154.4, 128.4, 87.1, 77.9, 52.1, 48.8, 46.8, 44.6, 42.8, 41.5, 37.4, 23.3, 11.2. HRMS calcd. for $C_{14}H_{19}O_2$ [MH^+] 219.1385. Found 219.1384

4.3 Supporting Information

α-β keton ester (54)

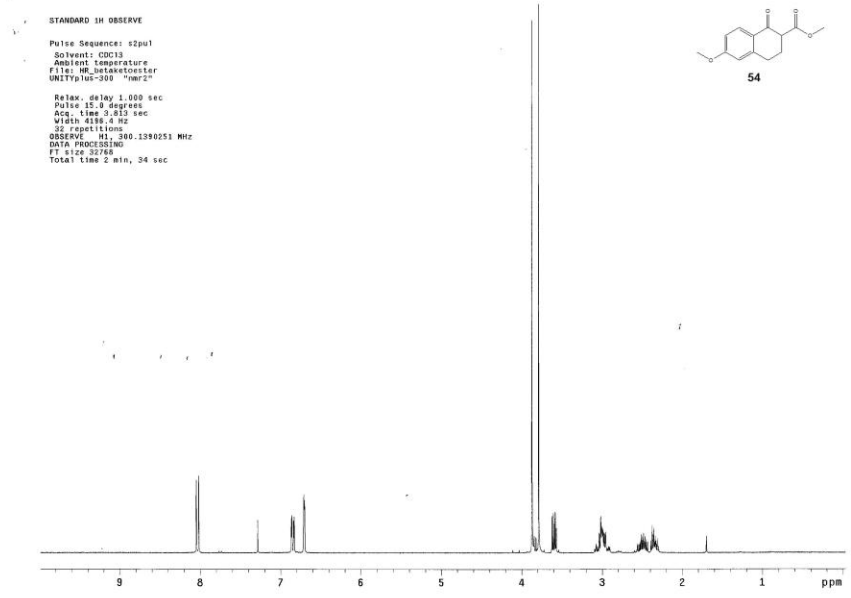

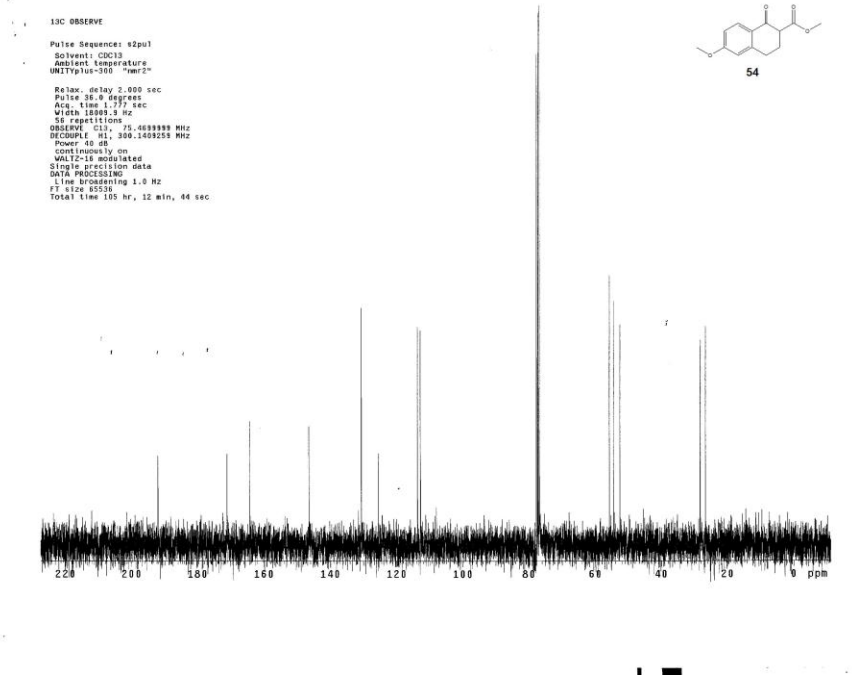

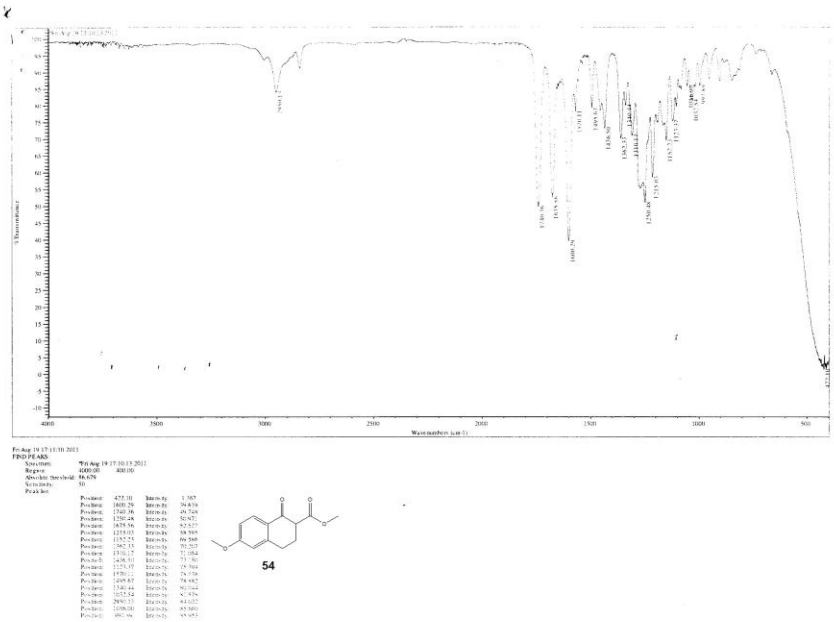

54

Carboxylic Acid 24

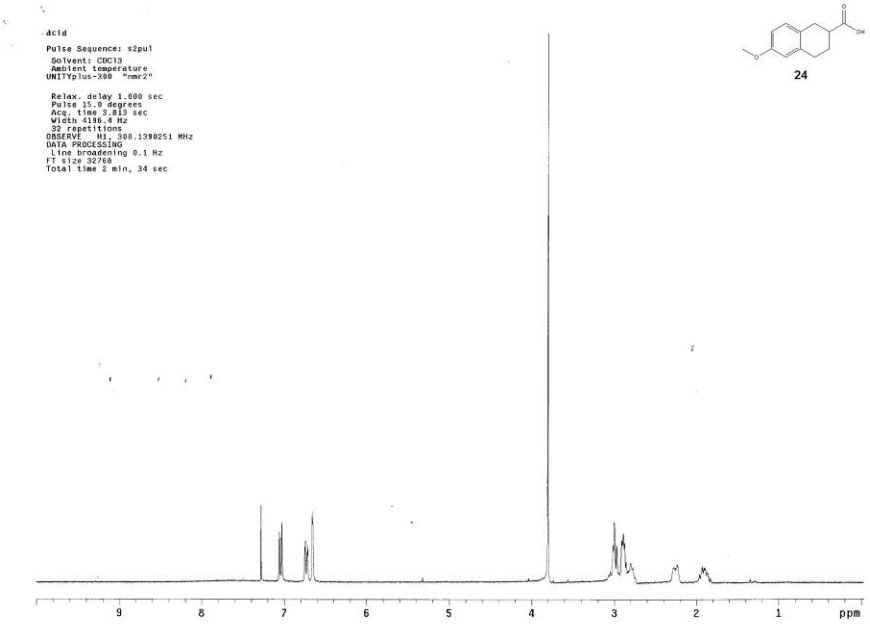

24

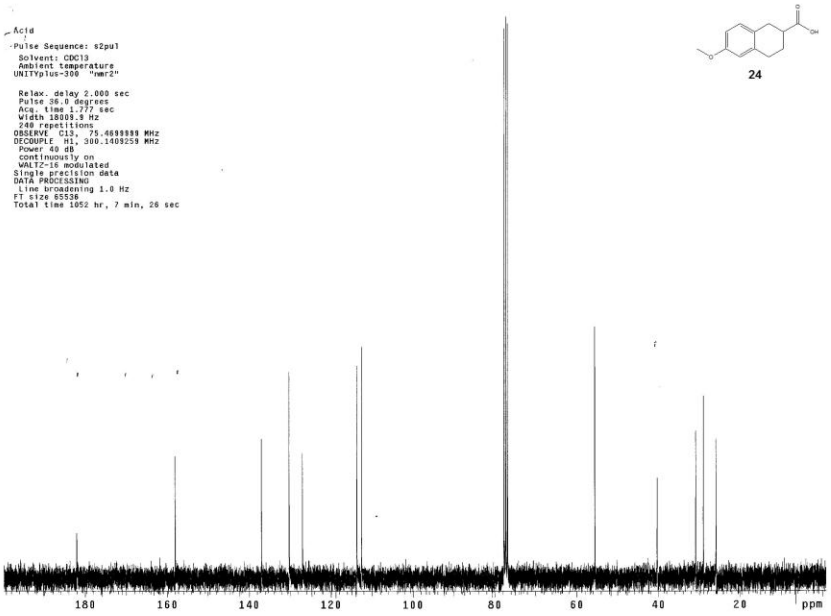
Acid
Pulse Sequence: s2pul
Solvent: CDCl3
Ambient temperature
UNITYplus-300 "nmr2"
Relax. delay 2.000 sec
Pulse 30.0 degrees
Acq. time 1.777 sec
Width 18009.9 Hz
240 repetitions
OBSERVE C13, 75.4699888 MHz
DECOUPLE H1, 300.1409259 MHz
Power 40 dB
continuously on
WALTZ-16 modulated
Single precision data
DATA PROCESSING
Line broadening 1.0 Hz
FT size 65536
Total time 1052 hr, 7 min, 26 sec
24
180
160
140
120
100
80
60
40
20
ppm


Acid
24

Diazoketone 57

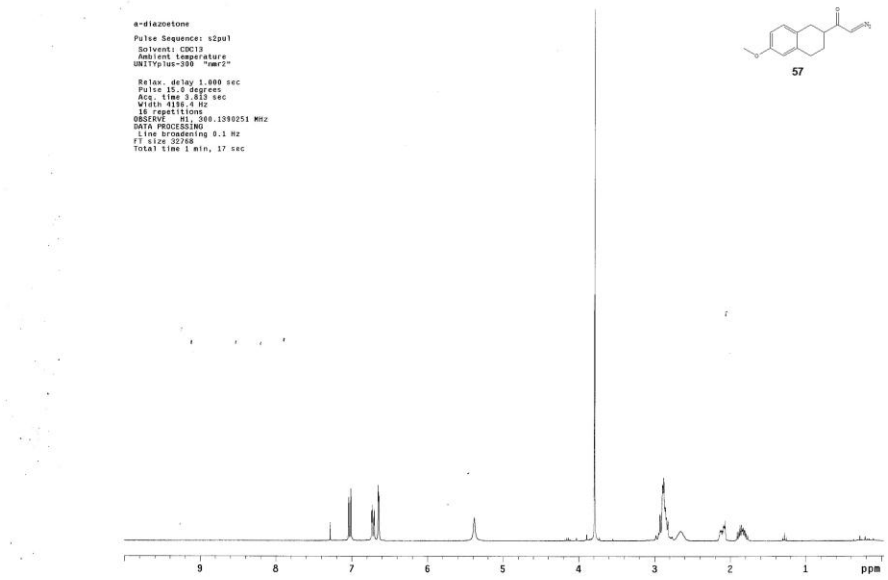

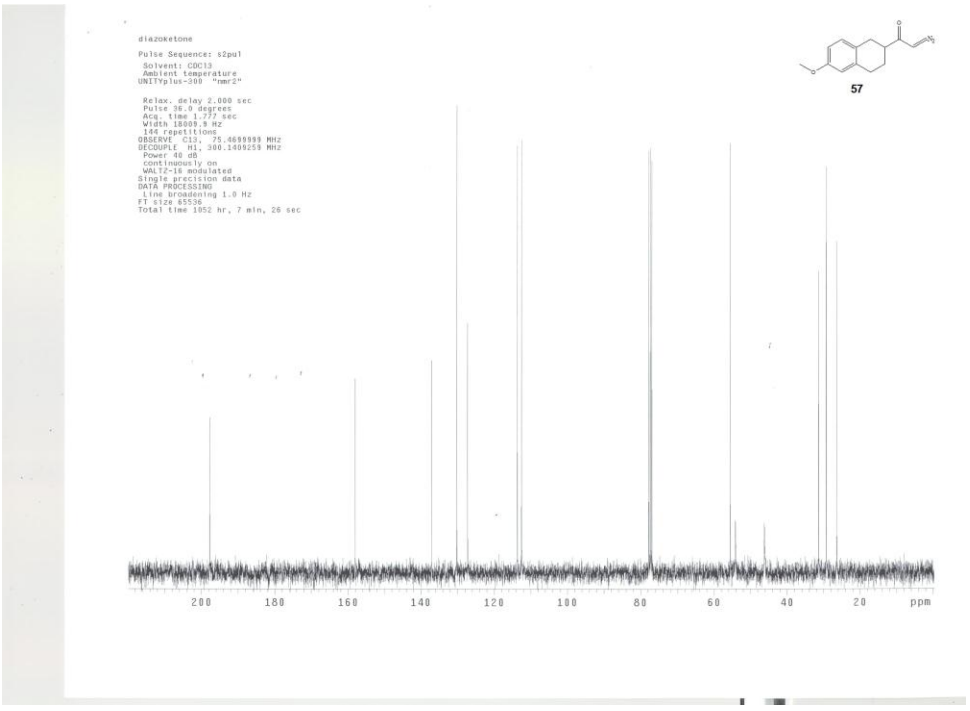

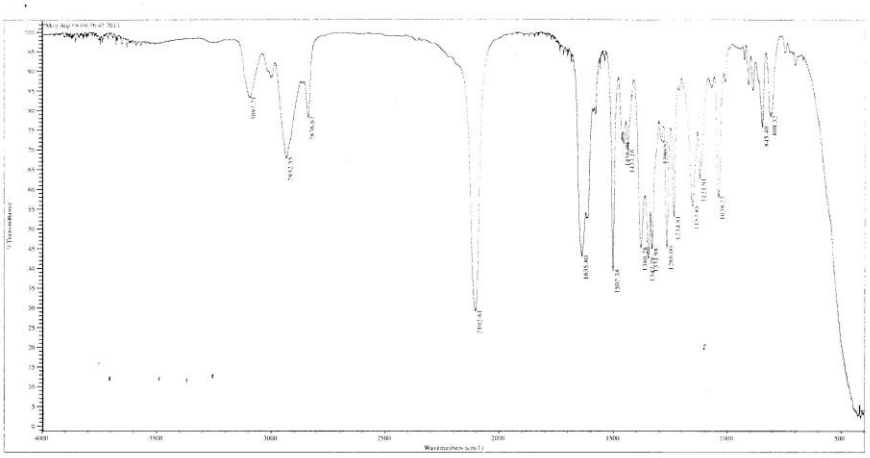

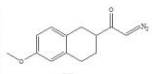

57

Dienone 25

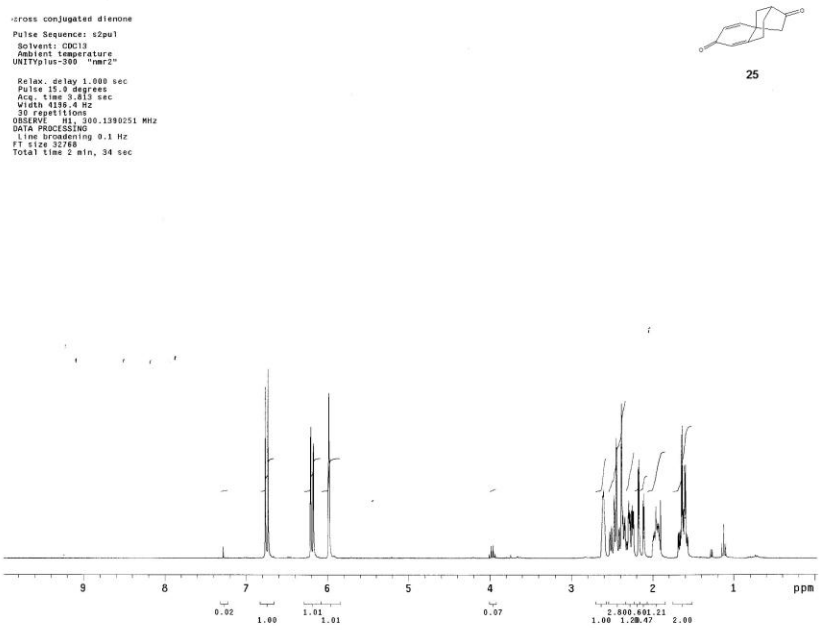
cross conjugated dienone
Pulse Sequence: s2pul
Solvent: CDCl3
Ambient temperature
UNITYplus-300 "nmr2"
Relax. delay 1.000 sec
Pulse 15.0 degrees
Acq. time 3.813 sec
Width 4186.4 Hz
30 repetitions
OBSERVE H1, 300.1390251 MHz
DATA PROCESSING
Line broadening 0.1 Hz
FT size 32768
Total time 2 min, 34 sec
25
9
8
7
6
5
4
3
2
1
ppm
0.02
1.00
1.01
1.01
0.07
1.00
1.20
0.47
1.21
2.00

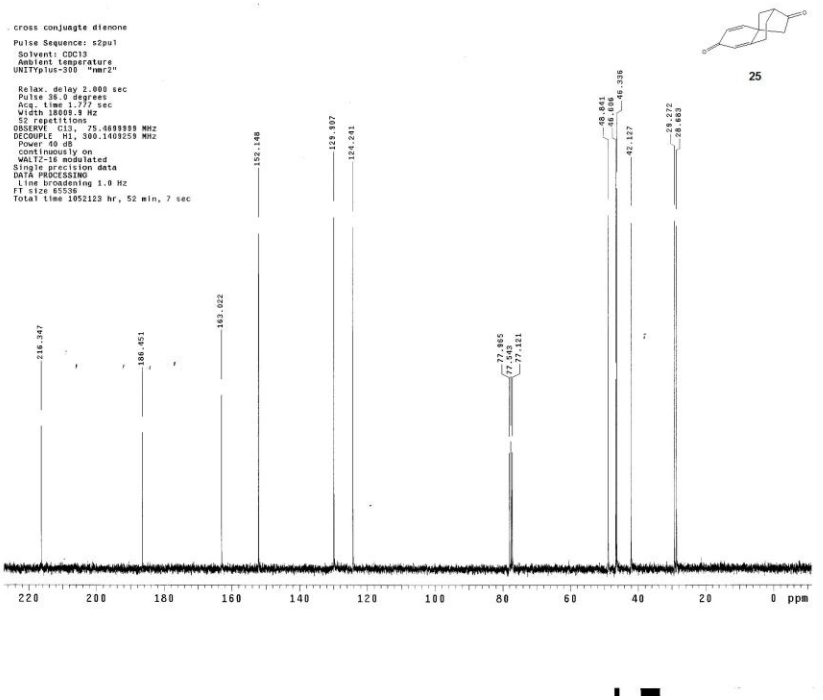
cross conjugte dienone
Pulse Sequence: s2pul
Solvent: CDCl3
Ambient temperature
UNITYplus-300 "nmr2"
Relax. delay 2.000 sec
Pulse 36.0 degrees
Acq. time 1.777 sec
Width 18009.9 Hz
52 repetitions
OBSERVE C13, 75.4699888 MHz
DECOUPLE H1, 300.1409259 MHz
Power 60 dB
continuously on
WALTZ-16 modulated
Single precision data
DATA PROCESSING
Line broadening 1.0 Hz
FT size 65536
Total time 1052123 hr, 52 min, 7 sec
25
216.347
186.451
163.022
152.148
129.907
124.241
77.465
77.143
77.121
48.841
48.686
46.336
42.127
28.272
28.083
220
200
180
160
140
120
100
80
60
40
20
0 ppm

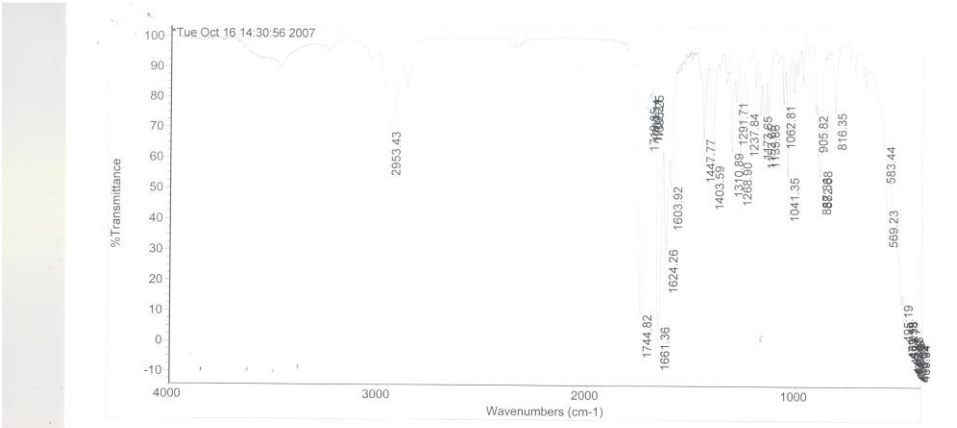

Tue Oct 16 14:33:05 2007
FIND PEAKS:
Spectrum: *Tue Oct 16 14:30:56 2007
Region: 4000.00 400.00
Absolute threshold: 82.130
Sensitivity: 100
Peak list:

Position:	409.34	Intensity:	-0.0045
Position:	418.02	Intensity:	-0.0582
Position:	424.99	Intensity:	0.0391
Position:	430.86	Intensity:	0.634
Position:	438.49	Intensity:	1.703
Position:	446.17	Intensity:	2.507
Position:	442.15	Intensity:	2.575
Position:	1661.36	Intensity:	5.285

25

Tertiary alcohol 26

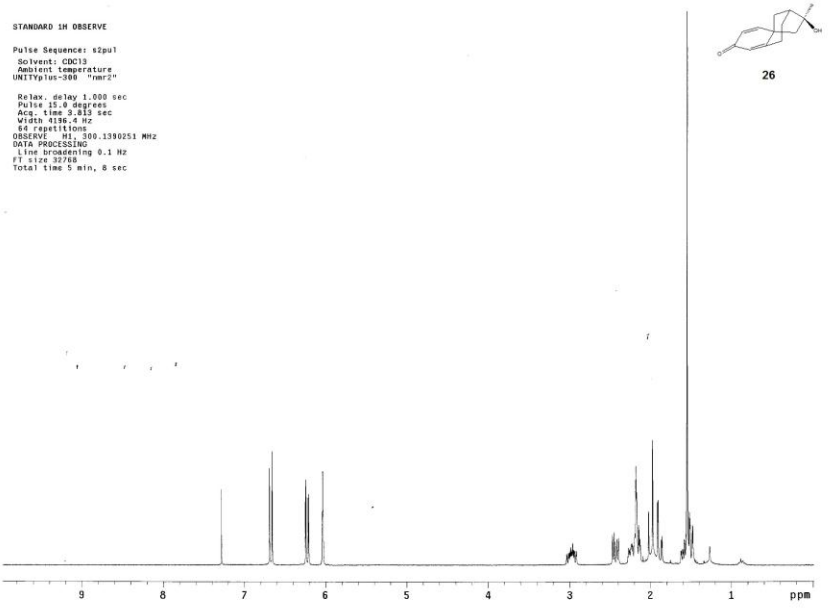

26

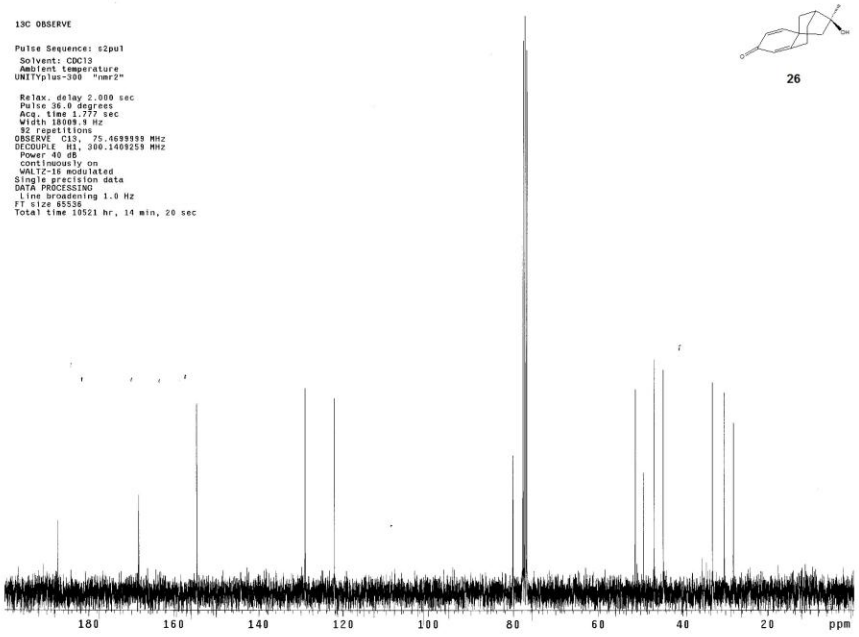
13C OBSERVE
Pulse Sequence: s2pul
Solvent: CDCl3
Ambient temperature
UNITYplus-300 "nmr2"
Relax. delay 2.000 sec
Pulse 36.0 degrees
Acq. time 1.777 sec
Width 18069.9 Hz
92 repetitions
OBSERVE C13, 75.4699998 MHz
DECOUPLE H1, 300.1409259 MHz
Power 40 dB
continuously on
WALTZ-16 modulated
Single precision data
DATA PROCESSING
Line broadening 1.0 Hz
FT size 65536
Total time 10521 hr, 14 min, 20 sec
26
180
160
140
120
100
80
60
40
20
ppm

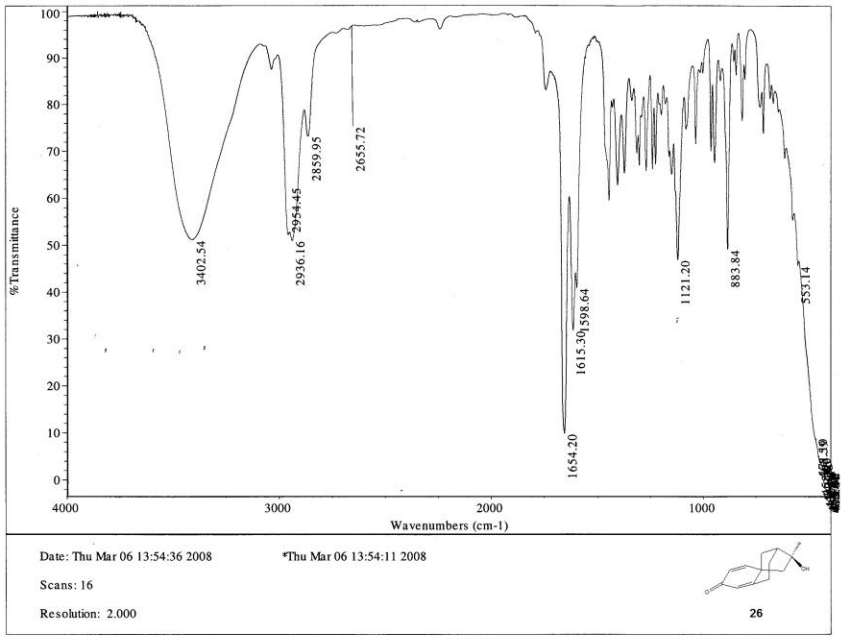
%Transmittance
Wavenumbers (cm-1)
3402.54
2936.16
2954.45
2859.95
2655.72
1654.20
1615.30
1598.64
1121.20
883.84
553.14
Date: Thu Mar 06 13:54:36 2008
*Thu Mar 06 13:54:11 2008
Scans: 16
Resolution: 2.000
26

α-Methyl dienone 58

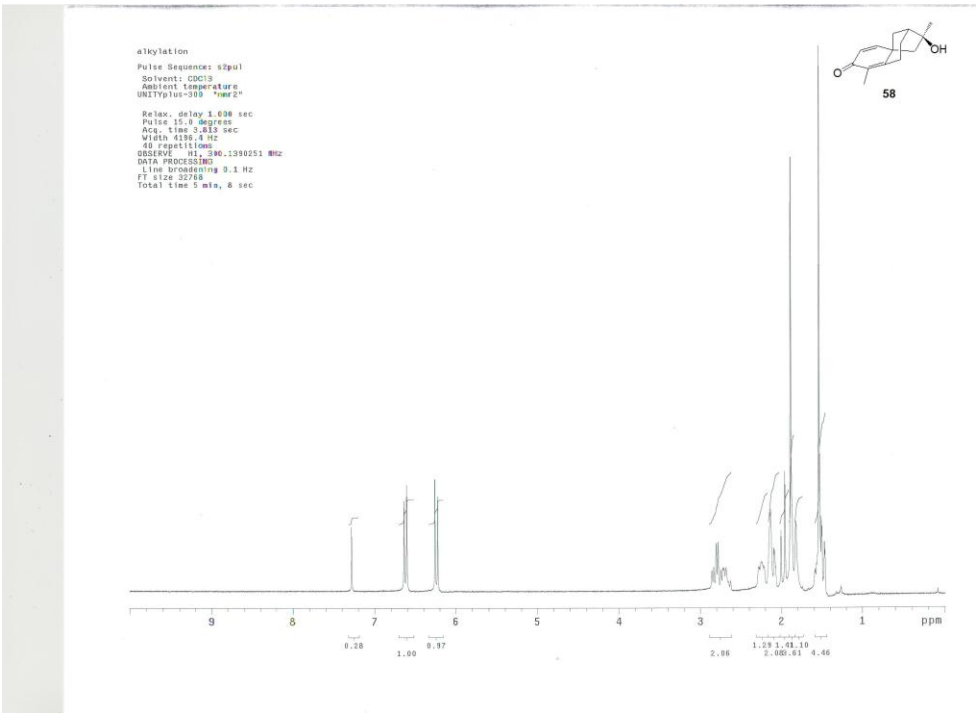

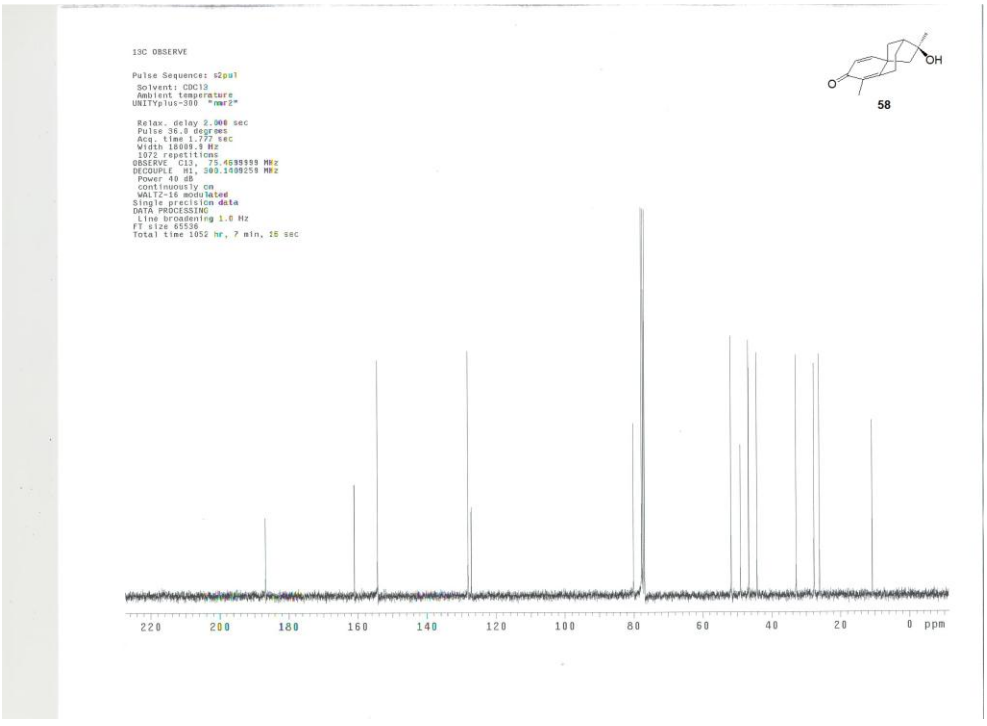

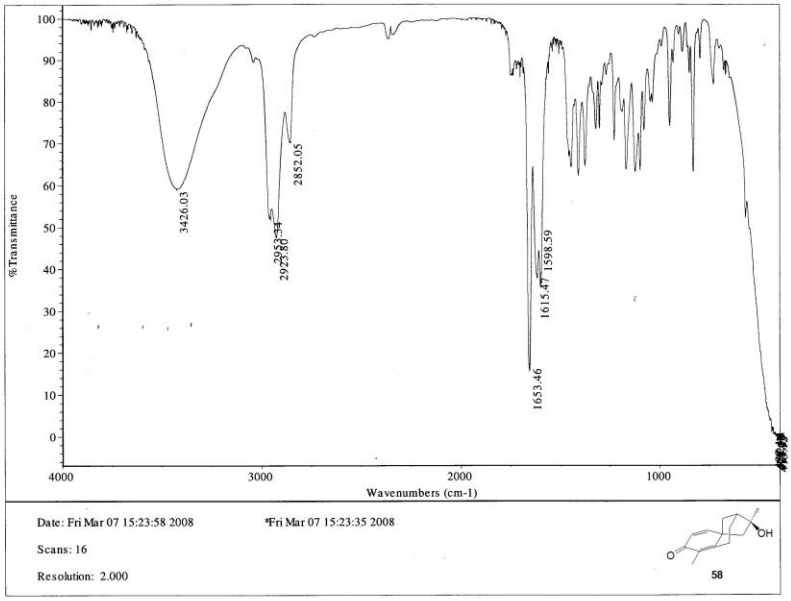

α-Allyl dienone 60

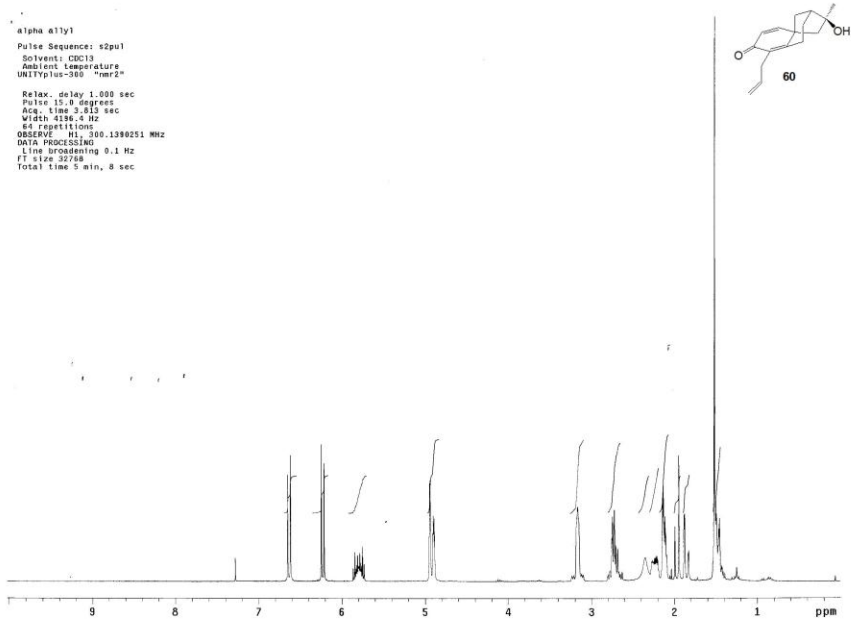

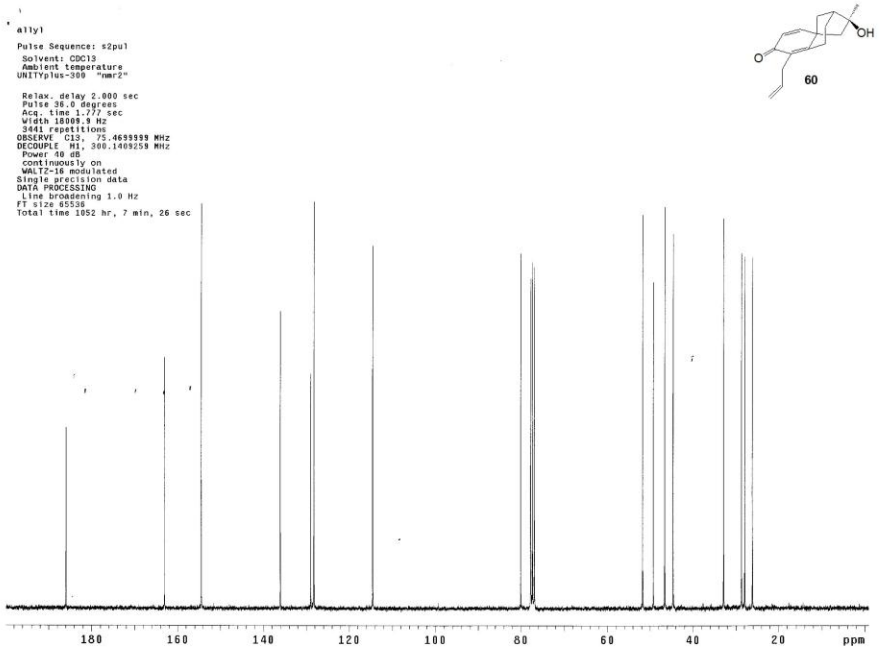

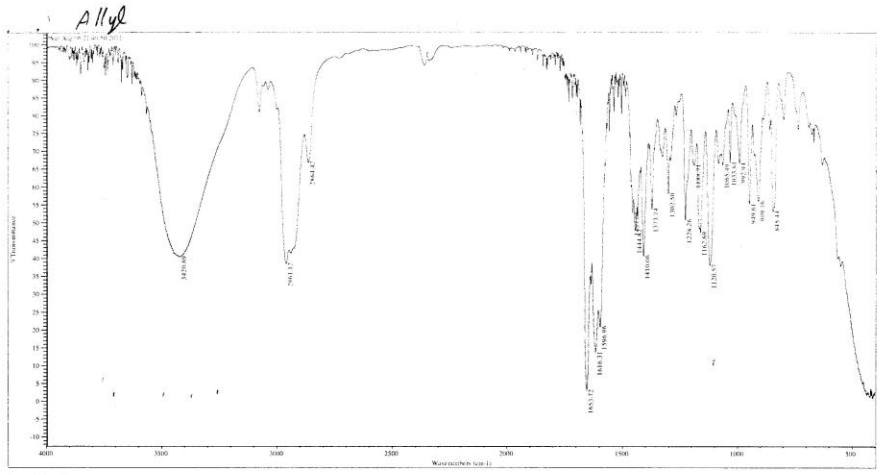

Sat Aug 06 21:41:49 2011
FIND PEAKS:
Spectrum: "Sat Aug 06 21:40:50 2011
Region: 4000.00 400.00
Absolute threshold: 87.264
Sensitivity: 50
Peak list:

Peak#	1633.72	Intensity	3.166
Peak#	1616.33	Intensity	13.664
Peak#	1598.98	Intensity	20.909
Peak#	1120.93	Intensity	38.131
Peak#	2961.12	Intensity	38.481
Peak#	3420.66	Intensity	40.356
Peak#	1410.06	Intensity	40.674
Peak#	1382.86	Intensity	47.140
Peak#	1444.82	Intensity	47.800
Peak#	1276.76	Intensity	50.725
Peak#	1457.08	Intensity	52.904
Peak#	845.44	Intensity	53.144
Peak#	1333.74	Intensity	53.781
Peak#	910.67	Intensity	55.194
Peak#	909.76	Intensity	55.850
Peak#	1525.52	Intensity	57.479
Peak#	1468.21	Intensity	66.170
Peak#	1965.46	Intensity	66.238
Peak#	997.84	Intensity	66.568
Peak#	1071.86	Intensity	66.870
Peak#	1954.37	Intensity	66.869

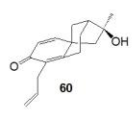

Enone 61

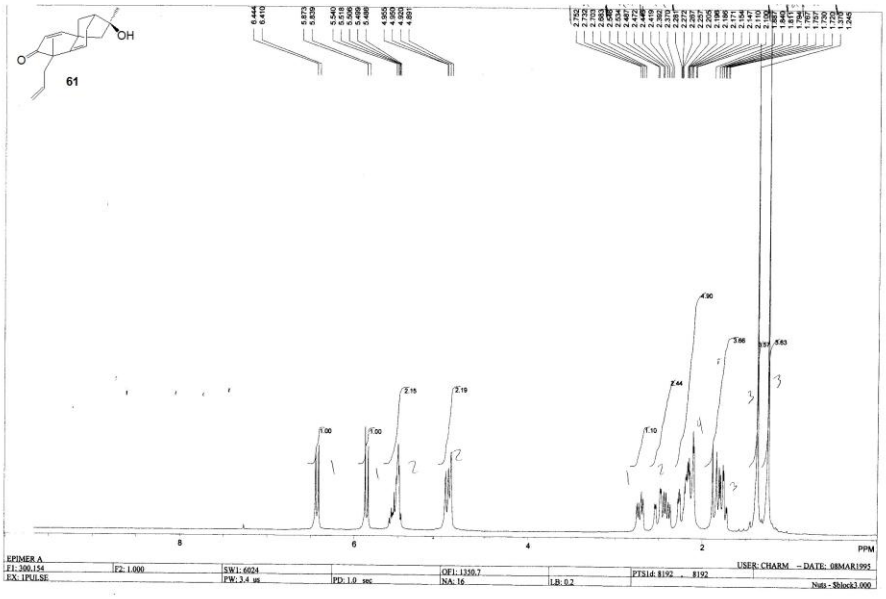
OH
O
61
PPM
EPIMER A
USER: CHARM -- DATE: 08MAR1995
F1: 300.154
F2: 1.000
SW1: 6024
PW: 3.4 us
PD: 1.0 sec
OF1: 1350.7
NA: 16
LB: 0.2
PTS1d: 8192 , 8192
EX: 1PULSE
Nuts - $block3.000

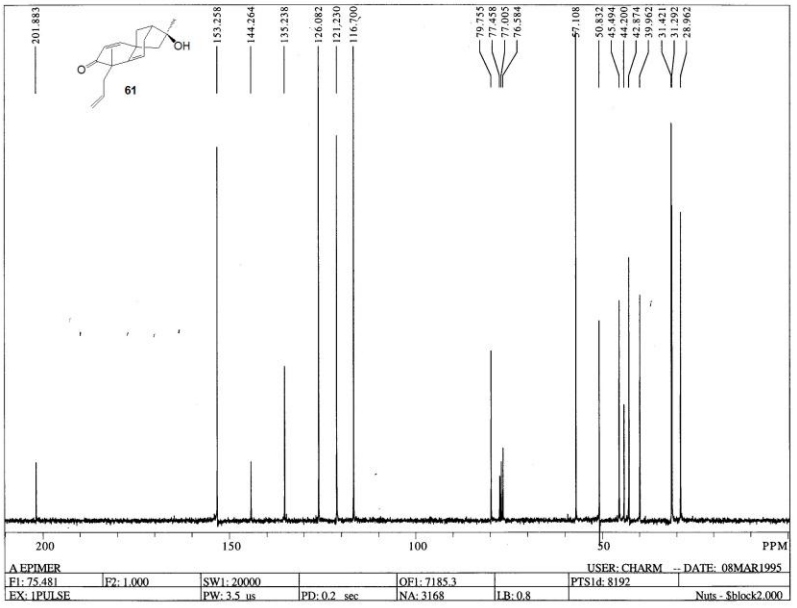
OH
O
61
201.883
153.258
144.264
135.238
126.082
121.230
116.700
79.755
77.458
77.005
76.584
57.108
50.832
45.494
44.200
42.874
39.962
31.421
31.392
28.962
200
150
100
50
PPM
A EPIMER
USER: CHARM -- DATE: 08MAR1995
F1: 75.481
F2: 1.000
SW1: 20000
PW: 3.5 us
PD: 0.2 sec
OF1: 7185.3
NA: 3168
LB: 0.8
PTS1d: 8192
EX: 1PULSE
Nuts - $block2.000

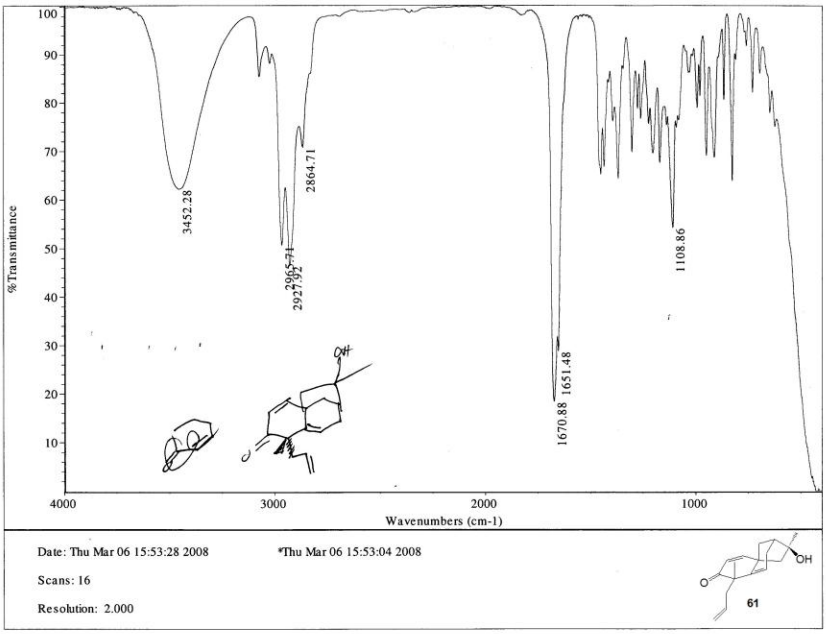
% Transmittance
Wavenumbers (cm-1)
3452.28
2927.92
2864.71
1670.88
1651.48
1108.86
OH
Date: Thu Mar 06 15:53:28 2008
*Thu Mar 06 15:53:04 2008
Scans: 16
Resolution: 2.000
61

Enone 65

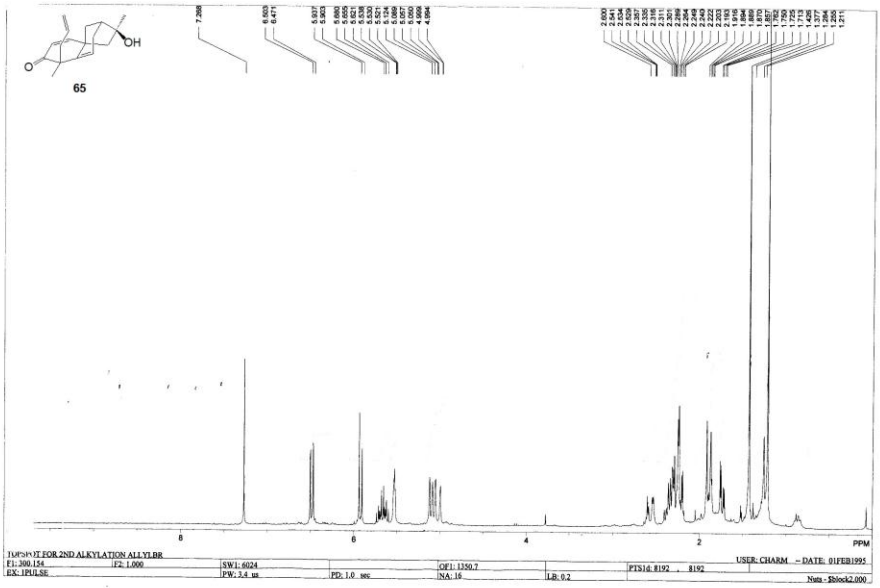
65
OH
PPM
USER: CHARM -- DATE: 01FEB1995

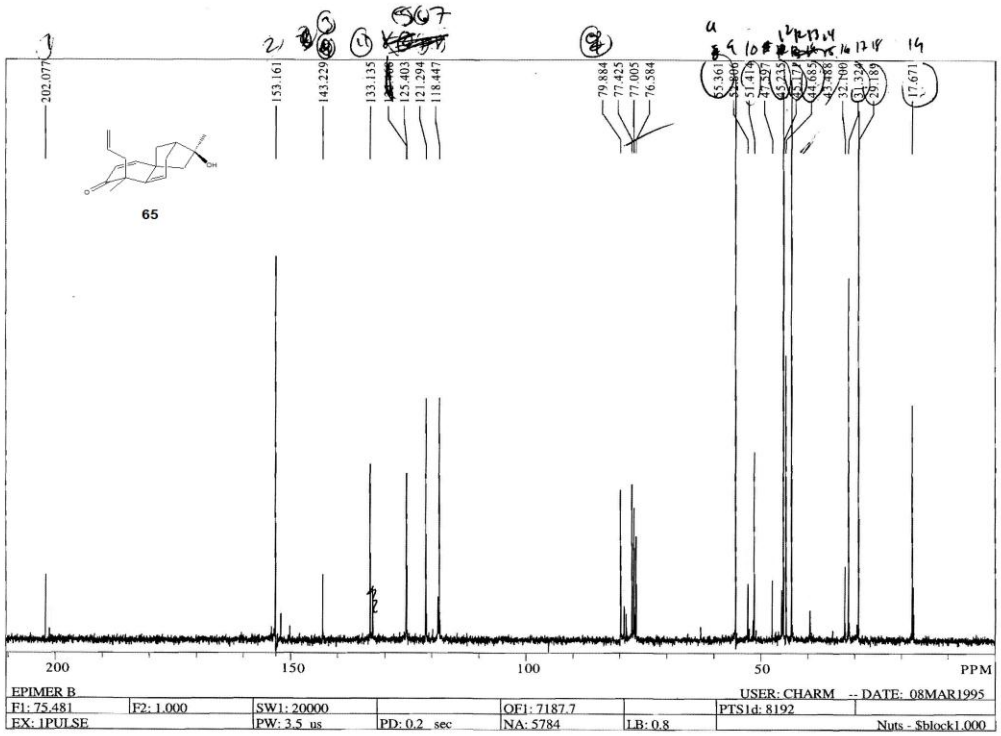
202.077
153.161
143.229
133.135
125.403
121.294
118.447
79.884
77.425
77.005
76.584
55.361
52.600
51.478
47.297
45.235
44.677
44.065
43.688
42.100
31.334
29.189
17.671
65
200
150
100
50
PPM
EPIMER B
USER: CHARM -- DATE: 08MAR1995
F1: 75.481
F2: 1.000
SW1: 20000
OF1: 7187.7
PTS1d: 8192
EX: 1PULSE
PW: 3.5 us
PD: 0.2 sec
NA: 5784
LB: 0.8
Nuts - $block1.000

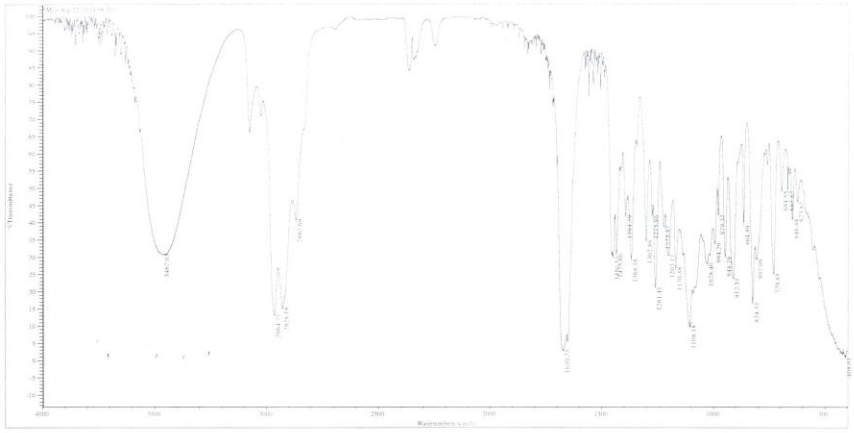
65

γ-Hydroxy dienone 74

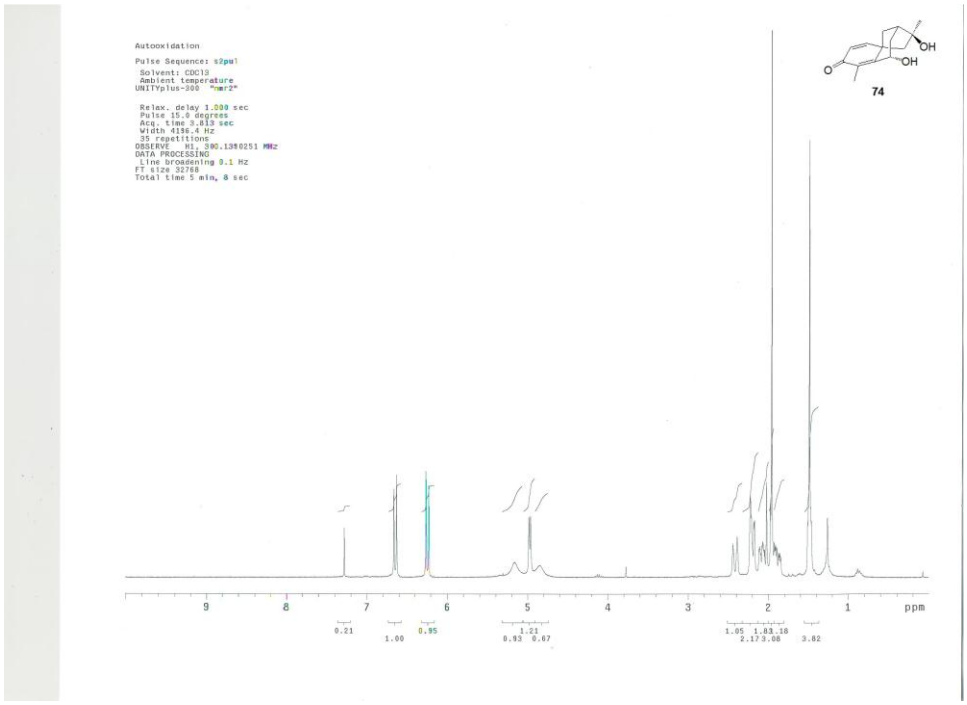

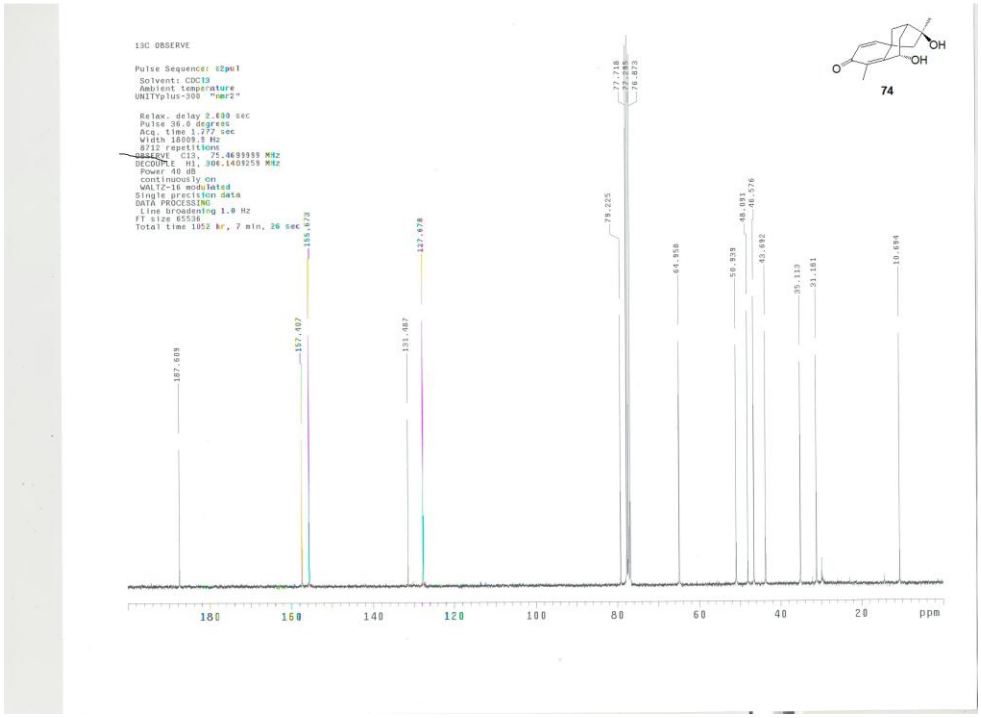

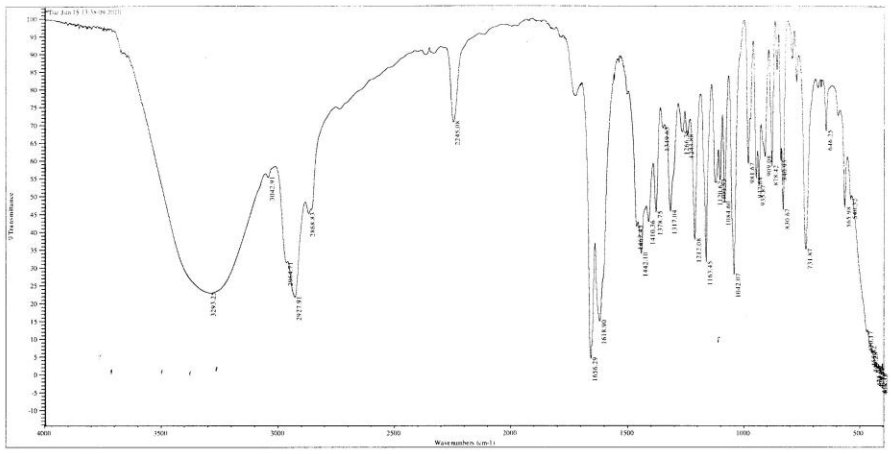

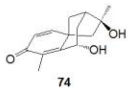

74

Ketone 76

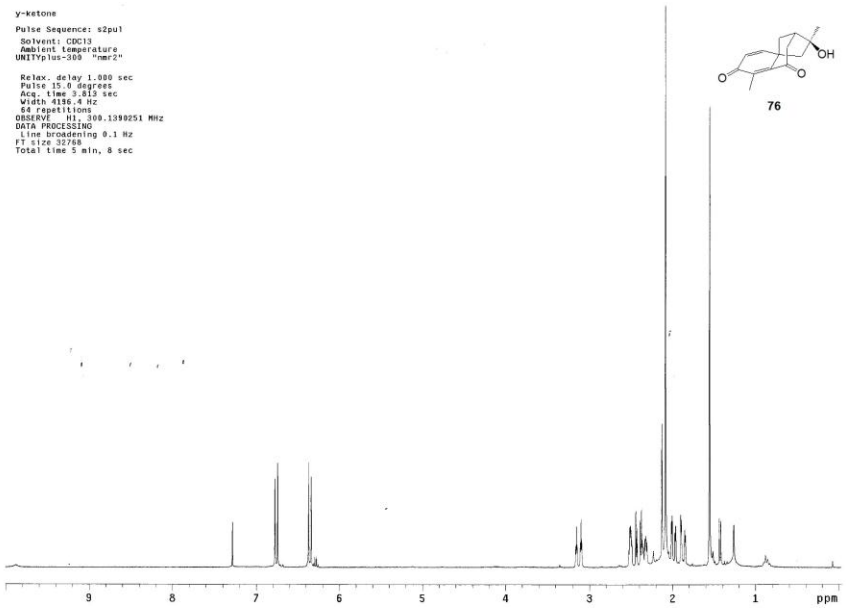

76

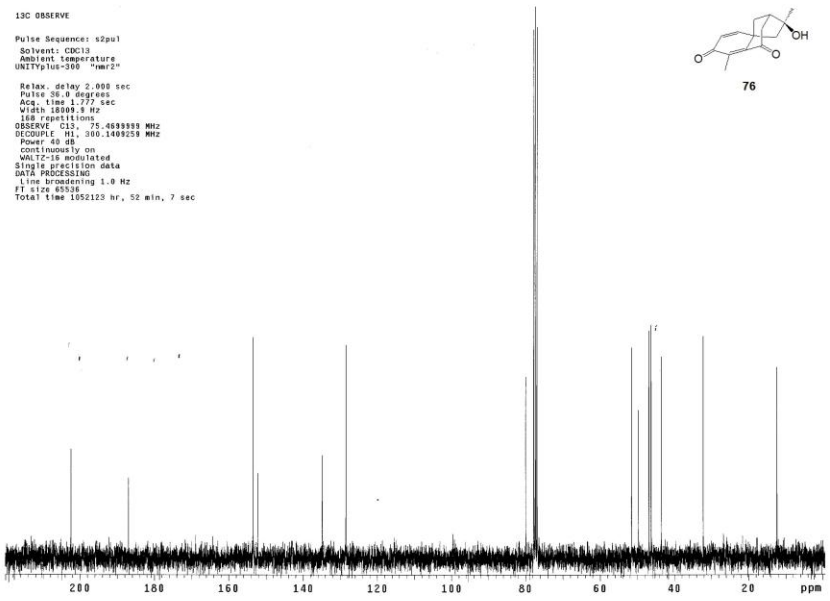

76

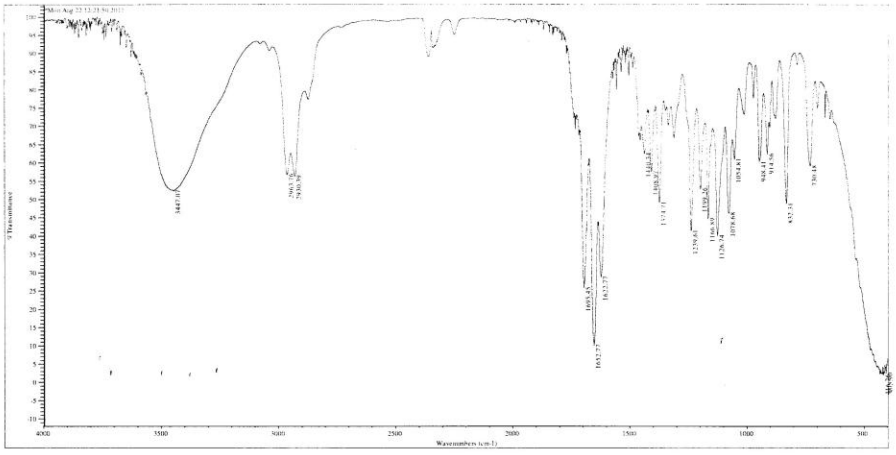

Mon Aug 22 12:22:54 2011
FIND PEAKS

Spectrum: *Mon Aug 22 12:21:50 2011
Region: 4000.00 400.00
Absolute threshold: 64.849
Sensitivity: 60
Peaklist:

Position:	416.26	Intensity:	1.976
Position:	465.90	Intensity:	3.453
Position:	1652.73	Intensity:	10.042
Position:	1665.45	Intensity:	28.727
Position:	1822.77	Intensity:	28.870
Position:	1726.74	Intensity:	36.995
Position:	1379.61	Intensity:	41.344
Position:	1368.99	Intensity:	44.631
Position:	1078.86	Intensity:	46.142
Position:	822.52	Intensity:	46.952
Position:	1374.71	Intensity:	49.074
Position:	3442.07	Intensity:	52.259
Position:	1399.26	Intensity:	52.866
Position:	2931.96	Intensity:	56.302
Position:	2963.36	Intensity:	56.886
Position:	2836.67	Intensity:	57.331
Position:	730.48	Intensity:	59.130
Position:	949.41	Intensity:	60.278
Position:	1354.91	Intensity:	60.965
Position:	1446.74	Intensity:	62.089
Position:	1014.96	Intensity:	62.363

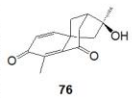

76

α-Hydroxy enone 77

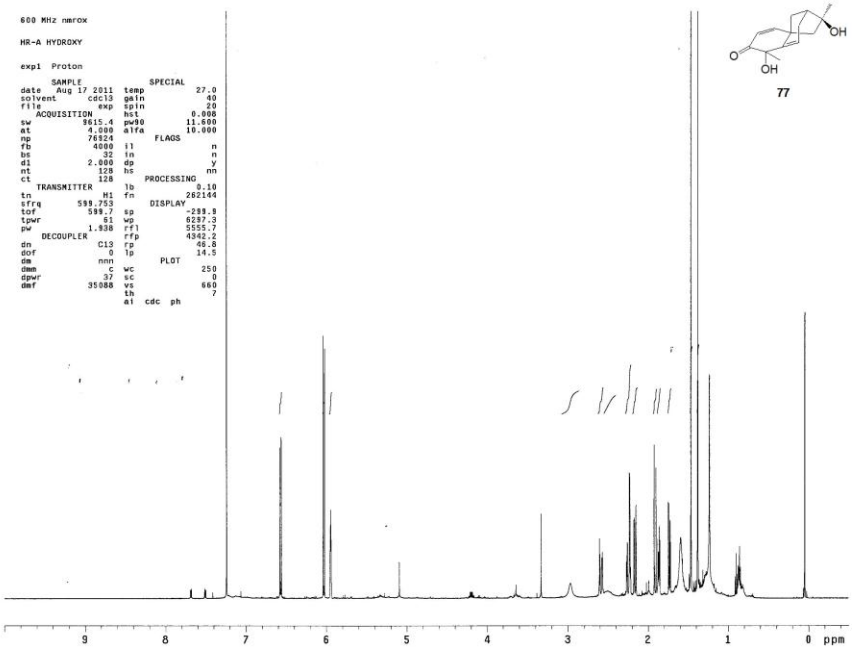

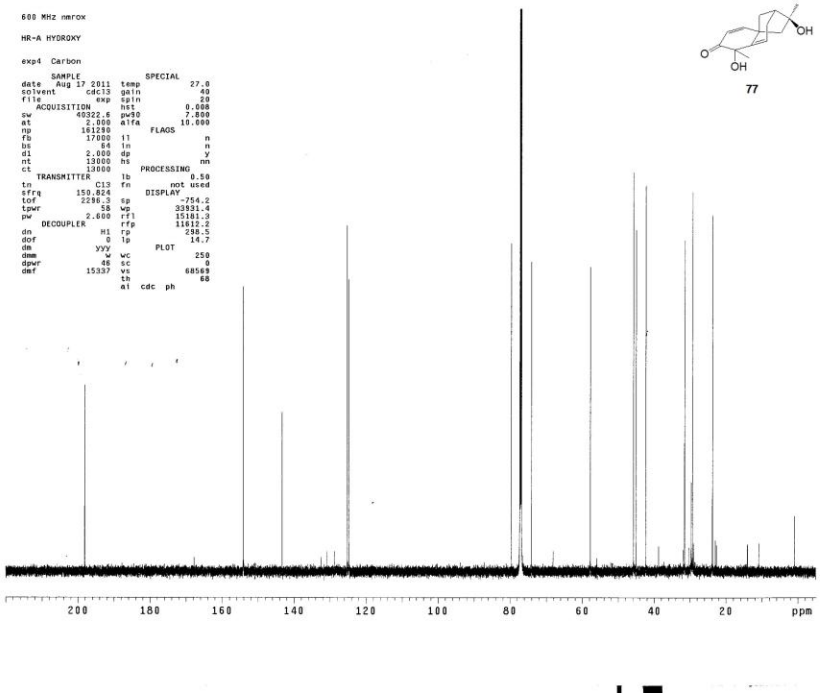

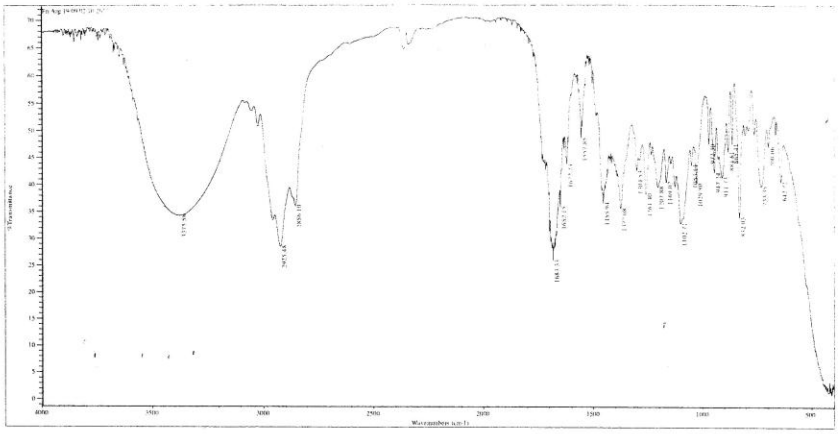

Silyloxy dienone 81

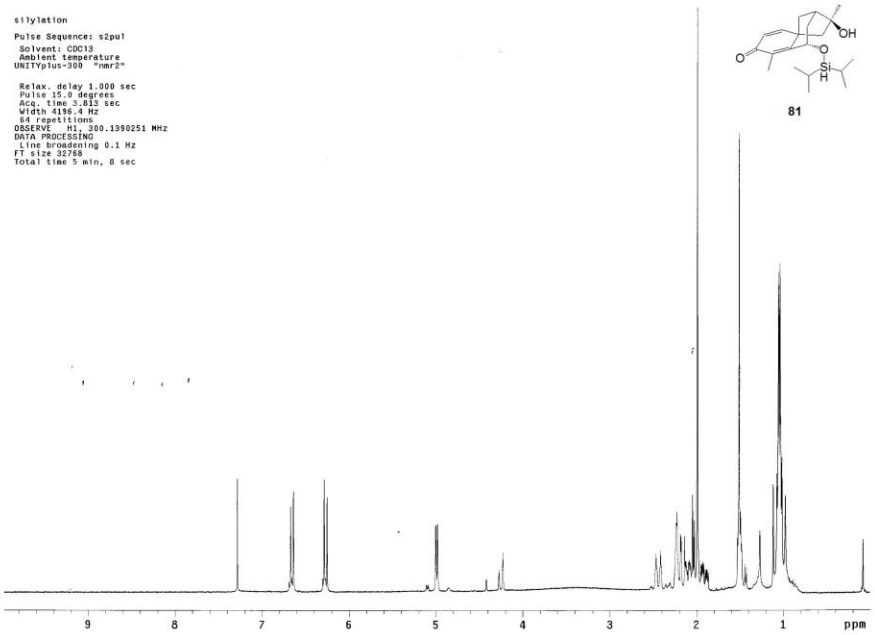
silylation
Pulse Sequence: s2pul
Solvent: CDCl3
Ambient temperature
UNITYplus-300 "nmr2"
Relax. delay 1.000 sec
Pulse 15.0 degrees
Acq. time 3.813 sec
Width 4196.4 Hz
64 repetitions
OBSERVE H1, 300.1390251 MHz
DATA PROCESSING
Line broadening 0.1 Hz
FT size 32768
Total time 5 min, 8 sec
OH
O
Si
H
81
9
8
7
6
5
4
3
2
1
ppm

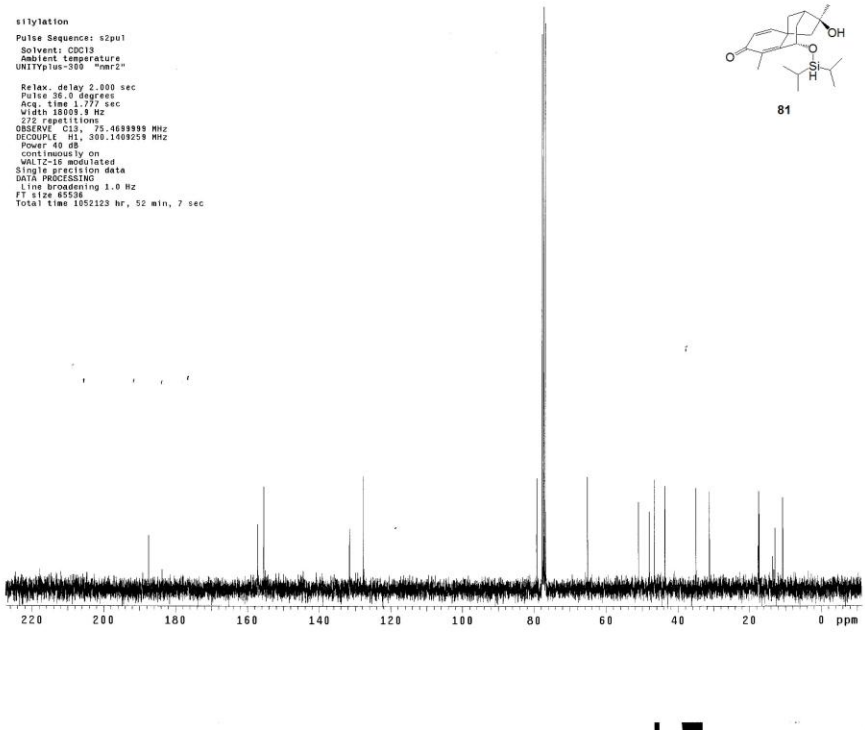
silylation
Pulse Sequence: s2pul
Solvent: CDCl3
Ambient temperature
UNITYplus-300 "nmr2"
Relax. delay 2.000 sec
Pulse 36.0 degrees
Acq. time 1.777 sec
Width 18009.9 Hz
272 repetitions
OBSERVE C13, 75.4699999 MHz
DECOUPLE H1, 300.1409259 MHz
Power 40 dB
continuously on
WALTZ-16 modulated
Single precision data
DATA PROCESSING
Line broadening 1.0 Hz
FT size 65536
Total time 1052123 hr, 52 min, 7 sec
OH
O
Si
H
81
220
200
180
160
140
120
100
80
60
40
20
0 ppm

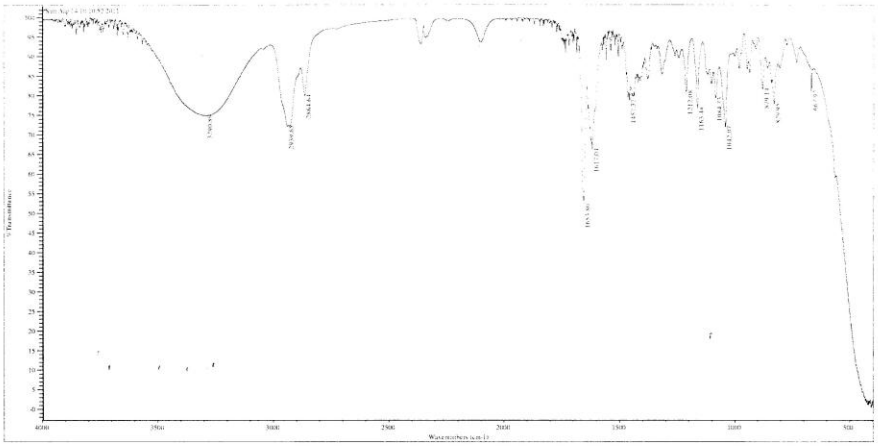

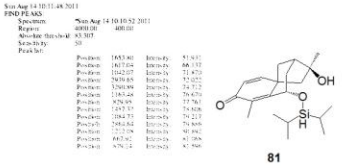

81

Enone 84

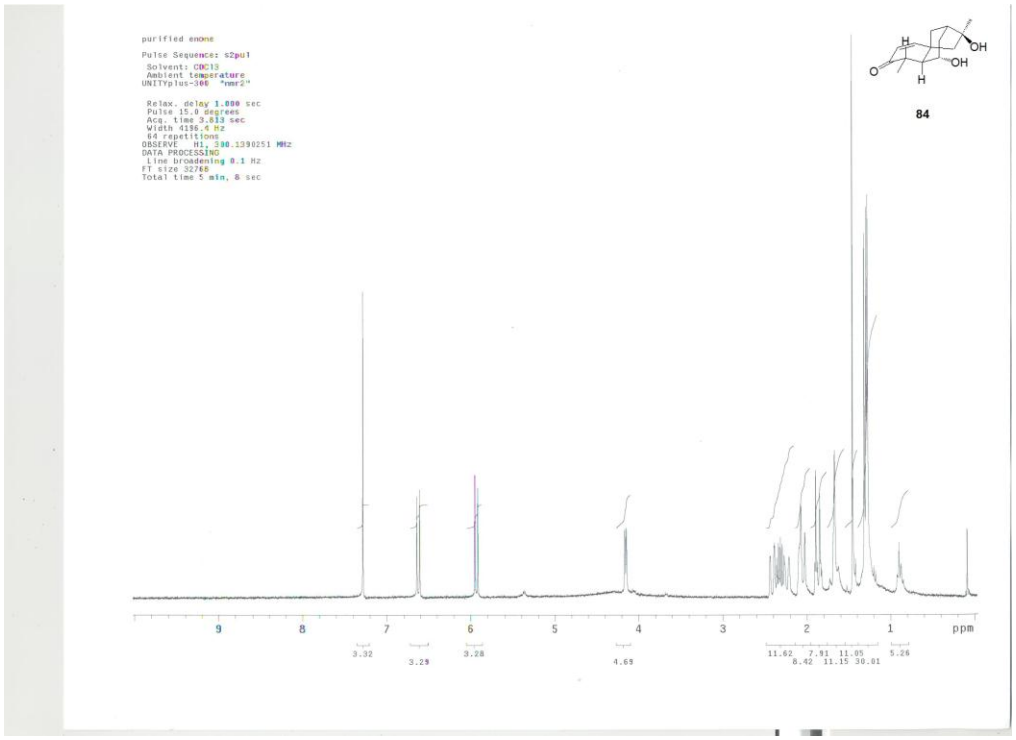
purified enone
Pulse Sequence: s2pul
Solvent: CDCl3
Ambient temperature
UNITYplus-300 "nmr2"
Relax. delay 1.000 sec
Pulse 15.0 degrees
Acq. time 3.813 sec
Width 4196.6 Hz
64 repetitions
OBSERVE H1, 300.1390251 MHz
DATA PROCESSING
Line broadening 0.1 Hz
FT size 32768
Total time 5 min, 8 sec
H
OH
O
OH
H
84
9
8
7
6
5
4
3
2
1
ppm
3.32
3.29
3.28
4.69
11.62
7.91
11.05
5.26
8.42
11.15
30.01

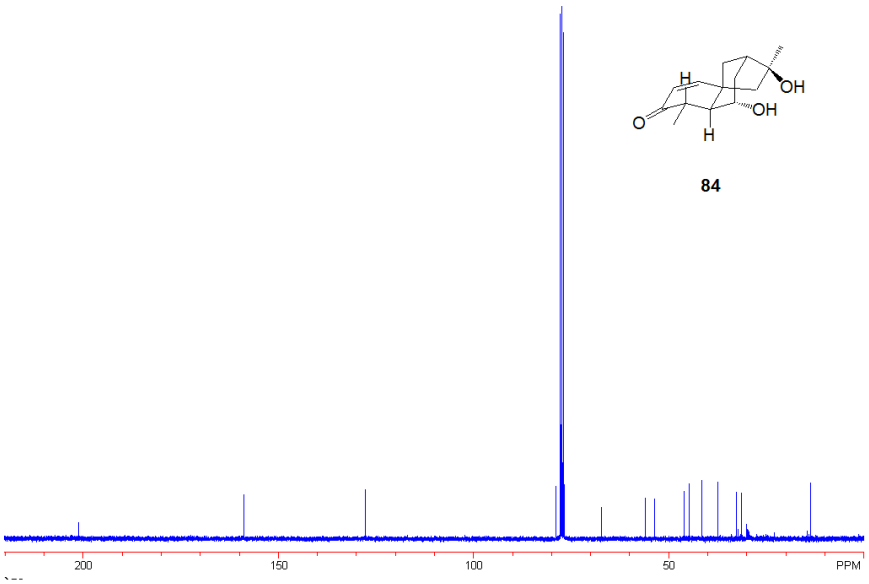
H
OH
O
OH
H
84
200
150
100
50
PPM

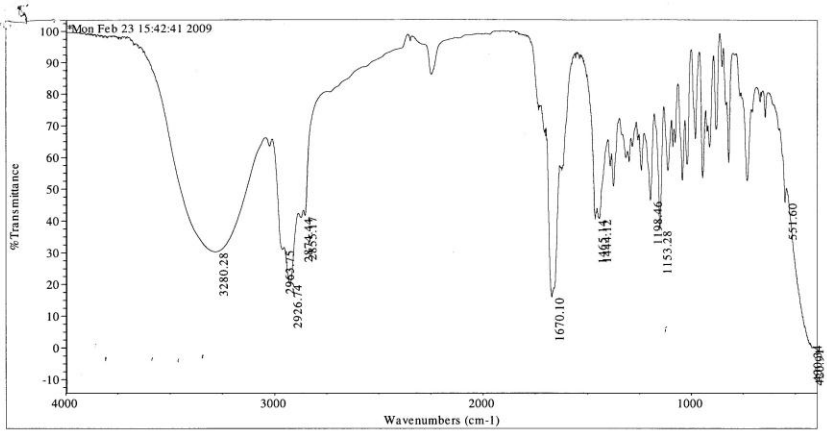

Mon Feb 23 15:44:42 2009
FIND PEAKS:
Spectrum: *Mon Feb 23 15:42:41 2009
Region: 4000.00 400.00
Absolute threshold: 50.000
Sensitivity: 94
Peak list:

Position:	420.91	Intensity:	-0.0024
Position:	430.34	Intensity:	1.109
Position:	1670.10	Intensity:	15.965
Position:	2926.74	Intensity:	20.128
Position:	3280.28	Intensity:	30.201
Position:	2963.75	Intensity:	30.929
Position:	1153.28	Intensity:	37.183

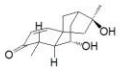

84

Cyclized enone 11

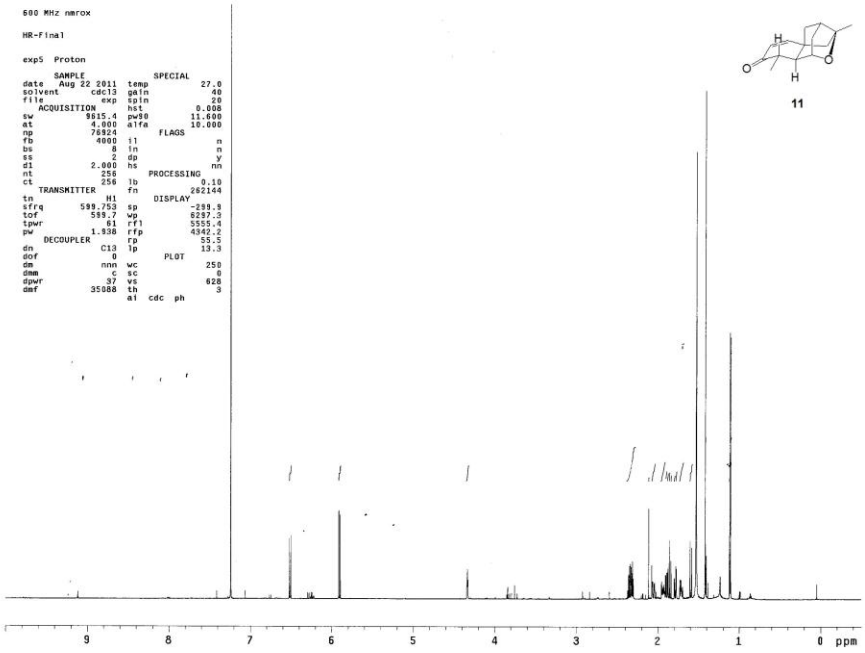

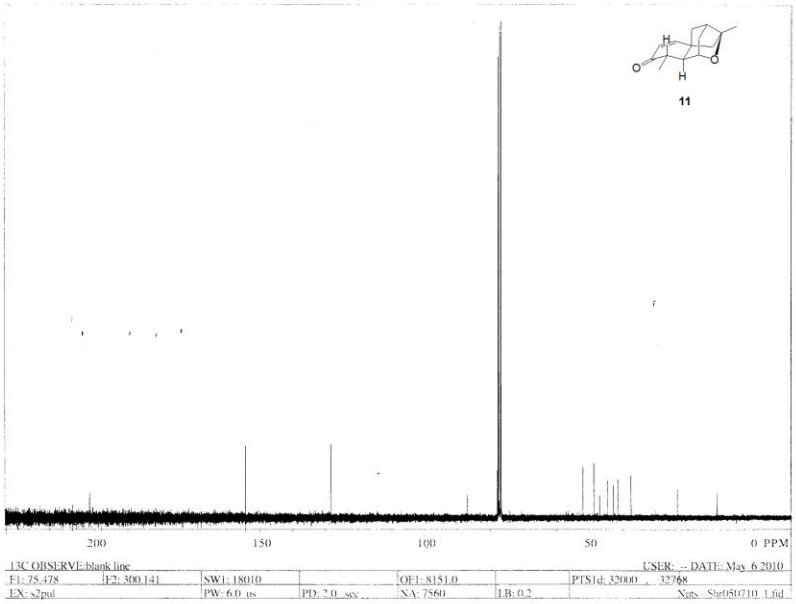
11
200
150
100
50
0 PPM
13C OBSERVE:blank line
USER: -- DATE: May 6 2010
F1: 75.478
F2: 300.141
SW1: 18010
OF1: 8151.0
PTS1d: 32000
32768
EX: x2pul
PW: 6.0 us
PD: 2.0 sec
NA: 7560
LB: 0.2
Nuts Shr050710 1.fid

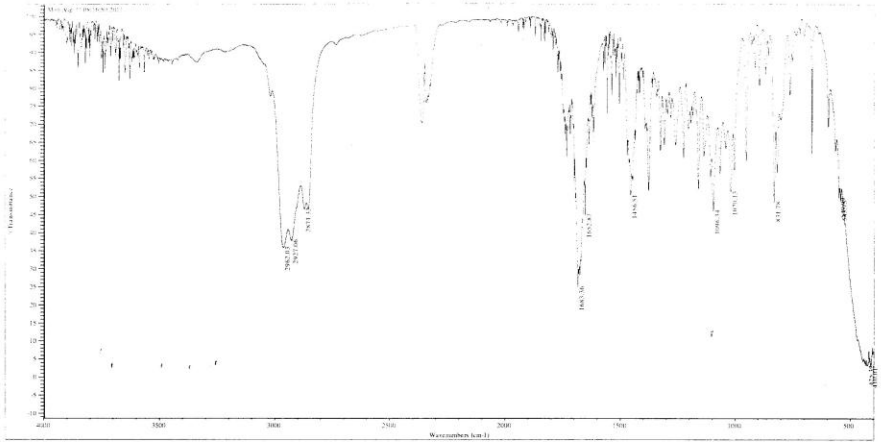
4000
3500
3000
2500
2000
1500
1000
500
Wavenumbers (cm-1)

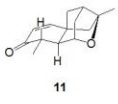
11

4.4 References

(1) Mal, D.; Dey, S. Synthesis of chlorine-containing angucycline BE-23254 and its analogs. *Tetrahedron* **2006**, *62*, 9589-9602.

(2) Beames, D.J.; Klose, T.R.; Mander, L.N., D. J. Studies on intramolecular alkylatoin. V. Intramolecular alkylation of the aromatic rinc in tetrahydronaphthyl diazomethyl ketones. *Aust. J. Chem.* **1974**, *27*, 1269-1275.

(3) Nicolaou, K. C. Li, A. Edmonds, D. J. Tria, G. S.; Ellery, S. P. Total Synthesis of Platensimycin and Related Natural Products. *Journal of the American Chemical Society* **2009**, *131*, 16905-16918.

Appendix A: X-Ray Data for Epimer 61

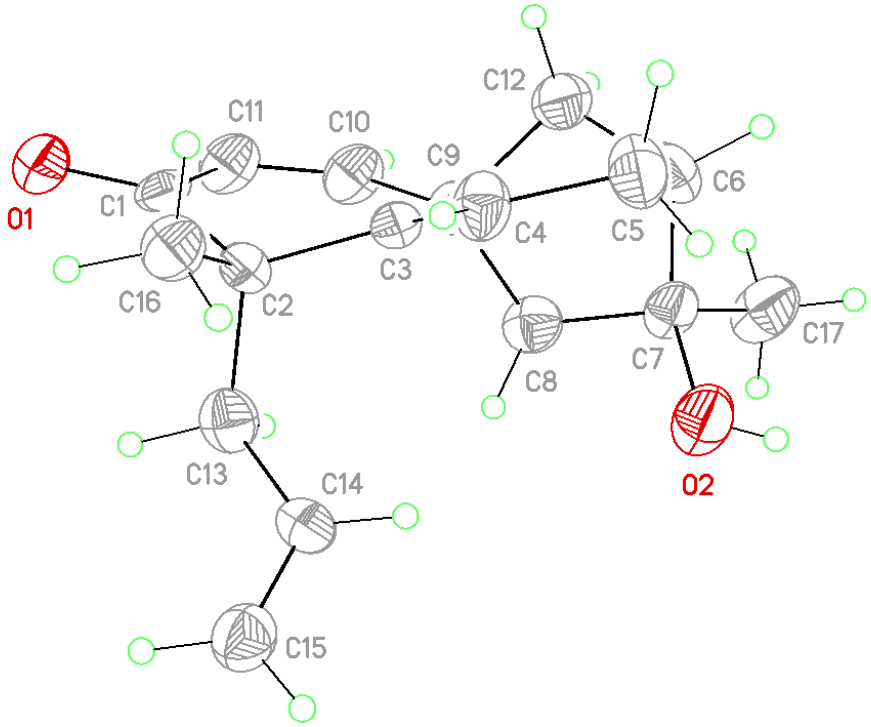

X-ray experimental for 61:

Crystals grew as colorless needles by slow evaporation of the mother liquor. The data crystal was a needle that had approximate dimensions; 0.38 x 0.09 x 0.06 mm. The data were collected on a Nonius Kappa CCD diffractometer using a graphite monochromator with MoKα radiation (λ = 0.71073Å). A total of 348 frames of data were collected using ω-scans with a scan range of 0.8° and a counting time of 140 seconds per frame. The data were collected at 153 K using an Oxford Cryostream low temperature device. Details of crystal data, data collection and structure refinement are listed in Table 1. Data reduction were performed using DENZO-SMN.[1] The structure was solved by direct methods using SIR97[2] and refined by full-matrix least-squares on F^2 with anisotropic displacement parameters for the non-H atoms using SHELXL-97.[3] The hydrogen atoms on carbon were calculated in ideal positions with isotropic displacement parameters set to 1.2xUeq of the attached atom (1.5xUeq for methyl hydrogen atoms). The hydrogen atoms bound to the hydroxyl oxygen atoms were observed in a ΔF map and refined with isotropic displacement parameters. The direction of the polar z axis could not be determined from the X-ray data and was arbitrarily assigned. The function, $\Sigma w(|F_o|^2 - |F_c|^2)^2$, was minimized, where $w = 1/[(\sigma(F_o))^2 + (0.0573*P)^2 + (0.8863*P)]$ and $P = (|F_o|^2 + 2|F_c|^2)/3$. $R_w(F^2)$ refined to 0.147, with R(F) equal to 0.0676 and a goodness of fit, S, = 1.06. Definitions used for calculating R(F), $R_w(F^2)$ and the goodness of fit, S, are given below.[4] The data were checked for secondary extinction effects but no correction was necessary. Neutral atom scattering factors and values used to calculate the linear absorption coefficient are from the International Tables for X-ray Crystallography (1992).[5] All figures were generated using SHELXTL/PC.[6]

Table 4.1. Crystal data and structure refinement for **71**

Empirical formula	C17 H22 O2	
Formula weight	258.35	
Temperature	153(2) K	
Wavelength	0.71073 Å	
Crystal system	Orthorhombic	
Space group	Pna21	
Unit cell dimensions	a = 17.7100(5) Å	□= 90°.
	b = 8.4320(10) Å	□= 90°.
	c = 19.4690(13) Å	□ = 90°.
Volume	2907.3(4) $Å^3$	
Z	8	
Density (calculated)	1.180 Mg/m^3	
Absorption coefficient	0.075 mm^{-1}	
F(000)	1120	
Crystal size	0.38 x 0.09 x 0.06 mm	
Theta range for data collection	2.09 to 24.99°.	
Index ranges	-20<=h<=21, -10<=k<=10, -23<=l<=23	
Reflections collected	4831	
Independent reflections	2635 [R(int) = 0.0990]	
Completeness to theta = 24.99°	99.9 %	
Absorption correction	None	
Refinement method	Full-matrix least-squares on F^2	
Data / restraints / parameters	2635 / 25 / 355	
Goodness-of-fit on F^2	1.062	
Final R indices [I>2sigma(I)]	R1 = 0.0676, wR2 = 0.1220	
R indices (all data)	R1 = 0.1417, wR2 = 0.1471	
Largest diff. peak and hole	0.223 and -0.187 $e.Å^{-3}$	

Table 2. Atomic coordinates (x 10^4) and equivalent isotropic displacement parameters ($Å^2$x 10^3) for **61**. U(eq) is defined as one third of the trace of the orthogonalized U^{ij} tensor.

	x	y	z	U(eq)
O1	-1747(3)	5207(6)	3522(3)	58(2)
O2	1773(3)	8388(6)	3528(2)	44(1)
C1	-1212(4)	5867(9)	3790(4)	43(2)
C2	-411(4)	5229(8)	3669(3)	37(2)
C3	196(4)	6078(9)	4101(4)	36(2)
C4	869(4)	5399(9)	4221(4)	41(2)
C5	1505(4)	6219(10)	4584(5)	43(2)
C6	1343(5)	7953(12)	4721(5)	43(2)
C7	1314(4)	9011(8)	4070(4)	39(2)
C8	465(4)	8922(9)	3825(4)	42(2)
C9	58(6)	7774(10)	4331(5)	38(2)
C10	-744(4)	8160(10)	4416(3)	40(2)
C11	-1310(6)	7322(8)	4178(5)	34(3)
C12	521(4)	8055(11)	4999(3)	39(2)
C13	-451(4)	3411(8)	3824(4)	50(2)
C14	-645(5)	3028(11)	4552(5)	59(2)
C15	-1301(7)	2447(10)	4764(7)	65(4)
C16	-241(4)	5477(9)	2896(4)	53(2)
C17	1542(4)	10712(8)	4228(4)	53(2)
O1A	4245(3)	4882(6)	2422(3)	56(1)
O2A	718(3)	1636(7)	2455(3)	48(1)
C1A	3707(4)	4192(8)	2160(4)	40(2)
C2A	2913(3)	4836(8)	2253(4)	41(2)
C3A	2302(4)	3958(9)	1846(4)	36(2)
C4A	1642(4)	4587(8)	1694(4)	42(2)
C5A	1013(5)	3708(11)	1353(5)	52(2)
C6A	1186(4)	1949(11)	1258(4)	41(2)

C7A	1196(4)	1001(8)	1931(4)	38(2)
C8A	2023(4)	1111(8)	2167(4)	35(2)
C9A	2421(5)	2228(10)	1663(5)	32(2)
C10A	3242(4)	1791(9)	1589(4)	40(2)
C11A	3817(7)	2697(9)	1785(6)	45(3)
C12A	1983(4)	1808(10)	1001(4)	43(2)
C13A	2940(4)	6608(9)	2077(4)	51(2)
C14A	3136(6)	6948(12)	1350(5)	66(3)
C15A	3750(8)	7610(9)	1133(8)	72(4)
C16A	2737(4)	4660(10)	3029(4)	53(2)
C17A	984(4)	-748(8)	1806(4)	49(2)

Appendix B: X-Ray Data for Epimer 65

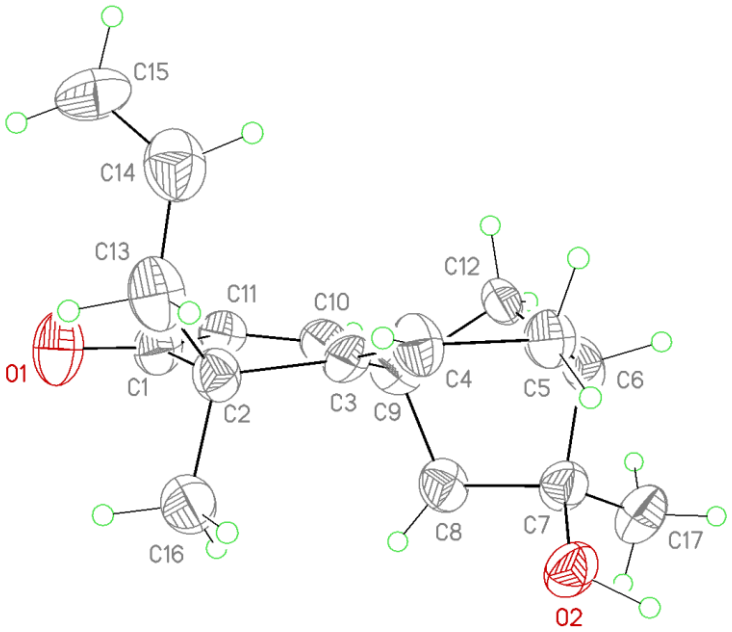

X-ray: Experiment for 65:

Crystals grew as clusters of small, colorless needles by evaporation of the mother liquor. The data crystal was cut from a cluster of crystals and had approximate dimensions; 0.19 x 0.09 x 0.08 mm. The data were collected on a Nonius Kappa CCD diffractometer using a graphite monochromator with MoKα radiation (λ = 0.71073Å). A total of 201 frames of data were collected using ω-scans with a scan range of 1.1° and a counting time of 260 seconds per frame. The data were collected at 153 K using an Oxford Cryostream low temperature device. Details of crystal data, data collection and structure refinement are listed in Table 1. Data reduction were performed using DENZO-SMN.[1] The structure was solved by direct methods using SIR97[2] and refined by full-matrix least-squares on F^2 with anisotropic displacement parameters for the non-H atoms using SHELXL-97.[3] The hydrogen atoms on carbon were calculated in ideal positions with isotropic displacement parameters set to 1.2xUeq of the attached atom (1.5xUeq for methyl hydrogen atoms). The hydrogen atom bound to O2 was observed in a ΔF map and refined with an isotropic displacement parameter. The absolute configuration of the molecule was assigned arbitrarily. The function, $\Sigma w(|F_o|^2 - |F_c|^2)^2$, was minimized, where $w = 1/[(\sigma(F_o))^2 + (0.0268*P)^2 + (0.5635*P)]$ and $P = (|F_o|^2 + 2|F_c|^2)/3$. $R_w(F^2)$ refined to 0.144, with R(F) equal to 0.0758 and a goodness of fit, S, = 1.03. Definitions used for calculating R(F), $R_w(F^2)$ and the goodness of fit, S, are given below.[4] The data were checked for secondary extinction effects but no correction was necessary. Neutral atom scattering factors and values used to calculate the linear absorption coefficient are from the International Tables for X-ray Crystallography (1992).[5]

Table 1. Crystal data and structure refinement for **65**

Empirical formula	C17 H22 O2	
Formula weight	258.35	
Temperature	153(2) K	
Wavelength	0.71073 Å	
Crystal system	Orthorhombic	
Space group	P212121	
Unit cell dimensions	a = 7.1420(6) Å	□= 90°.
	b = 10.0850(16) Å	□= 90°.
	c = 19.6410(10) Å	□ = 90°.
Volume	1414.7(3) $Å^3$	
Z	4	
Density (calculated)	1.213 Mg/m^3	
Absorption coefficient	0.078 mm^{-1}	
F(000)	560	
Crystal size	0.19 x 0.09 x 0.08 mm	
Theta range for data collection	2.07 to 24.99°.	
Index ranges	-8<=h<=8, -11<=k<=11, -23<=l<=23	
Reflections collected	2463	
Independent reflections	2463 [R(int) = 0.0000]	
Completeness to theta = 24.99°	99.7 %	
Absorption correction	None	
Refinement method	Full-matrix least-squares on F^2	
Data / restraints / parameters	2463 / 0 / 178	
Goodness-of-fit on F^2	1.031	
Final R indices [I>2sigma(I)]	R1 = 0.0758, wR2 = 0.1098	
R indices (all data)	R1 = 0.2182, wR2 = 0.1443	
Absolute structure parameter	5(4)	
Largest diff. peak and hole	0.212 and -0.212 $e.Å^{-3}$	

Table 2. Atomic coordinates (x 10^4) and equivalent isotropic displacement parameters ($Å^2$x 10^3) for **65**. U(eq) is defined as one third of the trace of the orthogonalized U^{ij} tensor.

	x	y	z	U(eq)
O1	2540(5)	5598(4)	4291(2)	44(1)
O2	2918(6)	4878(4)	7836(2)	48(1)
C1	2248(8)	5728(5)	4904(3)	29(1)
C2	3452(7)	5011(5)	5437(2)	29(1)
C3	3560(7)	5803(5)	6093(2)	26(1)
C4	5118(8)	5916(5)	6456(3)	36(2)
C5	5241(8)	6622(6)	7125(2)	43(2)
C6	3317(8)	7126(6)	7367(3)	42(2)
C7	1942(7)	6030(5)	7589(3)	34(2)
C8	888(7)	5666(6)	6938(3)	37(2)
C9	1789(7)	6460(6)	6353(2)	32(2)
C10	429(8)	6775(5)	5801(3)	40(2)
C11	626(8)	6479(6)	5149(3)	39(2)
C12	2338(8)	7740(6)	6749(2)	42(2)
C13	2413(8)	3668(5)	5557(2)	37(2)
C14	3379(7)	2791(6)	6068(3)	35(2)
C15	4039(7)	1590(6)	5932(3)	41(2)
C16	5375(7)	4702(5)	5128(2)	37(2)
C17	632(8)	6550(6)	8141(3)	55(2)

Appendix C: X-Ray Data for γ-Hydroxy Dienone 74

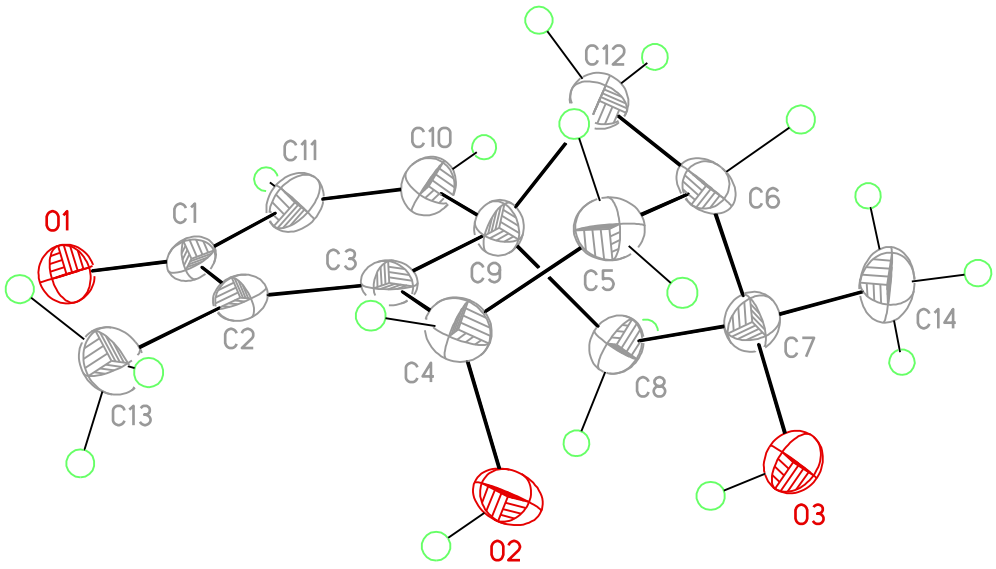

X-ray Experimental for 74:

Crystals grew as colorless needles by slow evaporation from dichloromethane and hexanes. The data crystal was a long lathe that had approximate dimensions; 0.53 x 0.08 x 0.07 mm. The data were collected on a Nonius Kappa CCD diffractometer using a graphite monochromator with MoK□ radiation (□ = 0.71073Å). A total of 165 frames of data were collected using □-scans with a scan range of 1.5° and a counting time of 108 seconds per frame. The data were collected at 153 K using an Oxford Cryostream low temperature device. Details of crystal data, data collection and structure refinement are listed in Table 1. Data reduction were performed using DENZO-SMN.[1] The structure was solved by direct methods using SIR97[2] and refined by full-matrix least-squares on F^2 with anisotropic displacement parameters for the non-H atoms using SHELXL-97.[3] The hydrogen atoms on carbon were calculated in ideal positions with isotropic displacement parameters set to 1.2xUeq of the attached atom (1.5xUeq for methyl hydrogen atoms). The hydroxyl group hydrogen atoms were observed in a ΔF map and refined with isotropic displacement parameters. The function, $\Sigma w(|F_o|^2 - |F_c|^2)^2$, was minimized, where $w = 1/[(\sigma(F_o))^2 + (0.044*P)^2 + (0.2463*P)]$ and $P = (|F_o|^2 + 2|F_c|^2)/3$. $R_w(F^2)$ refined to 0.0967, with R(F) equal to 0.0481 and a goodness of fit, S, = 1.04. Definitions used for calculating R(F), $R_w(F^2)$ and the goodness of fit, S, are given below.[4] Neutral atom scattering factors and values used to calculate the linear absorption coefficient are from the International Tables for X-ray Crystallography (1992).[5] All figures were generated using SHELXTL/PC.[6] Tables of positional and thermal parameters, bond lengths and angles, torsion angles, figures and lists of observed and calculated structure factors are located in tables 1 through through 7.

Table 1. Crystal data and structure refinement for **74**.

Empirical formula	C14 H18 O3	
Formula weight	234.28	
Temperature	153(2) K	
Wavelength	0.71070 Å	
Crystal system	Orthorhombic	
Space group	Pna21	
Unit cell dimensions	a = 7.7775(5) Å	□= 90°.
	b = 20.9924(12) Å	□= 90°.
	c = 7.4165(5) Å	□ = 90°.
Volume	1210.88(13) $Å^3$	
Z	4	
Density (calculated)	1.285 Mg/m^3	
Absorption coefficient	0.089 mm^{-1}	
F(000)	504	
Crystal size	0.53 x 0.08 x 0.07 mm	
Theta range for data collection	1.94 to 27.48°.	
Index ranges	-10<=h<=10, -26<=k<=26, -9<=l<=9	
Reflections collected	2542	
Independent reflections	1489 [R(int) = 0.0398]	
Completeness to theta = 27.48°	99.7 %	
Refinement method	Full-matrix least-squares on F^2	
Data / restraints / parameters	1489 / 1 / 164	
Goodness-of-fit on F^2	1.045	
Final R indices [I>2sigma(I)]	R1 = 0.0481, wR2 = 0.0892	
R indices (all data)	R1 = 0.0725, wR2 = 0.0967	
Largest diff. peak and hole	0.206 and -0.221 $e.Å^{-3}$	

Table 2. Atomic coordinates (x 10^4) and equivalent isotropic displacement parameters ($Å^2$x 10^3) for **74**. U(eq) is defined as one third of the trace of the orthogonalized U^{ij} tensor.

	x	y	z	U(eq)
O1	4177(2)	1755(1)	2960(3)	38(1)
O2	1419(3)	48(1)	7768(3)	31(1)
O3	-1517(3)	357(1)	9368(3)	31(1)
C1	3248(3)	1711(1)	4295(4)	27(1)
C2	3422(3)	1174(1)	5584(4)	26(1)
C3	2365(3)	1124(1)	7018(4)	22(1)
C4	2493(4)	571(1)	8328(4)	28(1)
C5	1967(4)	739(1)	10255(4)	29(1)
C6	480(3)	1220(1)	10381(4)	29(1)
C7	-1174(3)	1034(1)	9342(4)	29(1)
C8	-857(3)	1275(1)	7393(4)	27(1)
C9	945(3)	1606(1)	7390(4)	24(1)
C10	945(3)	2152(1)	6121(4)	30(1)
C11	1960(3)	2199(1)	4680(4)	31(1)
C12	1058(3)	1821(1)	9397(4)	29(1)
C13	4810(4)	703(1)	5114(5)	38(1)
C14	-2763(4)	1335(1)	10179(5)	41(1)

Appendix D: X-Ray Data for Enone 84

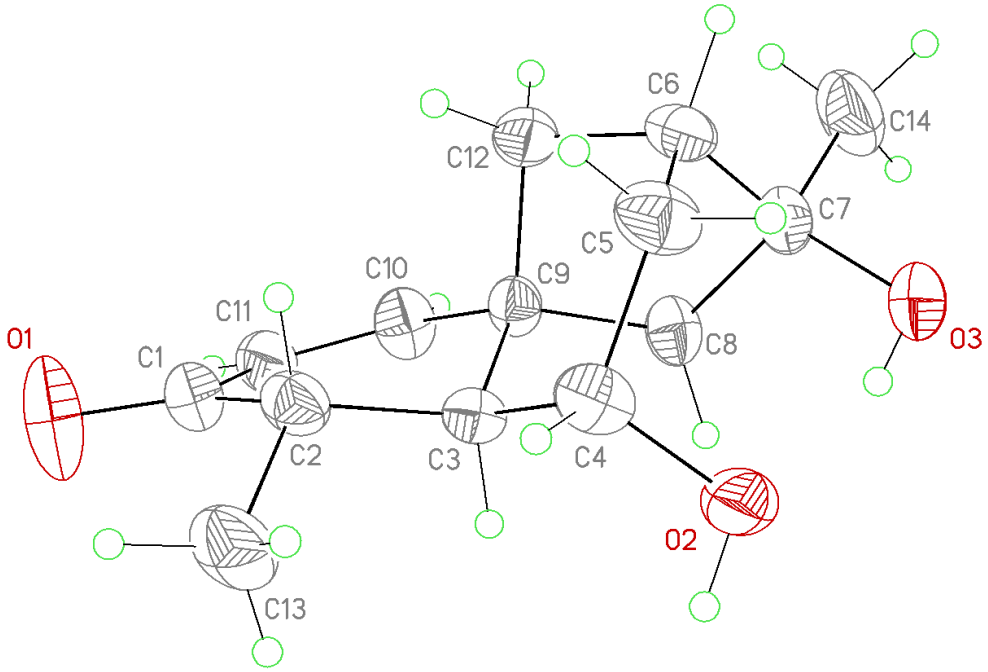

X-ray Experimental for 84:

X-ray Experimental for $C_{14}H_{20}O_3$: Crystals grew as colorless plates by slow evaporation from dichloromethane/hexanes. The data crystal had approximate dimensions; 0.25 x 0.25 x 0.08 mm. The data were collected on a Nonius Kappa CCD diffractometer using a graphite monochromator with MoKα radiation (λ = 0.71073Å). A total of 209 frames of data were collected using ω-scans with a scan range of 2° and a counting time of 288 seconds per frame. The data were collected at 153 K using an Oxford Cryostream low temperature device. Details of crystal data, data collection and structure refinement are listed in Table 1. Data reduction were performed using DENZO-SMN.[1] The structure was solved by direct methods using SIR97[2] and refined by full-matrix least-squares on F^2 with anisotropic displacement parameters for the non-H atoms using SHELXL-97.[3] The hydrogen atoms were calculated in ideal positions with isotropic displacement parameters set to 1.2xUeq of the attached atom (1.5xUeq for methyl hydrogen atoms). The function, $\Sigma w(|F_o|^2 - |F_c|^2)^2$, was minimized, where $w = 1/[(\sigma(F_o))^2 + (0.0493*P)^2 + (0.4359*P)]$ and $P = (|F_o|^2 + 2|F_c|^2)/3$. $R_w(F^2)$ refined to 0.122, with R(F) equal to 0.0488 and a goodness of fit, S, = 1.04. Definitions used for calculating R(F),$R_w(F^2)$ and the goodness of fit, S, are given below.[4] The data were checked for secondary extinction but no correction was necessary. Neutral atom scattering factors and values used to calculate the linear absorption coefficient are from the International Tables for X-ray Crystallography (1992).[5] All figures were generated using SHELXTL/PC.[6] Tables of positional and thermal parameters, bond lengths and angles, torsion angles and figures are found elsewhere.

Table 1. Crystal data and structure refinement for **84**.

Empirical formula	C14 H20 O3	
Formula weight	236.30	
Temperature	153(2) K	
Wavelength	0.71073 Å	
Crystal system	Monoclinic	
Space group	P21/c	
Unit cell dimensions	a = 10.516(2) Å	□= 90°.
	b = 8.0642(16) Å	□= 101.08(3)°.
	c = 15.392(3) Å	□ = 90°.
Volume	1281.0(4) $Å^3$	
Z	4	
Density (calculated)	1.225 Mg/m^3	
Absorption coefficient	0.085 mm^{-1}	
F(000)	512	
Crystal size	0.25 x 0.25 x 0.08 mm	
Theta range for data collection	1.97 to 27.49°.	
Index ranges	-13<=h<=13, -10<=k<=10, -19<=l<=19	
Reflections collected	5523	
Independent reflections	2928 [R(int) = 0.0224]	
Completeness to theta = 27.49°	99.4 %	
Absorption correction	None	
Refinement method	Full-matrix least-squares on F^2	
Data / restraints / parameters	2928 / 0 / 164	
Goodness-of-fit on F^2	1.043	
Final R indices [I>2sigma(I)]	R1 = 0.0488, wR2 = 0.1112	
R indices (all data)	R1 = 0.0723, wR2 = 0.1225	
Largest diff. peak and hole	0.233 and -0.153 $e.Å^{-3}$	

Table 2. Atomic coordinates (x 10^4) and equivalent isotropic displacement parameters ($Å^2$x 10^3) for **84**. U(eq) is defined as one third of the trace of the orthogonalized U^{ij} tensor.

	x	y	z	U(eq)
C1	5822(2)	1939(2)	6346(1)	39(1)
C2	6349(1)	3225(2)	7049(1)	33(1)
C3	7585(1)	4091(2)	6885(1)	27(1)
C4	7989(2)	5552(2)	7535(1)	36(1)
C5	7457(2)	7234(2)	7175(1)	41(1)
C6	7424(2)	7495(2)	6184(1)	36(1)
C7	8732(1)	7230(2)	5886(1)	36(1)
C8	8774(1)	5321(2)	5728(1)	34(1)
C9	7489(1)	4609(2)	5909(1)	27(1)
C10	7018(2)	3182(2)	5315(1)	36(1)
C11	6263(2)	1974(2)	5508(1)	36(1)
C12	6589(1)	6120(2)	5685(1)	35(1)
C13	6544(2)	2413(2)	7966(1)	52(1)
C14	8792(2)	8213(2)	5052(1)	55(1)
O1	5016(2)	922(2)	6470(1)	74(1)
O2	9376(1)	5710(2)	7761(1)	47(1)
O3	9829(1)	7763(2)	6529(1)	50(1)

Appendices References

1) DENZO-SMN. (1997). Z. Otwinowski and W. Minor, Methods in Enzymology, **276**: Macromolecular Crystallography, part A, 307 – 326, C. W. Carter, Jr. and R. M. Sweets, Editors, Academic Press.

2) SIR97. (1999). A program for crystal structure solution. Altomare A., Burla M.C., Camalli M., Cascarano G.L., Giacovazzo C. , Guagliardi A., Moliterni A.G.G., Polidori G.,Spagna R. J. Appl. Cryst. 32, 115-119.

3) Sheldrick, G. M. (1994). SHELXL97. Program for the Refinement of Crystal Structures. University of Gottingen, Germany.

4) $R_w(F^2) = \{\Sigma w(|F_o|^2 - |F_c|^2)^2/\Sigma w(|F_o|)^4\}^{1/2}$ where w is the weight given each reflection.
$R(F) = \Sigma(|F_o| - |F_c|)/\Sigma|F_o|\}$ for reflections with $F_o > 4(\sigma(F_o))$.
$S = [\Sigma w(|F_o|^2 - |F_c|^2)^2/(n - p)]^{1/2}$, where n is the number of reflections and p is the number of refined parameters.

5) International Tables for X-ray Crystallography (1992). Vol. C, Tables 4.2.6.8 and 6.1.1.4, A. J. C. Wilson, editor, Boston: Kluwer Academic Press.

6) Sheldrick, G. M. (1994). SHELXTL/PC (Version 5.03). Siemens Analytical X-ray Instruments, Inc., Madison, Wisconsin, USA.

Vita

Heriberto Rivera Jr. was born in Palm Springs, CA. After he was born his family returned to Mexico. After three years his family emigrated to Holtville, California where he graduated from Holtville High School in June of 2000. He went on to earn his B.Sc. in biochemistry from UCSD in 2005. Not knowing any better he made the decision to enroll in the Graduate Program at UT Austin in 2006.

Permanent address: F_O_A_D@hotmail.com

This dissertation was typed by Heriberto Rivera Jr.